TAMPERE UNIVERSITY OF APPLIED SCIENES
Environmental Engineering

Final thesis

Timo Flaspöhler

Design of the runner of a Kaplan turbine for small hydroelectric power plants

Supervisor Jaakko Mattila
Commissioned by Tampere University of Applied Sciences, Mechanical engineering department
Tampere 2007

TAMPERE UNIVERSITY OF APPLIED SCIENES
Environmental Engineering

Timo Flaspöhler	Design of the runner of a Kaplan turbine for small hydroelectric power plants
Final thesis	78 pages, 42 pages Appendix
Supervisor	Jaakko Mattila
November 2007	
Keywords	Electricity tariff, small hydroelectric power plant, Kaplan turbine, runner, adaptation mechanism, stress analysis, technical drawings

ABSTRACT

The final thesis deals with the design of the runner of a Kaplan turbine. It might be that due to the increasing of the electricity tariff in the last years small hydroelectric power plants become cost effective. Since the runner of a small hydroelectric power plant is quite small, it has to be reexamined if the hub of the runner provides enough room for a proper adaptation mechanism. For this purpose the main characteristics of the runner are determined. Then, important data such as the suction head, the occurring forces or the critical speed are established. After those data are known, a detailed stress analysis of the developed adaptation mechanism follows. The stress analysis shows that the mechanism to adjust the blades is able to withstand the occurring forces. Finally drafts of the runner and its parts are done.

TABLE OF CONTENTS

ABSTRACT ii
TABLE OF CONTENTS 1
LIST OF SYMBOLS 4
1 INTRODUCTION 8
1.1 Pelton turbine 9
1.2 Francis turbine 9
1.3 Kaplan turbine 10
1.4 Definition of a small hydroelectric power plant 11
1.5 Waterpower in Finland 11
1.6 The price of electricity in Finland 12
2 ASSIGNMENT OF TASKS 13
2.1 List of requirements 14
3 Variation matrix 16
3.1 Selection 17
4 CALCULATION OF THE MAIN CHARACTERISTICS 20
4.1 Power 21
4.2 Speed of the turbine 22
4.2.1 Specific speed 22
4.2.2 Rational speed 23
4.2.3 Runaway speed 23
4.3 Runner diameter section 24
4.4 Hub diameter 24
4.5 Blade characteristics of some different heads and discharges 25
5 CAVITATION 26
6 DESIGN OF THE BLADE 28
6.1 Distortion of the blade under ideal circumstances 28
6.2 The “Tragflügeltheorie” 31
6.2.1 Procedure 32
7 CALCULATION OF THE FORCES 36
7.1 Tangential force 36
7.2 Axial force 37
7.3 Resulting force 38
7.4 Hydraulic moment 38
7.5 Centrifugal force 41

7.6 Weight of the blade 42
8 CRITICAL SPEED 43
9 STRESS ANALYSES 45
9.1 Axle 46
9.2 Blade 47
9.2.1 Bending 47
9.2.2 Torsion 48
9.3 Pivot 50
9.3.1 Contact pressure 50
9.3.2 Torsion 51
9.3.3 Bending 51
9.4 Lever 53
9.4.1 Bending 53
9.4.2 Shear 54
9.4.3 Contact pressure 55
9.5 Link 56
9.5.1 Buckling 57
9.5.2 Stress calculation of the links eye 58
9.6 Crosshead 60
9.7 Bolt 62
9.7.1 Bending 62
9.7.2 Shear 63
9.7.3 Contact pressure 64
9.8 Shaft 66
9.9 Hub 67
10 CALCULATION OF THE SCREWS 68
10.1 Screw connection of the lever and the pivot 68
10.2 Screw connection between the blade and the pivot 73
10.3 Screw connection between the upper and the middle hub 74
10.4 Screw connection between the middle and the lower hub 75
11 EXPLANATION OF THE RUNNER DESIGN 76
12 ASSEMBLING 78
13 CONCLUSION 79
14 APPENDIX 81
14.1 Calculation of the mains characteristics 81
14.1.1 Power 81
14.1.2 Rational speed 81
14.1.3 Runaway speed 81
14.1.4 Runner diameter 82
14.1.5 Hub diameter 82

14.2 Cavitation 83
14.3 Design of the blade 84
14.3.1 Velocities and the angles angle of distortion (180°-β_∞) 84
14.3.2 Calculation of the blade characteristics 85
14.4 Calculation of the forces 89
14.4.1 Tangential force 89
14.4.2 Axial force 89
14.4.3 Resulting force 90
14.4.4 Hydraulic moment 90
14.4.5 Centrifugal force 91
14.5 Critical speed 92
14.6 Stress analysis 92
14.6.1 Axle 92
14.6.2 Blade 93
14.6.3 Pivot 94
14.6.4 Lever 96
14.6.5 Link 98
14.6.6 Crosshead 100
14.6.7 Bolt 100
14.6.8 Shaft 102
14.7 Calculation of the screws 104
14.7.1 Screw connection of the lever and the pivot 104
14.7.2 Screw connection of pivot and flange 108
14.7.3 Screw connection between the upper and the middle hub 112
14.8 Drawings 116
14.9 Tables 125
15 REFERENCES 133

LIST OF SYMBOLS

A	Area
A_3	Core cross section of the thread
A_b	Blade area
A_{ers}	Ersatz area
A_N	Nominal cross section of the screw shank
A_{proj}	Projection screen
B	Wide
b	Wide
b	Length
c	Velocity
c	Absolute velocity
c	Wide
c_q	Spring constant for elastic lateral oscillation
D	Diameter
D_e	Runner diameter
D_i	Hub diameter
d	Diameter
d_w	Outer diameter of the annular surface of the screw
d_h	Hole diameter
E	Elastic modulus
E	Specific hydraulic energy of machine
e_y	Length
F	Force
F_a	Axial force
F_B	Longitudinal force
F_c	Centrifugal force
F_{Kl}	Clamping force
F_l	Lifting force
F_r	Resulting force
F_{sp}	Tension force
F_t	Tangential force
f_z	Setting amount

G	Weight
G	Weightiness
g	Acceleration of gravity
H	Wide
H	Head
H	Gross head
H_n	Net head
H_s	Suction head
h	Wide
I	Moment of inertia
K	profile characteristic number
K_A	Application factor
k_A	Snap factor
l	Chord
l	Length
l_k	Buckling length
l_k	Clamping length
M	Moment
M_h	Hydraulic moment
M_{sp}	Tension torque
n	Speed
n_{max}	Runaway speed
n_{QE}	Specific speed
n_{max}	Runaway speed
n_{max}	Runaway speed
n_{QE}	Specific speed
P	Power
p	Contact pressure
p_{atm}	Atmospheric pressure
p_v	Vapor pressure
p_{min}	minimal water pressure
Q	Discharge
R	Radius
R_e	Runner radius

R_i	Hub radius
R_m	Tensile strength
$R_{po.2}$	Elastic limit
r	Radius
t	Grating dispartment
u	Tangential velocity
W_b	Section modulus
W_t	Polar section modus
w	Relative velocity
y	Thickness
y	Length
z	Number of blades
z	Number of the screws
z	Length
α	Angle
β	Angle
δ	Angle of attack
δ_T	Flexibility of the uptight parts
δ_S	Flexibility of the screw
ε	Angle
ζ_a	Lifting coefficient
ζ_A	Lifting coefficient
ζ_W	Drag coefficient
η_h	Hydraulic efficiency
η_s	efficiency of the energy change
λ	Thickness ratio
λ	Angle of slip
$\lambda_{g0.2}$	Marginal strength
μ	Friction factor at the interstice
Φ	Force ratio
Φ_k	Simplified force ratio
ρ	Density of water
σ	Cavitation coefficient
σ_b	Bending stress

σ_k	Buckling stress
τ_s	Shear stress
τ_t	Tensional stress
ω	Angular velocity

1 INTRODUCTION

The demand for increasing the use of renewable energy has risen over the last few years due to environmental issues. The high emissions of greenhouse gases have led to serious changes in the climate. Although the higher usage of renewable energy would not solve the problems over night, it is an important move in the right direction. The field of renewable energy includes, for example wind power, solar power and waterpower. /1/

The first use of waterpower as an energy source dates back centuries. The energy was utilized, for instance, to grinding grain. The applied machinery for this purpose was based on simple water wheels. Over the years the machinery has been developed and become more and more advanced. Hydropower was the first renewable source which was used to generate electricity over 100 years ago. Today, hydropower is an important source of producing electrical energy; approximately 20% of the world electricity is supplied by hydroelectric power plants. /1, 2, 3, 4/

Depending on the head and discharge of the sites, the hydroelectric power plant has to be equipped with a specific turbine in order to get the highest efficiency. There are several different kinds of water turbines and can be divided into impulse and reaction turbines. An impulse turbine is where the water pressure is transformed into kinetic energy before the water reaches the runner of the turbine. The energy hits the runner in a form of a high-speed jet. A turbine, where the water pressure applies a force on the face of the runner blade is called a reaction turbine. The following three following turbines are usually utilized in the modern field of hydropower:

- Pelton turbine
- Francis turbine
- Kaplan turbine

These are discussed in more detail below.

/1/

1.1 Pelton turbine

The Pelton turbine belongs to the group of impulse turbines. It consists of a wheel which has a large number of buckets on its perimeter. One or more jets thud on the buckets which cause the torque. The wheel and generator are generally directly connected by a shaft. The range of head, in which the Pelton turbine is used, is between 60m and more than 1,000m. The Pelton turbine has quite a high efficiency and can be in the range of 30% and 100% of the maximum design discharge for a one-jet turbine and between 10% and 100% for a multi-jet turbine. /1, 3/

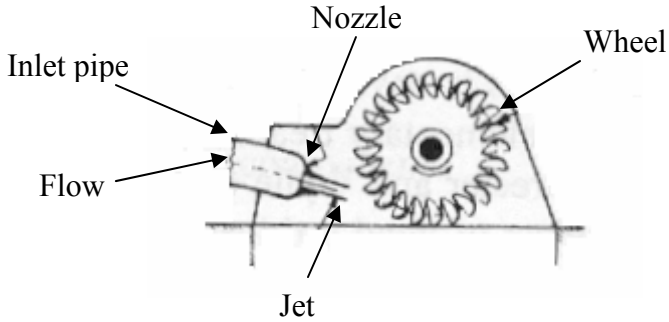

Figure 1.1: Pelton Turbine /3/

1.2 Francis turbine

The Francis turbine is a reaction turbine. It has fixed runner blades and adjustable guide vanes. Francis turbines are generally arranged so that the axis is vertical although smaller turbines can have a horizontal axis. The admission of a Francis turbine is radial and the outlet is axial. The field of application of the turbine is from a head of 25m up to 350m. It has an efficiency of over 80% in a ranging from approximately 40% to 100% of the maximum discharge. /1, 3/

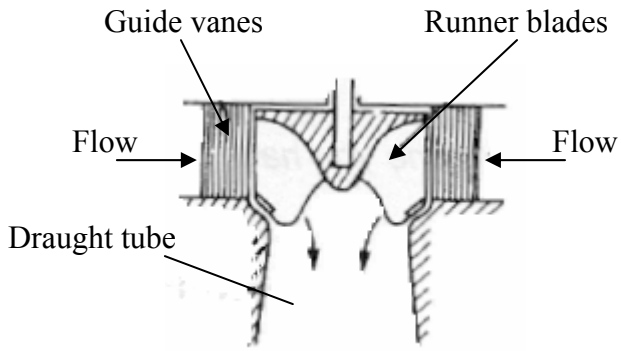

Figure 1.2: Francis Turbine /3/

1.3 Kaplan turbine

The Propeller turbine and the Kaplan turbine are reaction turbines. They have relatively small dimensions combined with a high rational speed. Hence the generator dimension is rather small and inexpensive. In addition, both the Propeller and the Kaplan turbines show a large overload capacity. The intake of the flow is radial. After the inlet the flow makes a right angle turn and enters the runner in an axial direction.

The difference between the Propeller and Kaplan turbines is that the Propeller turbine has fixed runner blades while the Kaplan turbine has adjustable runner blades. Propeller turbines can only be used on sites with a comparatively constant flow and head while Kaplan turbines are quite flexible.

The Kaplan turbine can be divided in double and single regulated turbines. A Kaplan turbine with adjustable runner blades and adjustable guide vanes is double regulated while one with only adjustable runner blades is single regulated. The application of Kaplan turbines are from a head of 2m to 40m. The advantage of the double regulated turbines is that they can be used in a wider field. The double regulated Kaplan turbines can work between 15% and 100% of the maximum design discharge; the single regulated turbines, however, can only work between 30% and 100% of the maximum design discharge. /1, 3, 5/

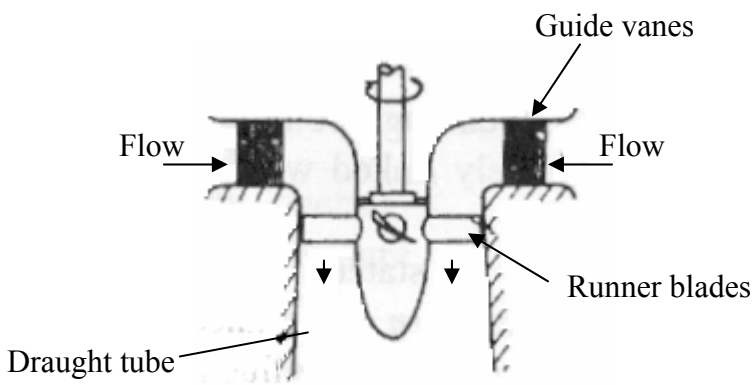

Figure 1.3: Kaplan turbine /3/

1.4 Definition of a small hydroelectric power plant

To define whether a hydroelectric power plant is a small one or not depends on its capacity. However, European countries do not agree where the capacity limit for a small hydroelectric power plant should be. In the UK, for example, the limit is fixed at 20MW while in France the capacity limit is 12MW. In Finland, the capacity limit is only 1MW. /1, 6/

1.5 Waterpower in Finland

Although Finland is called the land of 1,000 lakes, hydropower does not play a significant role in energy production.

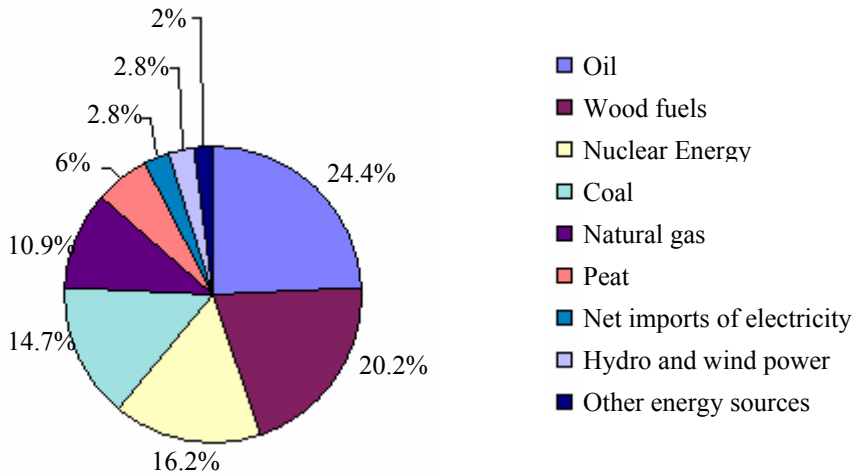

Figure 1.4: Total energy consumption of Finland in the year 2006 /7/

As shown in figure 1.4, hydropower, together with wind power, comprises just 2.8% of the total energy. The main energy sources in Finland are oil (24.4%) and wood fuels (20.2%). Nuclear energy, coal and natural gas are also important energy sources.

The main reason for the small share of hydropower as a source of energy lies with the characteristics of the natural landscape. Although Finland has many water sources, it is a relatively flat country. For this reason, the heads are mostly to low to build large or medium-size hydroelectric power plants. Furthermore, areas where the heads are high are normally under environmental protection. The only way to increase the electricity production by water power, therefore, would be to build small hydroelectric power plants. This option has not been cost effective due

to the low electricity tariff - the income would have been too little to cover investments. However, due to the price rise in electricity over the last few years, this option might be reconsidered.

1.6 The price of electricity in Finland

Figure 1.4 shows the price development of electricity in Finland over the last 6 years. Although the years 2004 and 2005 show a downturn, the electricity tariff increased approximately by a factor of three from 2000 to 2006.

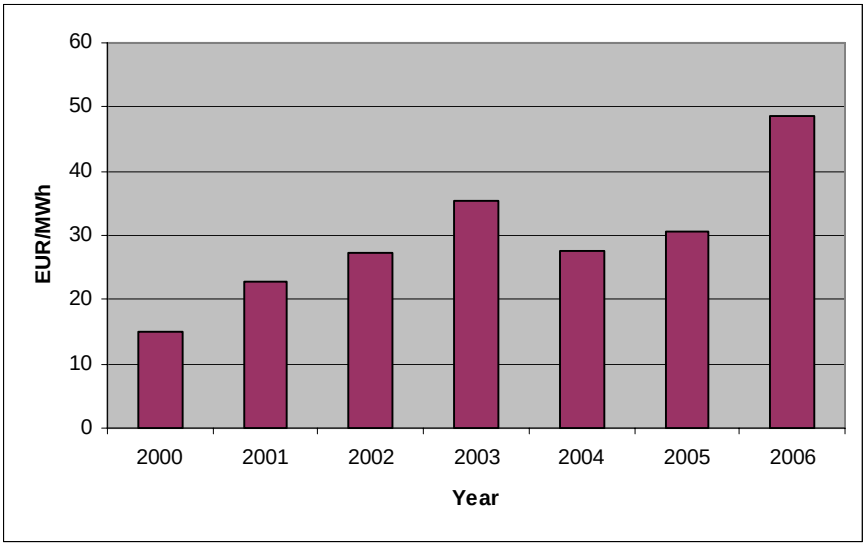

Figure 1.4: Electricity tariff 2000-2006 /8/

In Figure 1.5 it can be seen that the annual average of the electricity tariff in 2007 will be less than in 2006. However a new increase in the price of electricity can be expected for the few next years.

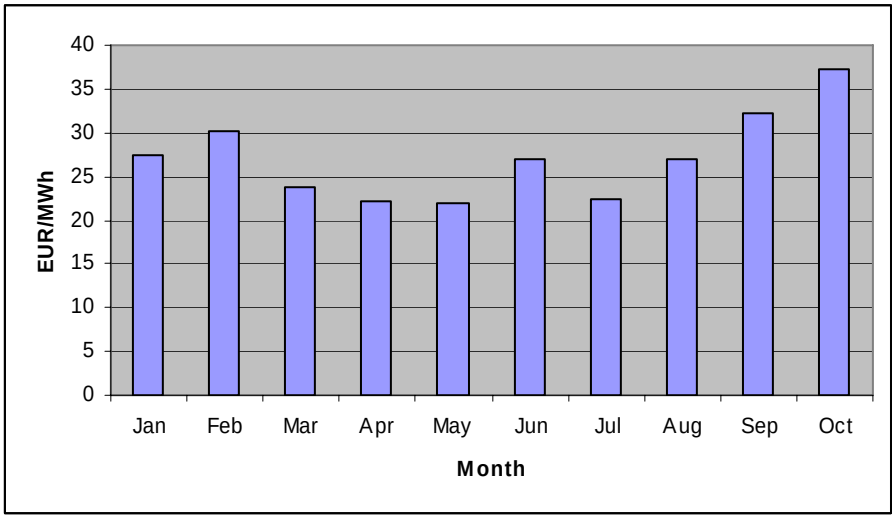

Figure 1.5: Electricity tariff January- October 2007/8/

2 ASSIGNMENT OF TASKS

This final thesis is one part of a project carried out by Tampere Polytechnic which, at the time of writing, was in its initial staged. The aim of the project is to explore if it is worth building small hydroelectric power plants in Finland.

The aim of this final thesis is to develop a Kaplan turbine's runner with adjustable blades - adaptive for small hydroelectric power plants. For this purpose, a prototype of the runner is to be designed with a proper mechanism for adjusting the blades. The concern is that the hub of the turbines for small heads does not provide much space for the adaptation mechanism. The mechanism's parts have to be big enough to resist the occurring forces and small enough to fit in the hub. This thesis determines whether this is possible or not. If the stress analysis shows that the mechanism is suitable, a draft of the runner will be drawn. The requirements of the discharge and the head are set at the site where an experimental rig for the prototype can be founded.

Jaakko Matila project supervisor, owns a small hydroelectric power plant equipped with a Francis turbine. The Korpikosky power plant, built on Lake Korpijärvi, provides enough space to build an experimental rig for the runner and as it would allow a direct comparison between a Kaplan and a Francis turbine. The turbine is designed to work in a maximal head of 3.7 meters and a highest discharge of $3m^3/s$.

To guarantee a smooth running of the project, experts from different fields are involved: Jaakko Matila and Simo Marjamäki are responsible for technical issues: Antti Klaavo for economical matters and Juha Paukkala for any legal questions.

2.1 List of requirements

Timo Flaspöhler		**List of requirements**	R = Requirement W = Wish	
Project: Kaplan Turbine				
R W	No.	Description	Value, Dates, Comments,	Responsible
	1	Purpose		
R	1.1	Small hydroelectric power plant		
	2	Working range		
R	2.1	Discharge	3 m^3/s	
R	2.2	Head	3.7m	
	3	Geometry		
R	3.1	Number	1	
R	3.2	Blade diameter	730mm	Timo
R	3.3	Hub diameter	240mm	Flaspöhler
	4	Blades		
R	4.1	Adjustable blades		
	5	Forces		
W	5.1	Mechanical transmission		
	6	Material		
R	6.1	Corrosion-resistant		
R	6.2	Cold-resistant		
Date: 01.10.2007				Page 1

Timo Flaspöhler		**List of requirements**		R = Requirement W = Wish
Project: Kaplan Turbine				
R W	No.	Description	Value, Dates, Comments,	Responsible
	7	Manufacturing		
W	7.1	In the Tampere Polytechnic		
W	7.2	Using purchased parts		
	7.3	Prototype		
	8	Assembling		
R	8.1	Accessibly assembling		
R	8.2	Simple assembling		
	9	Maintenance		Timo
R	9.1	Simple maintenance		Flaspöhler
	10	Safety		
R	10.1	Accident prevention rule		
	11	Power		
R	11.1	High efficiency		
	12	Dates		
R	12.1	Deadline	17.12.2007	
Date: 01.10.2007				Page 2

3 Variation matrix

Table 3.1: Variation matrix

	A	B	C
1: Axle	Material: X3CrNb17	Material: X20Cr13	Material: X17CrNi16-2
2: Shaft	Material: X3CrNb17	Material: X20Cr13	Material: X17CrNi16-2
3: Upper hub	Material: X3CrNb17	Material: X5CrNi18-10	Material: X8CrNi18-10
4: Middle hub	Material: X3CrNb17	Material: X20Cr13	Material: X8CrNi18-10
5: Lower hub	Material: X3CrNb17	Material: X20Cr13	Material: X8CrNi18-10
6: Blade	Material: X3CrNb17	Material: X3CrNiMo13-4	Material: X8CrNi18-10
7: Blade number	4	6	8
8: Pivot	Material: X3CrNb17	Material: X20Cr13	Material: X17CrNi16-2
9: Bearing pivot	Roller-bearing 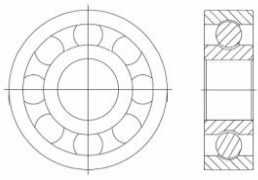	Bush bearing dry operation 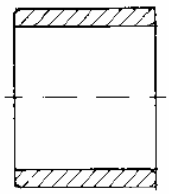	Bush bearing with greasing 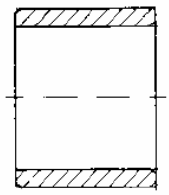
10: Bearing material	iglidur®H370	iglidur®H	—
11: Lever	Material: X3CrNb17	Material: X20Cr13	Material: X17CrNi16-2
12: Link	Material: X3CrNb17	Material: X20Cr13	Material: X8CrNi18-10

	A	B	C
13: Bearing link	Bush bearing dry operation 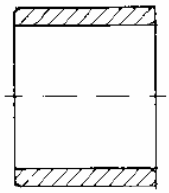	Bush bearing with greasing 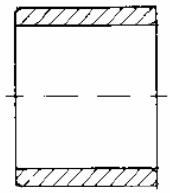	—
14: Bearing	iglidur®H370	iglidur®H	
15: Crosshead	Material: X3CrNb17	Material: X20Cr13	Material: X17CrNi16-2
16: Bolt	Bolt without head	Bolt with head and splint pin hole	Bolt with head and threaded pin 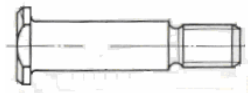
17: Bolt	Material: X6CrMoS17	Material: X20Cr13	Material: X17CrNi16-2
18: Fuse element	Locking ring 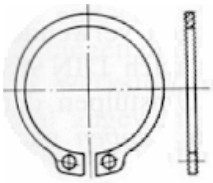	Splint 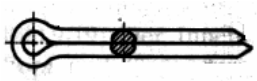	Spring cotter 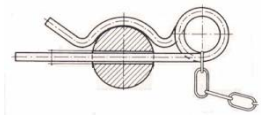

3.1 Selection

Chosen	Statement
1:A	The axle is made out of stainless steel and will be welded on the upper hub. Thus the chosen material is corrosion-resistant with good weldability.
2:A	The shaft has to be corrosions resistant and will be welded to the crosshead. The chosen material is a stainless steel with a good weldability.

3:B	The upper hub is corrosion resistant. Since the upper hub and the axel will be connected by welding, the upper hub should also be from a weldable material. The chosen material fulfills both these requirements and thus a good choice.
4:B	The middle hub needed to be highly machinable because of the holes needed to fit the pivot. It is corrosions-resistant.
5:A	The lower hub needs only to be corrosion resistant. Thus this inexpensive material is sufficient.
6:B	The blade has to be as thin as possible: thus the material should have a high resistance against bending and be stainless. The material chosen for the blade was stainless steel with the highest strength against bending.
7:A	Four blades are usually used at heads up to approximately 25-30m. /9/
8:B	The pivot is of stainless steel and the steel highly machinable. The material satisfies both these properties.
9:B	The bearing was chosen because it should not have any additives which could contaminate the water (oil and grease): it is also inexpensive compared to roller bearings.
10:B	The bearing must be specified to work under water and it fulfills all the stress requirements; the bearing chosen is an inexpensive alternative to the iglidur®H370.
11:B	The lever is supposed to manufacture via milling; so its material must be machinable. Furthermore, it must be corrosions resistance. The chosen material fulfills the mentioned requirements.
12:A	The link must to be corrosion resistance and withstand the occurring forces. The link chosen fulfills both requirements and it is less expensive than other stainless steels.
13:B	See statement 8
14:B	See statement 9

15:B	The material for the crosshead must be stainless steel, have a high machinability and be weldable. The chosen material has a good machinability and conditional weldability which should be sufficient.
16:C	The chosen bolt is to the best for fixing the bolt at the crosshead.
17:A	The chosen material is corrosion resistant and it is able to withstand all the forces which occur at the bolt. Furthermore, it is a common bolt material.
18:C	For maintenance purposes, the runner should be easy to disassemble. This spring cotter is easy to dismantle and it is not always necessary to replace it after each dismantling.

4 CALCULATION OF THE MAIN CHARACTERISTICS

In this section and also in the following sections, only equations and results will be presented. The detailed calculation of this thesis can be found step by step in the Appendix.

The main characteristics are the data on which the design of the runner is based. To calculate, for instance, the forces on the blade or to determine the dimensions of the adaptation mechanism the characteristics of the turbine are needed.

In figure 4.1, a sketch of a Kaplan turbine is given. On this sketch, those heads and points which play a significant roll in this thesis are marked.

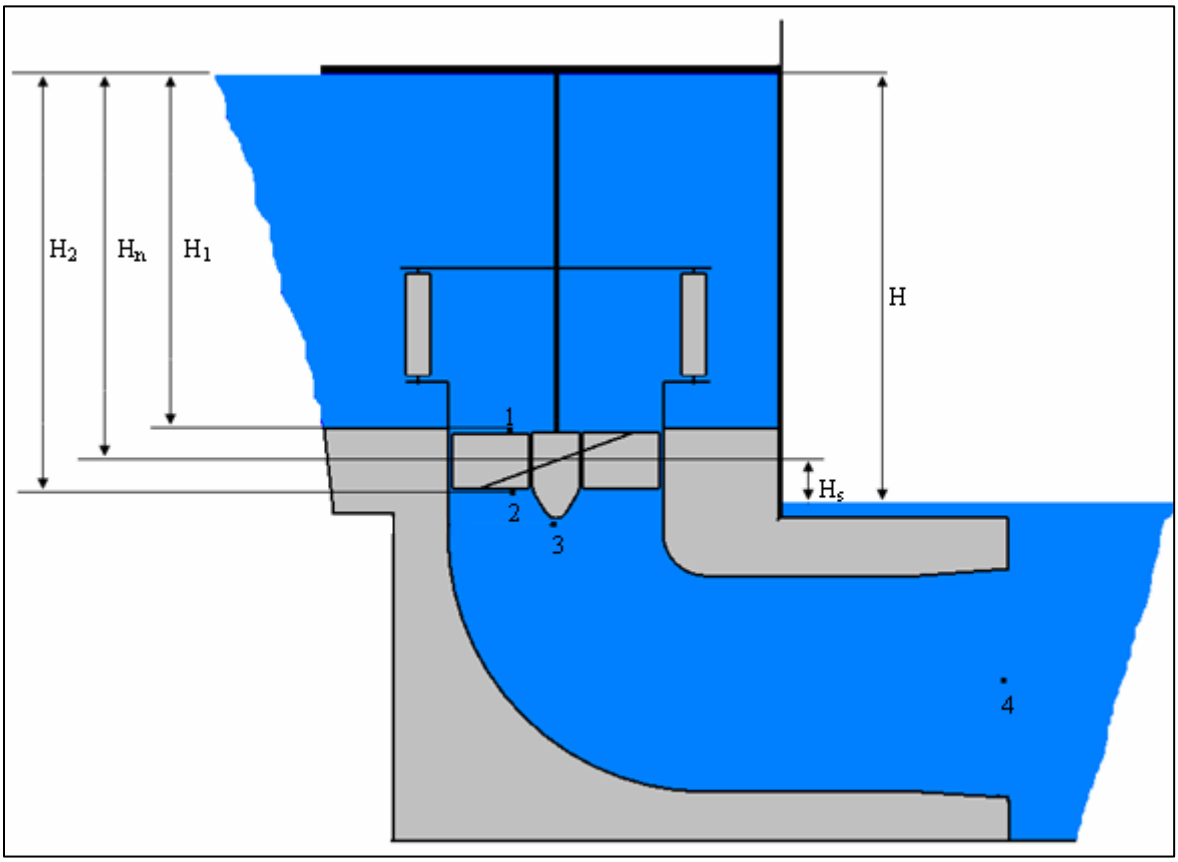

Figure 4.1: Sketch of a Kaplan turbine

4.1 Power

The power of the runner can be calculated with the following equation:

$$P = Q * H * \eta_h * \rho * g \qquad [W] \qquad (4.1)$$

Where:

Q	discharge	[m^3/s]
H	gross head	[m]
η_h	hydraulic efficiency	[-]
ρ	water density	[kg/m^3]
g	acceleration of gravity	[m/s^2]

The efficiency depends on the level of the losses which depend on the construction of the water passage of the turbine. However, the design of the runner is just theoretical. This means that the runner is not designed for a specific plant and the water passage does not exist. Thus, the value of efficiency must be assumed. The site where the experimental rig of the turbine can be built provides a maximum gross head of 3.7m. An efficiency of 0.9 can be assumed for a Kaplan turbine. Also, the discharge arises from the site of the experimental rig. The daily maximum discharge of lake Korpijärvi is approximately $3m^3/s$.

In addition, the following values are known:

$$\rho = 998 kg/m^3$$

$$g = 9.81 m/s^2$$

The outcome of this is a turbine's power of **<u>98kW</u>**. /1/

4.2 Speed of the turbine

4.2.1 Specific speed

The different types of water turbines can be classified by their specific speed. Different definitions of the specific speed exist which can be found in the technical literature. As stated in the "Guide on how to develop a small hydropower plant", the specific speed is a dimensionless parameter and characterizes the hydraulic properties of a turbine in terms of speed and discharge capacity; it is based on similitude rules.

The specific speed is defined as:

$$n_{QE} = \frac{n * \sqrt{Q}}{E^{3/4}} \qquad [-] \qquad (4.2)$$

Where:

E	specific hydraulic energy of machine	[J/kg]
n	rational speed of the turbine	[s^{-1}]

The specific hydraulic energy of machine can be established with the following equation:

$$E = H_n * g \qquad [J/kg] \qquad (4.3)$$

Where:

H_n	net head	[m]

A net head of 3.33m arises from the product of the gross head and the efficiency:

$$H_n = H * \eta_h \qquad [m] \qquad (4.4)$$

Due to statistical studies of schemes, F. Schweiger and J. Gregory established the following correlation between the specific speed and the net head for Kaplan turbines:

$$n_{QE} = \frac{2.294}{H_n^{0.486}} \qquad [-] \qquad (4.5)$$

Since the rational speed is unknown, the specific speed has to be calculated with the formula (4.5). Hence, a resulting specific speed of **1.28** arises. /1/

4.2.2 Rational speed

The rational speed can be calculated by putting equation (4.3) in equation (4.2). The resulting equation has to be re-arranged to the rational speed of the turbine. From this a rational speed of **$10s^{-1}$** follows. This value of the rational speed is optimal because it is synchronous to the generator speed. Thus, the turbine can be directly coupled to it.

Table 4.1: Generator synchronisation speed /1/

Number of poles	50 Hz	60 Hz	Number of poles	50 Hz	60 Hz
2	3000	3600	16	375	450
4	1500	1800	18	333	400
6	1000	1200	20	300	360
8	750	900	22	272	327
10	600	720	24	250	300
12	500	600	26	231	277
14	428	540	28	214	257

In table 4.1 gives the synchronous speeds (in the unit min^{-1}) which the runner should reach to connect it directly to the generator. /1/

4.2.3 Runaway speed

The runaway speed is the maximum speed which the turbine can theoretically attain; it is achieved during a load rejection. Depending on the regulation of the Kaplan turbine, the following guidelines can be used to determine the runaway speed:

Table 4.2: Runaway speed /1/

Turbine type	Runaway speed n_{max}/n
Single regulated Kaplan turbine	2.0 – 2.6
Double regulated Kaplan turbine	2.8 – 3.2

The turbine is supposed to work double regulated. Hence, a maximum runaway speed of **$32s^{-1}$** arises. /1/

4.3 Runner diameter section

The runner diameter D_e can be calculated by the following equation:

$$D_e = 84.5 * (0.79 + 1.602 * n_{QE}) * \frac{\sqrt{H_n}}{60 * n} \quad [m] \qquad (4.6)$$

All the values which are needed to calculate the runner diameter were established in Section 4.2. By using these values, a runner diameter of **0.73m** results from the equation (4.6). /1/

4.4 Hub diameter

The hub diameter D_i can be calculated with the following equation:

$$D_i = \left(0.25 + \frac{0.0951}{n_{QE}}\right) * D_e \quad [m] \qquad (4.7)$$

A hub diameter of **0.24m** arises from the equation (4.7). /1/

4.5 Blade characteristics of some different heads and discharges

Table 4.2: Characteristics under different circumstances

D_e [m]	0.71	0.75	0.78	0.81	0.84	0.87	0.90	0.93	0.95	0.98	1.01	
D_i [m]	0.22	0.23	0.24	0.25	0.26	0.27	0.28	0.29	0.29	0.30	0.31	H_n
P [kW]	50	55	60	65	70	75	80	85	90	95	100	
Q [m^3/s]	2.55	2.81	3.06	3.32	3.57	3.83	4.09	4.34	4.60	4.85	5.11	2
n [s^{-1}]	9.56	9.11	8.72	8.38	8.08	7.80	7.55	7.33	7.12	6.93	6.76	
n_{max} [s^{-1}]	28.67	27.33	26.17	25.14	24.23	23.41	22.66	21.99	21.37	20.80	20.27	
P [kW]	66	73	80	86	93	99	106	113	119	126	133	
Q [m^3/s]	2.71	2.98	3.25	3.52	3.79	4.06	4.34	4.61	4.88	5.15	5.42	2.5
n [s^{-1}]	9.84	9.38	8.98	8.63	8.32	8.03	7.78	7.55	7.33	7.14	6.96	
n_{max} [s^{-1}]	29.52	28.14	26.95	25.89	24.95	24.10	23.34	22.64	22.00	21.41	20.87	
P [kW]	83	92	100	108	117	125	133	142	150	158	167	
Q [m^3/s]	2.83	3.12	3.40	3.68	3.97	4.25	4.54	4.82	5.10	5.39	5.67	3
n [s^{-1}]	10.09	9.62	9.21	8.85	8.53	8.24	7.98	7.74	7.52	7.32	7.14	
n_{max} [s^{-1}]	30.28	28.87	27.64	26.56	25.59	24.73	23.94	23.23	22.57	21.97	21.41	
P [kW]	101	111	121	131	141	151	161	171	181	191	201	
Q [m^3/s]	2.94	3.23	3.53	3.82	4.11	4.41	4.70	4.99	5.29	5.58	5.88	3.5
n [s^{-1}]	10.33	9.85	9.43	9.06	8.73	8.43	8.16	7.92	7.70	7.49	7.30	
n_{max} [s^{-1}]	30.98	29.54	28.28	27.17	26.18	25.30	24.49	23.76	23.09	22.48	21.91	
P [kW]	118	130	142	154	166	178	190	201	213	225	237	
Q [m^3/s]	3.02	3.33	3.63	3.93	4.23	4.54	4.84	5.14	5.44	5.75	6.05	4
n [s^{-1}]	10.54	10.05	9.62	9.25	8.91	8.61	8.33	8.09	7.86	7.65	7.45	
n_{max} [s^{-1}]	31.63	30.16	28.87	27.74	26.73	25.82	25.00	24.26	23.57	22.95	22.36	
P [kW]	137	150	164	177	191	205	218	232	246	259	273	
Q [m^3/s]	3.10	3.41	3.72	4.03	4.34	4.65	4.96	5.27	5.58	5.89	6.20	4.5
n [s^{-1}]	10.74	10.24	9.81	9.42	9.08	8.77	8.49	8.24	8.01	7.80	7.60	
n_{max} [s^{-1}]	32.23	30.73	29.43	28.27	27.24	26.32	25.48	24.72	24.03	23.39	22.79	
P [kW]	155	170	186	201	217	232	248	263	279	294	310	
Q [m^3/s]	3.16	3.48	3.80	4.11	4.43	4.74	5.06	5.38	5.69	6.01	6.33	5
n [s^{-1}]	10.94	10.43	9.98	9.59	9.24	8.93	8.64	8.39	8.15	7.93	7.73	
n_{max} [s^{-1}]	32.81	31.28	29.95	28.77	27.73	26.79	25.93	25.16	24.45	23.80	23.20	
P [kW]	173	191	208	225	243	260	277	295	312	329	347	
Q [m^3/s]	3.22	3.54	3.86	4.18	4.51	4.83	5.15	5.47	5.79	6.12	6.44	5.5
n [s^{-1}]	11.12	10.60	10.15	9.75	9.39	9.08	8.79	8.53	8.29	8.06	7.86	
n_{max} [s^{-1}]	33.35	31.80	30.44	29.25	28.18	27.23	26.36	25.58	24.86	24.19	23.58	
P [kW]	192	211	230	250	269	288	307	326	346	365	384	
Q [m^3/s]	3.27	3.60	3.92	4.25	4.58	4.90	5.23	5.56	5.88	6.21	6.54	6
n [s^{-1}]	11.29	10.76	10.30	9.90	9.54	9.22	8.92	8.66	8.41	8.19	7.98	
n_{max} [s^{-1}]	33.86	32.29	30.91	29.70	28.62	27.65	26.77	25.97	25.24	24.57	23.95	

Table 4.2 was completed by using the above equations from this chapter. This table allows the reader to get an overview of the main characteristics of a Kaplan turbine under different head and discharge circumstances.

5 CAVITATION

In the fact that the vapor pressure of a liquid exceeds the hydrodynamic pressure of the liquid flow, a small part of the water changes into the vapor phase; this causes the formation of steam bubbles. The bubbles join the water flow and the more the water changes into the vapor phase the bigger the bubbles get. Finally, the water carries the bubbles to a spot where the liquid pressure increases again. The steam bubbles are not able to withstand the higher pressure and they condense in an imploding manner. This implosion releases very fast micro streams and pressure peaks of up to some hundred MPa occur.

Cavitation occurs especially at spots where the pressure is low. In the case of a Kaplan turbine, the inlet of the runner is quite susceptible to it. At parts with a high water flow velocity cavitation might also arise.

Cavitation should be avoided because it has several negative effects on the turbine. First it decreases the efficiency and causes crackling noises. However, the main problem is the wear or rather the damage of the turbine's parts such as the blades. Cavitation does not just destroy the parts, chemical properties are also lost; for example, the material is not able to recover its protective layer which is tutelary against corrosion.

The suction head H_s is the head where the turbine is installed; if the suction head is positive, the turbine is located above the trail water; if it is negative, the turbine is located under the trail water. To avoid cavitation, the range of the suction head is limited. The maximum allowed suction head can be calculated using the following equation:

$$H_s = \frac{p_{atm} - p_v}{\rho * g} + \frac{c_4^2}{2 * g} - \sigma * H_n \qquad [m] \qquad (5.1)$$

Where:

p_{atm}	atmospheric pressure	[Pa]
p_v	water vapor pressure	[Pa]
ρ	water density	[kg/m^3]
g	acceleration of gravity	[m/s^2]

c_4	outlet average velocity	[m/s]
σ	cavitation coefficient	[-]
H_n	net head	[m]

The cavitation coefficient, calculated by modeling tests, is usually given by the turbine manufacture. However, statistical studies related the cavitation coefficient to the specific speed. Thus the σ for the Kaplan turbine can also be established with the following equation:

$$\sigma = 1.5241 * n_{QE}^{1.46} + \frac{c_4^2}{2 * g * H_n} \quad [-] \qquad (5.2)$$

Where:

n_{QE}	specific speed	[-]

The outlet velocity c_4 can be established via the discharge and the diameter at the outlet of the water passage. Since the dimensions of the water passage are not known, the outlet velocity has to be assumed. An outlet velocity of 2m/s is chosen. Using this velocity a diameter of 1.38m would arise at the outlet of the water passage - a quite realistic value.

The specific speed is known from Section 4.2.1 and has a value of $1.28s^{-1}$. Thus a cavitation coefficient of 2.2 arises.

The vapor pressure depends on the water temperature. The water temperature of rivers in Finland can vary from 0°C in the winter to a maximum of 24°C in the summer. Since the vapor pressure increases with higher temperatures the vapor pressure at 24°C is relevant for the cavitation calculation. At a water temperature of 24°C, the vapor pressure is 2985.7 Pa (see Table 14.1). Since the site, where the experimental rig can be build, is just 100m above the sea level, an atmospheric pressure of 101300 Pa can be used.

Hence, a maximum suction head of **2.9m** results from equation (5.1). As long the chosen suction head is below the established suction head no cavitation occurs. A suction head of **0.45m** is chosen. /1, 9, 10/

6 DESIGN OF THE BLADE

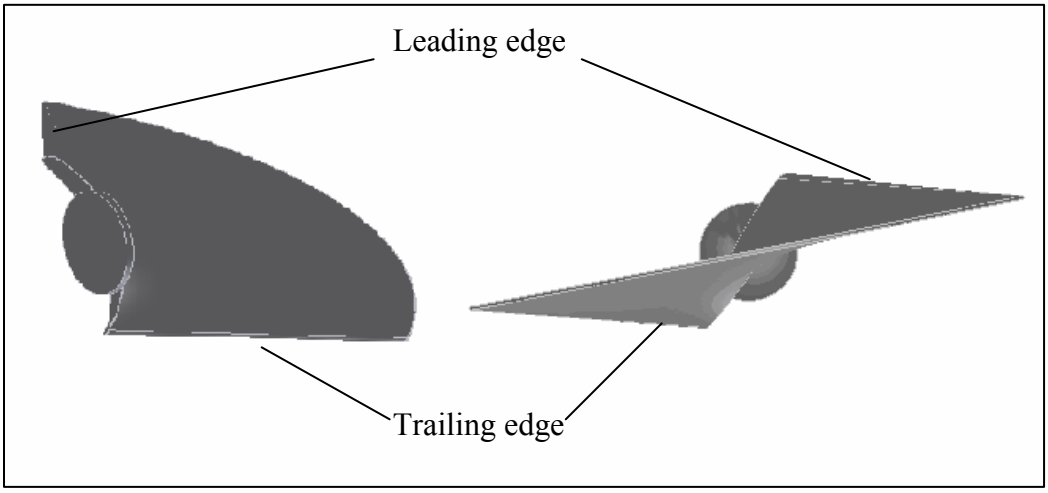

Figure6.1: Two different views of a blade

The design of the blade does not just depend on the stress analysis; several other factors play significant roles as well. The leading edge is thicker than the trailing edge for a streamlined flow. Furthermore, the blade should to be as thin as possible to improve the cavitation characteristics; it is thicker near the flange becoming thinner and thinner towards the tip. In addition, the blade has to be distorted on the basis of the tangential velocity. The “Tragflügeltheorie” is also an important factor in defining the shape of the profile and the distortion of the blade. /9, 11/

6.1 Distortion of the blade under ideal circumstances

The velocity triangles, which occur on the blade, play a significant role in determining its distortion. The velocities at the velocity triangle are shown in Figure 6.2.

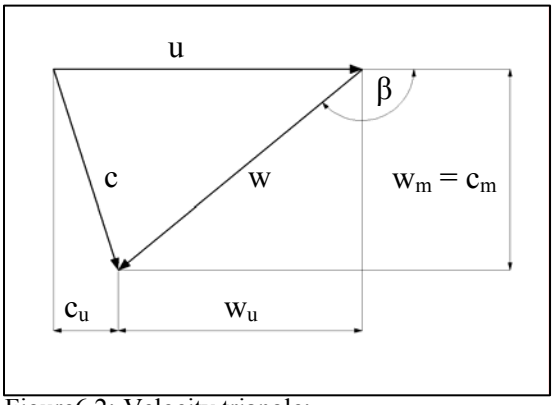

u	tangential velocity	[m/s]
c	absolute velocity	[m/s]
w	relative velocity	[m/s]

Figure6.2: Velocity triangle:

When a cylindrical cut is set at the runner and the cut is developed into a drawing pane, a grating like that shown in Figure 6.3 occurs. Velocity triangle 1 occurs directly before the grating and the velocity triangle 2 occurs directly after the grating. The meridian components w_{1m} and w_{2m} are equal. The medial relative velocity can be determined via the average of w_1 and w_2 and its direction is specified due to the angle β_∞. Value t represents the grating partition and value l denotes the chord.

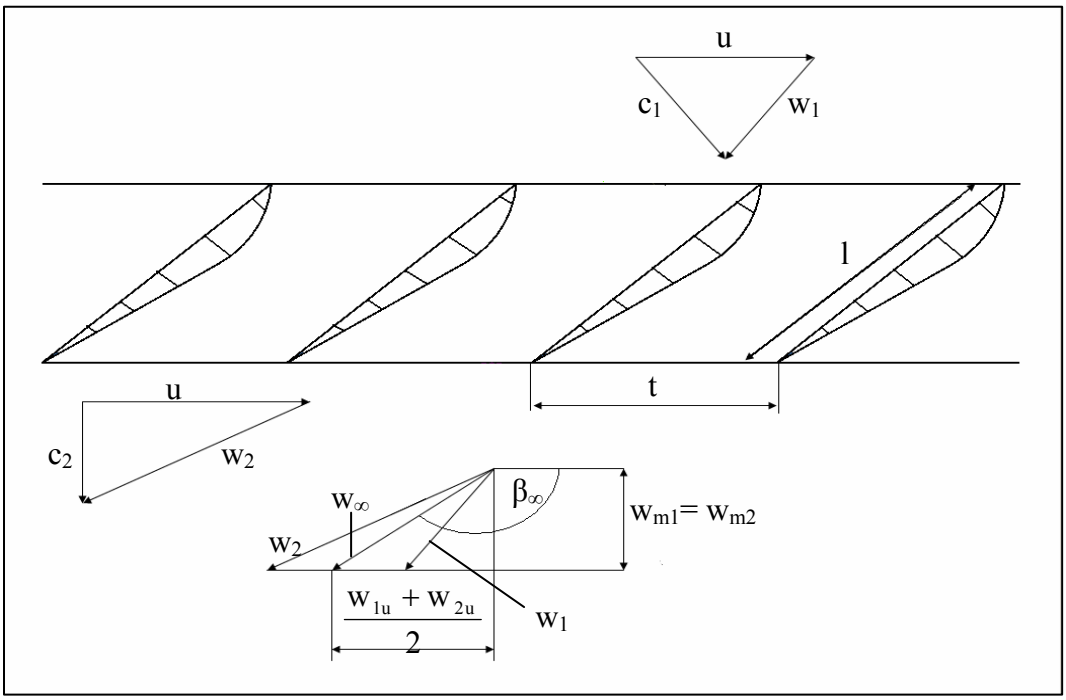

Figure 6.3: Grating /9/

To define the distortion of the blade, the velocity triangles of six different radiuses of the blade are determined. The angle β_∞ of each radius gives conclusions on the distortion of the blade.

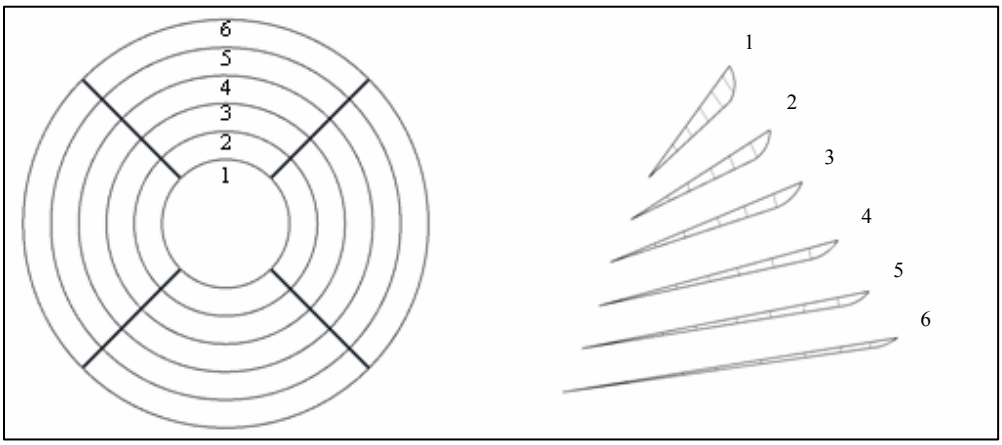

Figure6.4: Cylindrical cuts of the blade /9/

Table 6.1: Velocities and angles of the occurring velocity triangles

d	0.73	0,63	0,54	0,43	0,33	0,24
u	22.93	19.79	17.03	13.51	10.37	7.54
c_{u1}	1.39	1.62	1.88	2.37	3.08	4.24
c_{u2}	1.45	1.69	1.96	2.47	3.22	4.42
w_{u1}	-21.54	-18.18	-15.15	-11.14	-7.28	-3.30
w_{u2}	-21.48	-18.11	-15.07	-11.04	-7.15	-3.12
$w_{u\infty}$	-21.51	-18.14	-15.11	-11.09	-7.22	-3.21
w_m	8.00	8.00	8.00	8.00	8.00	8.00
w_1	22.98	19.86	17.13	13.72	10.82	8.65
w_2	22.92	19.80	17.06	13.63	10.73	8.59
w_∞	22.95	19.83	17.10	13.67	10.77	8.62
β_∞	160	156	152	144	132	112
$(180-\beta_\infty)$	20	24	28	36	48	68

Table 6.1 shows the velocities and the significant angles of the velocity triangles for each of the radiuses. The equations, which were used to establish the table, are as follows:

$$u = \pi * n * d \qquad [m/s] \qquad (6.1)$$

$$c_u = \frac{H_n * g}{u} \qquad [m/s] \qquad (6.2)$$

$$w_u = c_u - u \qquad [m/s] \qquad (6.3)$$

$$w_m = \frac{Q}{A} \qquad [m/s] \qquad (6.4)$$

$$w = \sqrt{w_u^2 + w_m^2} \qquad [m/s] \qquad (6.5)$$

$$\beta_\infty = \arccos\frac{w_u}{w} \qquad [m/s] \qquad (6.6)$$

The angles, however, are not 100% accurate. To get the exact angles of the distortion the “Tragflügletheorie” has to be considered. /9/

6.2 The "Tragflügeltheorie"

The "Tragflügeltheorie" was developed by Ludwig Prandtl. According to the "Tragflügeltheorie" a lifting force F_l applies at the blades of the runner due to the configuration of the parallel stream and the circulation stream, which occur at the blade. Hence, values such as the lift coefficient and the attack angel δ also play a significant role in the design of the blade. These coefficients can be determined via model tests. In the book "Vesiturbiinit", the results of such model tests are shown. Using these results the profile, the chord and the exact distortion of the blade can be determined. /9, 12/

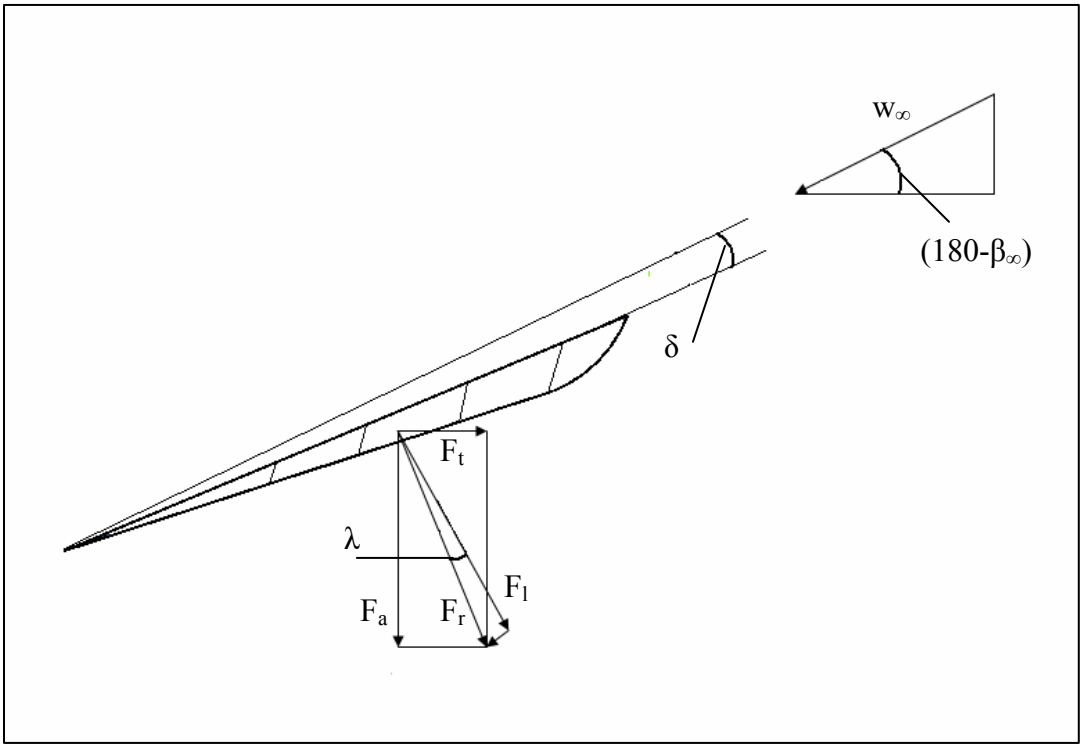

Figure 6.5: "Tragflügeltheorie" /9/

6.2.1 Procedure

For a better understanding, this section examines the precise procedure of the determining the blade's main characteristics.

Step 1:

With the following equation, the lifting coefficients for each radius are determined:

$$\zeta_a = \frac{w_2^2 - w_\infty^2 + 2*g*\left(p_{atm} - H_s - p_{min} - \eta_s * \frac{c_3^2 - c_4^2}{2*g}\right)}{K*w_\infty^2} \quad [-] \qquad (6.7)$$

Where:

w_2	relative velocity after the grating	[m/s]
w_∞	medial relative velocity	[m/s]
p_{atm}	atmospheric pressure	[m]
H_s	suction head	[m]
p_{min}	minimal water pressure	[m]
η_s	efficiency of the energy change	[-]
c_3	velocity after the runner	[m/s]
c_4	outlet velocity	[m/s]
K	profile characteristic number	

Almost all the values of the equation (6.7) are known either from previous section or they can easily be established. The other values have to be assumed but can be found in "Vesiturbiinit" where a range for these values is given. The ranges of these values are as follows:

p_{min} = 2÷2.5

η_s = 0.88÷0.91

K = 2.6÷3

Step 2:

When the lifting coefficient is known, the ratio l/t can be established as follows:

$$\frac{l}{t} = \frac{g*\eta_h*H}{w_\infty^2} * \frac{c_m}{u} * \frac{\cos\lambda}{\sin(180 - \beta_\infty - \lambda)} * \frac{1}{\zeta_a} \quad [-] \qquad (6.8)$$

Where:

g	acceleration of gravity	[m/s^2]
η_h	hydraulic efficiency	[-]
H	gross head	[m]
c_m	meridian velocity	[m/s^2]
λ	angle of slip	[°]
u	tangential velocity	[m/s^2]
$(180-\beta_\infty)$	inflow angle	[°]

In equation (6.8), the angle of slip λ has to be assumed; the range for the assumption is as follows:

$\lambda = 2.5° \div 3°$

Using this assumption, an approximate value of the ratio l/t can be established.

Step 3:

During Step 3, the reciprocal value of the ratio l/t has to be established. Via the reciprocal value, the ratio of the lifting coefficients ζ_a/ζ_A can be read off in the following chart. Using this ratio the lifting coefficient ζ_A can be established.

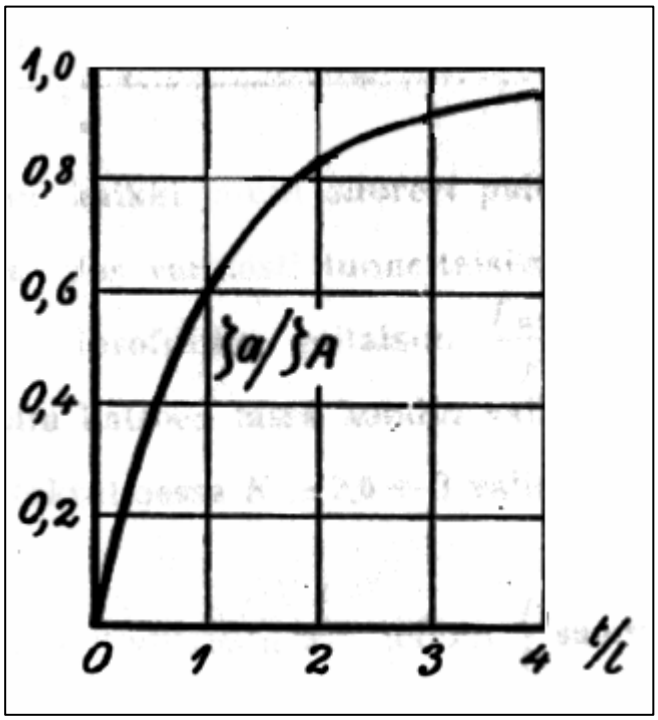

Figure 6.6: Ratio of ζ_a/ζ_A and t/l /12/

Step 4:

The chart in the following figure gives information on the drag coefficient ζ_W of the different profiles.

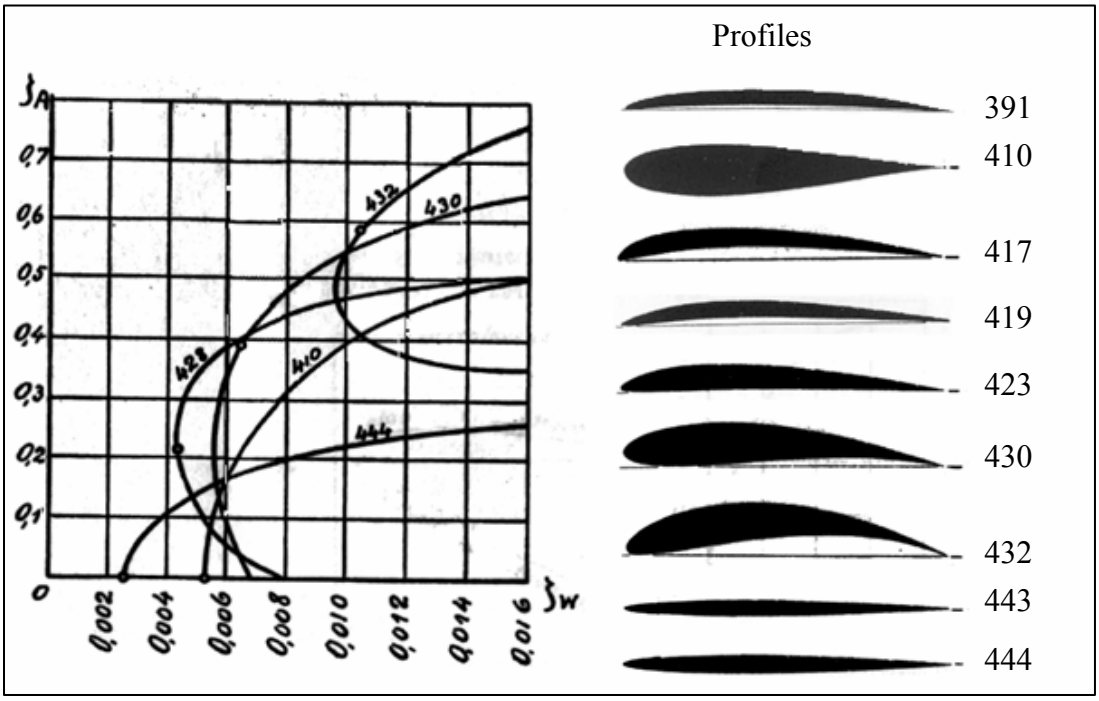

Figure 6.7: Ratio of ζ_A and ζ_A for different profils /12/

Each of the curves represents one of the profiles which are listed beside the chart. First, it has to be decided which of the profiles should be chosen; following this, the drag coefficient of this profile can be determined by using the chart.

Step 5:

With the following equation, the angle of slip can be calculated:

$$\lambda = \arctan \frac{\zeta_W}{\zeta_A} \qquad [°] \qquad (6.9)$$

It has to be checked whether the assumed angle of slip and the calculated angle of slip are similar or not. If the difference is too great, the procedure of the calculation has to be repeated using the angle of slip calculated in equation (6.9). Steps 2 to 5 must be repeated until the angles of slip do not change anymore; however, it is necessary to always choose the same profile in Step 4. When the angle λ is fixed, it can be assumed that the last calculated values of Steps 2 to 5 are accurate enough. Thus the ratio l/t and the profile are determined.

Step 6:

The angle of attack δ of the chosen profile can now be established using the following figure.

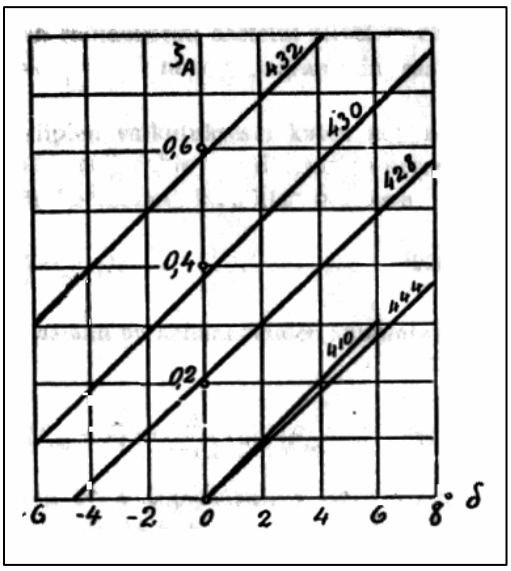

Figure6.8: Ratio of ζ_A and δ for different profils /12/

The above Steps have to be followed for the same diameters as in Section 6.1. The listed values in Table 6.2 arise using the profile 430:

Table6.2: Characteristics of the blade

d	0.73	0.63	0.54	0.43	0.33	0.24
l/t	0.95	0.90	0.87	0.85	0.85	0.94
ζ_A	0.12	0.16	0.21	0.32	0.52	0.87
ζ_W	0.0062	0.0063	0.0065	0.006	0.009	0.04
λ	2.9	2.3	1.8	1.1	1.0	2.6
δ	-5.40	-4.60	-3.30	-1.20	3.00	9.60

At a diameter of 0.24m, the value of the lift coefficient ζ_A is so high that it is not indicated in the Figures 6.7 and 6.8. Thus, the further development of the curves in these charts had to be assumed in order to obtain the drag coefficient and the angle of slip.

To get the accurate angle of distortion, the angle δ has to be subtracted from the angle ($180-\beta_\infty$). The outcome of this is shown in Table 8.3.

Table6.3: Angle of the blade distortion

d	0.73	0.63	0.54	0.43	0.33	0.24
($180-\beta_\infty-\delta$)	26	28	31	37	45	59

/12/

7 CALCULATION OF THE FORCES

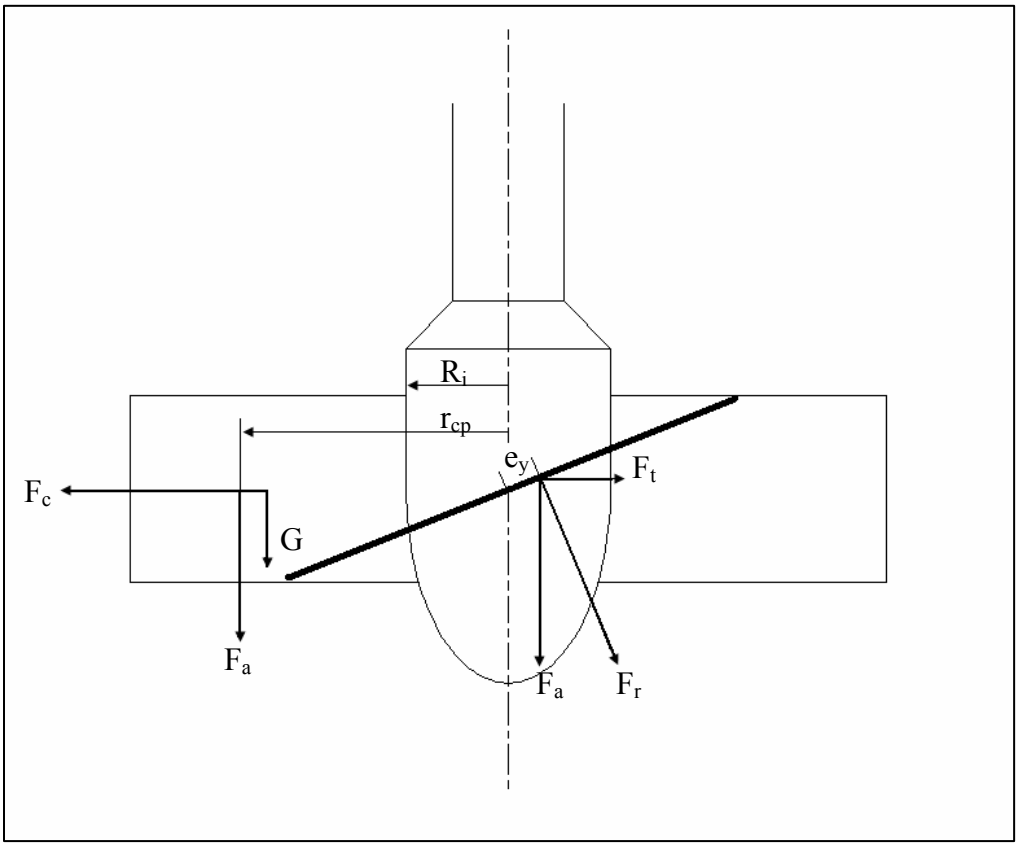

Figure 7.1: Occurring forces upon the blade /11/

7.1 Tangential force

The tangential force is defined as:

$$F_t = \frac{P}{2 * \pi * n * z * r_{cp}} \qquad [N] \qquad (7.1)$$

Where:

P	power	[W]
n	rational speed	[s^{-1}]
z	number of blades	[-]
r_{cp}	radius of the center of pressure (cp)	[m]

The radius r_{cp} can be calculated using the following equation:

$$r_{cp} = \sqrt{\frac{R_e^2 + R_i^2}{2}} \qquad [mm] \qquad (7.2)$$

The outcome of this is a radius of 0.272m and from this follows a tangential force of **1,434N**. /11/

7.2 Axial force

The axial force can be established in two ways. The first possibility is to calculate F_a via the water pressure and the second possibility is to calculate it via the tangential force and the distortion of the blade. Understandably, the results are supposed to be the same. Using both ways to calculate the axial force is a good method of ensuring that the design of the blade fits.

1. Calculation via water pressure:

Assuming that the water is dormant and the blade is a plate, the force F_a, which is caused by the water, can be approximately calculated with the following equation:

$$F_a = g * \rho * H_n * A_b \quad [N] \qquad (7.3)$$

Where:

g	acceleration of gravity	$[m/s^2]$
ρ	water density	$[kg/m^3]$
H_n	net head	[m]
A_b	area of the blade	[m]

To calculate the area A_b, a further assumption must be made. Assuming that the ratio of l/t (see chapter 6.2.1) of the blade is constant, a simplified blade area as shown in Figure 7.2 arises.

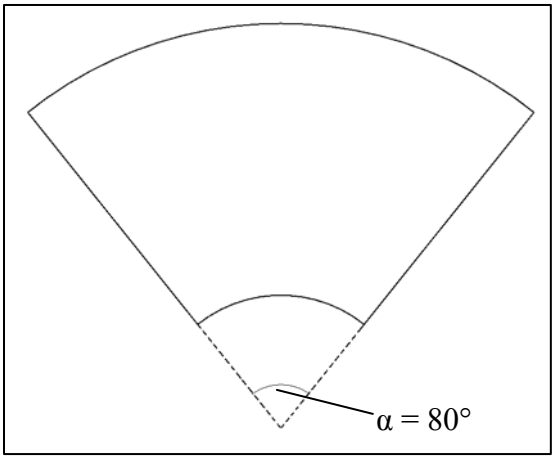

Figure 7.2: Sketch of the simplified blade area

Hence, an A_b of 0.083m^2 has been established using the following equation:

$$A_b = \frac{\pi * \alpha * (R_e^2 - R_i^2)}{360^\circ} \qquad [m^2] \qquad (7.4)$$

Thus a force of **2,706N** results from the equation (7.3). /13/

2. Calculation via the tangential force and blade distortion:

The blade distortion ($180-\beta_\infty-\delta$) at the radius r has a value of 31°. The force F_a can be established using the following equation:

$$F_a = \frac{F_t}{\tan(180 - \beta_\infty - \delta)} \qquad [N] \qquad (7.5)$$

The outcome from equation (7.5) is an axial force of **2,387N**.

The results do not match 100%; however, that can be based on the assumption of the dormant water and the simplification of the blade. One can thus say that the blade characteristics which were established in Chapter 6 are accurate. In the following calculations, the higher value of **2,706N** will be used. /9/

7.3 Resulting force

The force F_r can be established by using following equation:

$$F_r = \sqrt{F_t^2 + F_a^2} \qquad [N] \qquad (7.6)$$

A resulting force of **3,062N** results from the equation (7.6). /11/

7.4 Hydraulic moment

The force F_r causes a turning moment which tends to turn the blade about its axis of rotation - the 'hydraulic moment'. The value of the moment changes due to the adjustment of the blade. The main forces that the adaptation mechanism has to withstand are caused by this moment. Hence, the moment has a high influence on the design of the adaptation mechanism and can be calculated with the following equation:

$$M_h = F_r * e_y \qquad [Nmm] \qquad (7.7)$$

Where:

e_y distance from the cp to the rotation axis of the blade [mm]

The center of pressure cp is not a fixed point; it changes its position depending on the adjustment of the blade. Thus the arm e_y also changes its value. Under simplified circumstances as those in Section 7.2, the arm e_y can be calculated, although the evaluation is not 100% accurate. The exactly center of pressure and consequently the exactly length of the arm e_y can only be precisely established by using model tests. However, to get an idea of the length of e_y the calculation under simplified circumstances is sufficient.

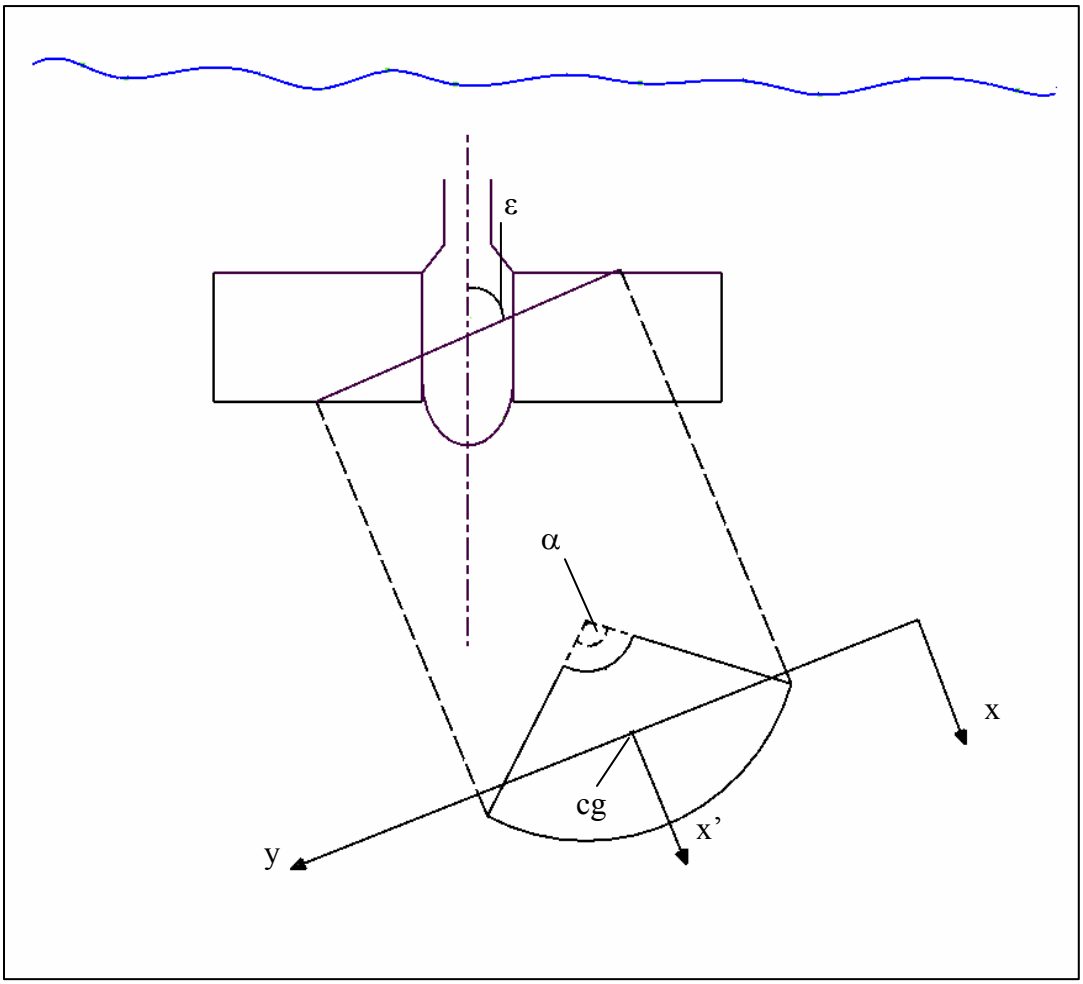

Figure 7.3: Turbine with projected view of the blade

The distance between the center of gravity cg and respectively the rotation axis of the blade and the center of pressure in y-direction can be calculated with the following equation:

$$e_y = \frac{I_s}{y_s * A} \qquad [mm] \qquad (7.8)$$

Where:

I_s	moment of inertia of the area A related to the x'-axis which runs parallel to the x-axis over the center of gravity	[mm^4]
y_s	the distance between the x-axis and the center of gravity	[mm]
A_b	area of the blade	[mm^2]

The moment of inertia is defined as:

$$I_s = \frac{R_e^4 - R_i^4}{4} * \left(\frac{\hat{\alpha}}{2} - \sin\frac{\alpha}{2} * \cos\frac{\alpha}{2} \right) \qquad [mm^4] \qquad (7.9)$$

With a blade-radius R_e of 365mm, a hub-radius R_i of 120mm and an angle α of 80° ($\hat{\alpha}$ = 1.396) a moment of inertia of 901,718,555mm^4 results.

The distance y_s can be calculated as follows:

$$y_s = \frac{F_a}{g * \rho * A_b * \cos\varepsilon} \qquad [m] \qquad (7.10)$$

Where:

F_a	force of the water on the plate	[N]
g	acceleration of gravity	[m/s^2]
ρ	water density	[kg/m^3]
A_b	area of the plate	[m^2]
ε	angle of the adjustment of the blade	[°]

Angle ε changes with the adjustment of the blade. The smaller the angle the bigger is e_y. The smallest possible angle of 20° was chosen. Hence, a y_s of 3.5m results.

All the necessary values are now known to calculate e_y - a value of **3.1mm** results from the equation (7.8). /13/

Using the results from equation (7.8) and (7.6) in equation (7.7) a maximum turning moment of **9,422Nmm** results. /11/

7.5 Centrifugal force

The blade, the blade flange, the pivot, the lever and the link of the runner cause the centrifugal force, which is defined as:

$$F_c = M_G * R_{cg} * \omega^2 \qquad [N] \qquad (7.11)$$

Where:

M_G	total weight of the five parts	[kg]
R_{cg}	radius to the center of gravity	[mm]
ω	angular velocity	[s^{-1}]

The total weight of the five parts results out of the sum of the weight of each part:

$$M_G = \sum G_i \qquad [kg] \qquad (7.12)$$

Where:

G_i	weight of a single part	[kg]

The radius to the center of gravity can be calculated with the following equation:

$$R_{cg} = \frac{\sum G_i * R_i}{\sum G_i} \qquad [mm] \qquad (7.13)$$

Where:

R_i	radius to the center of gravity of a single part	[mm]

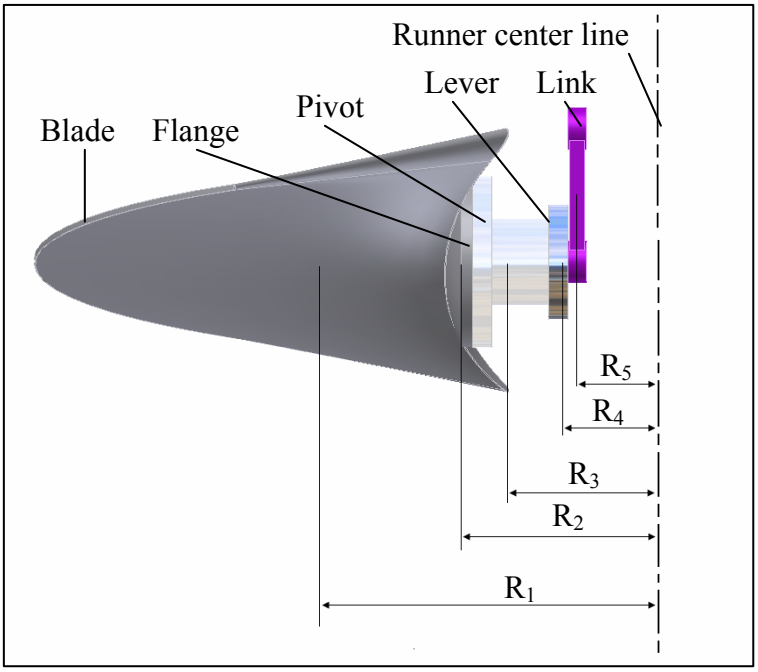

Figure 7.4: Radiuses to the center of gravity of each part

The angular of velocity can be calculated with the following equation:

$$\omega = 2 * \pi * n_{max} \qquad [s^{-1}] \qquad (7.14)$$

Where:

n_{max} runaway speed $[s^{-1}]$

Table 7.1: Weight and radius to the center of gravity

Part	G_i [kg]	R [mm]	G*R [kgmm]
1. Blade	5.6	272	1523
2. Blade flange	0.55	110.6	61
3. Pivot	1.15	90	103.5
4. Lever	0.27	55	14.85
5. Link	0.08	45	3.6
Total	7.65		1,706

A radius to the center of gravity R_{cg} of 223mm as the case may be of 0.223m results. To calculate the angular velocity, the runaway speed is needed. In Section 4.2.3, a maximum runaway speed of $32s^{-1}$ has been determined. Thus an angular velocity of $201s^{-1}$ results from equation (7.14). The outcome of this is a centrifugal force of **68,922N**. /11/

7.6 Weight of the blade

The weight of the blade can be calculated by using the following equation:

$$F_B = G_B * g \qquad [N] \qquad (7.15)$$

A weight of **55N** results from equation (7.15). /11/

8 CRITICAL SPEED

The critical speed is that where the runner has its natural frequency. When the runner operates at or close to the critical speed, a high vibration occurs which may damage the runner.

To assure that the rational speed is not equal or close to the critical speed, the critical speed can be determined as follows:

$$n_c = \frac{1}{2*\pi} * \sqrt{\frac{c_q}{G}} \qquad [s^{-1}] \qquad (8.1)$$

Where:

c_q	spring constant for elastic lateral oscillation	[N/m]
G	total weightiness of the runner	[kg]

The total weight of the runner results from the sum of the weight of the single parts which are listed in the following table:

Table 7.1: Weight of the runner parts

Part	G_i [kg]
Blade	4*5.6
Blade flange	4*0.55
Pivot	4*1.15
Lever	4*0.27
Link	4*0.08
Upper hub	1.8
Middle hub	17
Lower hub	4.8
Total	54.2

The runner of a turbine is overhung-mounted; thus the spring constant for elastic lateral oscillation is defined as:

$$c_q = \frac{3*E*I}{l^3} \qquad [N/mm] \qquad (8.2)$$

Where:

E	elastic modulus	[N/mm^2]
I	axial moment of inertia	[mm^4]
l	length of the axle to the bearing	[mm]

The material which was chosen for the axle has an elastic modulus of 220,000N/mm^2.

The axial moment of inertia can be established as follows:

$$I = \frac{\pi}{64} * (D^4 - d^4) \qquad [mm^4] \qquad (8.3)$$

Where:

D	outer diameter of the axle	[mm]
d	interior diameter of the axle	[mm]

Value D is equal to 168.3mm and value d equal of 159.3mm. Hence, an axial moment of inertia of 7,772,160mm^4 results. The axel is supposed to be borne at a length of 200mm. The outcome of this is a spring constant for an elastic lateral oscillation of 6,41,203N/mm.

A critical speed of **17.3s^{-1}** results from equation (8.1) which is 7.3s^{-1} higher than the rational speed. Thus the difference between rational speed and the critical speed is big enough. In the case of a load rejection, the speed reaches its maximum of approximately 32s^{-1} (see Section 4.2.3). However, a load rejection only lasts a short time and as the speed passing through the critical field rather quick there is no danger of damage. /13/

9 STRESS ANALYSES

The moment M_h which was calculated in Section 7.4 is one of the main characteristics on which the stress analysis is based. Since it was established under simplified circumstances, it might be that it is different under real circumstances and a bigger turning moment occurs. Thus a safety factor of 10 has been chosen to be sure that the parts of the runner can withstand the forces which might occur. Hence, a turning moment of **94,920Nmm** will be utilized in the stress analysis. Furthermore, it will be assumed that the parts are stressed statically. The stress of the parts changes with the head and the discharge. These changes take place rather slowly, though. Thus the assumption of statically stress is rather convenient than dynamically stress.

When a load rejection occurs, the forces at the blade suddenly decrease and after the load rejection suddenly increase again. This causes an impact on the runner. Thus an application coefficient K_A of 1.25 is utilized to consider the impulsive stress.

The strength factors of the material of the parts can be read off Table 14.2 in the Appendix.

9.1 Axle

The maximum tensional stress which the axle can withstand is **125N/mm²**.

The present tensional stress can be calculated as follows:

$$\tau_t = \frac{K_A * M_t}{W_t} \qquad [N/mm^2] \quad (9.1)$$

Where:

M_t	turning moment	[Nmm]
W_t	polar section modulus	[mm³]

The turning moment M_t is the moment caused by the tangential forces and it can be establish using the following equation:

$$M_t = K_A * 4 * r_{cp} * F_t \qquad [Nmm] \quad (9.2)$$

The tangential force has a value of 1,434N and the r_{cp} has a value of 272mm. Thus a turning moment of 1,560,192Nmm results from equation (9.2).

The polar section modulus is defined as:

$$W_t = \frac{\pi}{16} * \frac{D^4 - d^4}{D} \qquad [mm^3] \quad (9.3)$$

Where:

D	outer diameter of the axle	[mm]
d	interior diameter of the axle	[mm]

The outer diameter is 168.3mm and the interior diameter is 159.3mm; a polar section modulus of 184,722mm³ results.

The outcome of this is a present tensional stress of **<u>10.6N/mm²</u>** which is significantly smaller then the permissible tensional stress. /13, 14/

9.2 Blade

At the stress analysis, the blade is treated as a flat plate. Furthermore, the blade is not considered over its whole width only over the width h, which has a value of 60mm. This is because the main forces are at work in this area. Accordingly, one can say that the stress analysis of this part represents the whole blade.

9.2.1 Bending

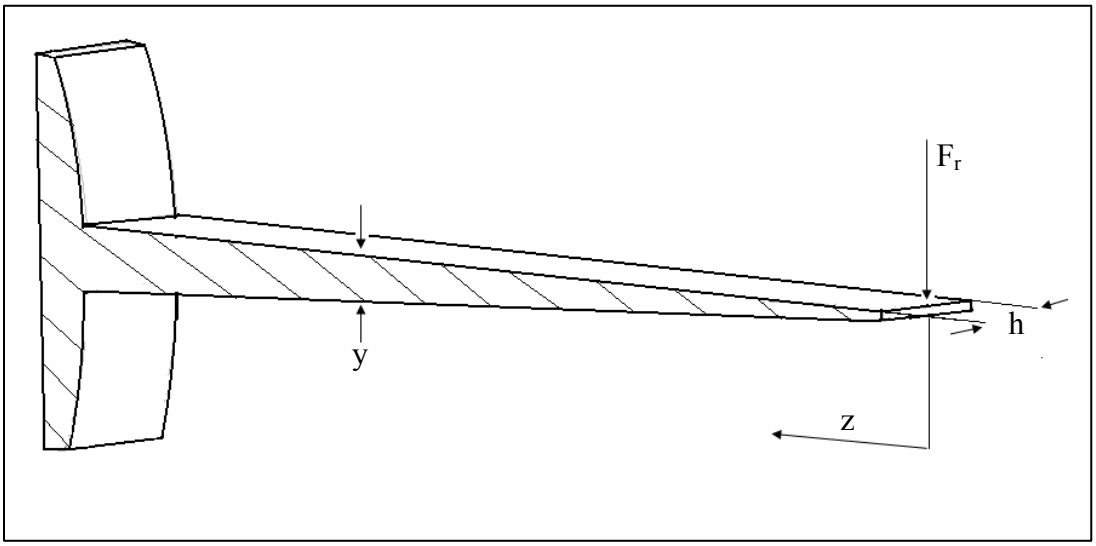

Figure 9.1: Sketch of the significant cutaway of the blade

With the assumption that force F_r applies at the tip of the blade instead of the center of pressure, equation (9.4) can be used to calculate the minimum required thickness y at every radius. Since the bending moment at the assumption is even higher than in reality, a safety factor of approximately 1.6 is included. Due to this fact, utilizing the application coefficient K_A is not necessary. Furthermore, as the weight of the blade is relatively small compared with the force F_r, it can be neglected.

Equation to calculate the minimum required thickness of the blade:

$$y = \sqrt{\frac{6 * F_r * z}{h * \sigma_{bpermissible}}} \qquad [mm] \qquad (9.4)$$

The permissible bending stress of the blade is **450N/mm²**.

Using equation (9.4), the following table of the blade thickness is created; whereas the thickness at 0.73m was set with a value of 2mm without using the equation:

Table 9.1: Blade thickness at different radiuses

r	120	165	215	265	315	365
y	13	12	10	8	6	2

According, to the source /10/ the in the table, the shown values should be safe against bending and thus further bending stress analyses are not necessary.
/13, 15/

9.2.2 Torsion

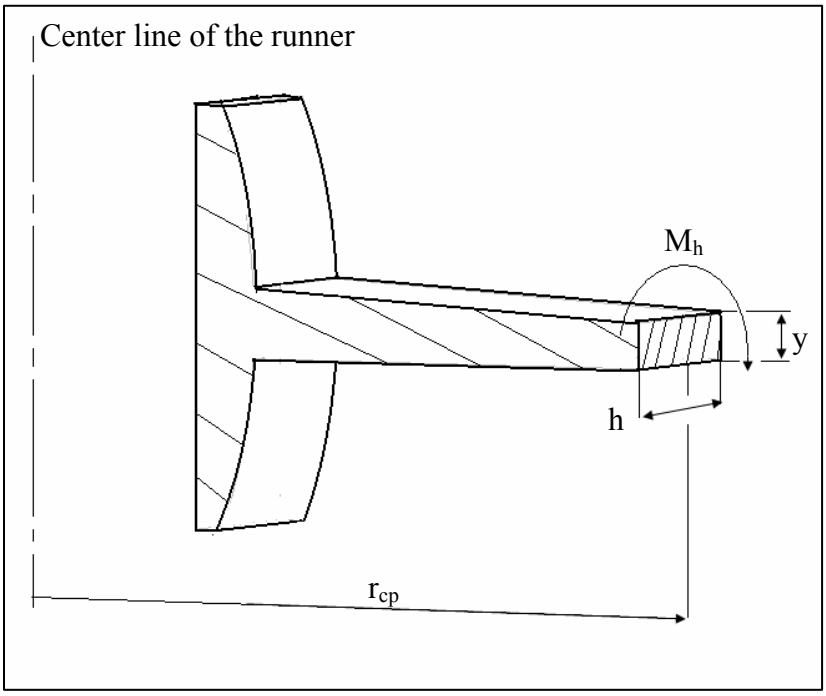

Figure 9.2: Sketch of the significant cutaway of the blade with cylindrical cut

The main force F_r, which causes the hydraulic moment, is applied at the radius r_{cp}. A cut is therefore made at this radius to get the relevant cross-section form.

The maximum permissible tensional stress of the blade is **270N/mm²**.
The present tensional stress can be determined as follows:

$$\tau_t = \frac{K_A * M_h}{W_t} \qquad [N/mm^2] \quad (9.5)$$

Where:

M_h	hydraulic moment	[Nmm]
W_t	polar section modulus	[mm^2]

The polar section modulus for the present cross-section form is defined as:

$$W_t = \frac{c_1}{c_2} * h * y^2 \qquad [mm^2] \qquad (9.6)$$

The values of c_1 and c_2 depend on the ratio of h and y and they can be read off the Table 14.3 in the Appendix. The value of h is 60mm and y is equal to 8mm. From this follows a c_1 of 0.307 and a c_2 of 0.999 and a polar section modulus of 1,180mm^2 results. The hydraulic moment has a value of 94,920Nmm and the outcome of this is a present tensional stress of **101N/mm^2**, which is less than the maximum permissible stress. /13, 15/

9.3 Pivot

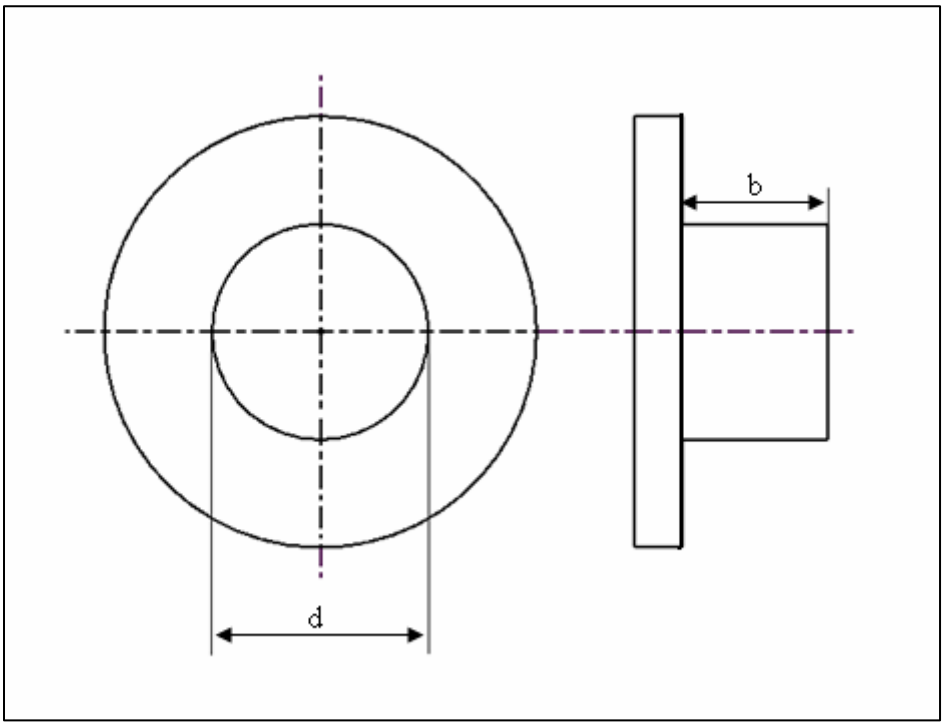

Figure 9.3: Sketch pivot

Material: X20Cr13 (1.4021)

9.3.1 Contact pressure

The maximum permissible contact pressure of the pivot is **300N/mm²**. The maximum permissible contact pressure of the bearing (HSM-4550-30) must, however, also be considered. The permissible contact pressure of the bearing is **90N/mm²** and is therefore used as the reference value for the maximum contact pressure.

The present contact pressure can be calculated with the following equation:

$$p = \frac{K_A * F_r}{A_{proj}} \qquad [N/mm^2] \quad (9.7)$$

Where:

F_r	resulting force	[N]
A_{proj}	projection screen	[m²]

The projection screen can be established as follows:

$$A_{proj} = b * d \qquad [mm^2] \quad (9.8)$$

Where:

b	length of the pivot	[mm]
d	diameter of the pivot	[mm]

With a diameter d of 45mm and a length b of 30mm, a projection screen of 1,350mm^2 results. As the resulting force has a value of 3,062N, a present contact pressure of **2.8N/mm^2** results from the equation (9.7). /13, 15, 16/

9.3.2 Torsion

The maximum permissible tensional stress is **225N/mm^2**.

The present tensional stress can be established using the following equation:

$$\tau_t = \frac{K_A * M_h}{W_t} \qquad [N/mm^2] \quad (9.9)$$

Where:

M_h	hydraulic moment	[Nmm]
W_t	polar section modulus	[mm^3]

Equation of the polar section modulus:

$$W_t = \frac{\pi * d^3}{16} \qquad [mm^3] \quad (9.10)$$

With a hydraulic moment M_h of 94,920Nmm and a polar section modulus of 17,892mm^3 a present tensional stress of **6.6N/mm^2** results. /13, 15/

9.3.3 Bending

The significant maximum permissible bending stress is the value of the bearing which is **175N/mm^2**.

The present bending stress can be determined as follows:

$$\sigma_b = \frac{K_A * M_b}{W_{b\,min}} \qquad [N/mm^2](9.11)$$

Where:

M_b	bending moment	[Nmm]
$W_{b\,min}$	minimal section modulus	[mm^3]

The length l of the arm which causes the bending moment is 212mm. Thus a bending moment of 649,144Nmm can be established from the following equation:

$$M_b = l * F_r \qquad [Nmm] \quad (9.12)$$

The section modulus can be calculated as follows:

$$W_{b\,min} = \frac{\pi * d^3}{32} \qquad [mm^3] \quad (9.13)$$

The diameter d is 45mm; so a section modulus of 8,946mm^4 results.

The outcome of this is a present bending stress of **<u>90N/mm²</u>**.

/13, 15, 16/

9.4 Lever

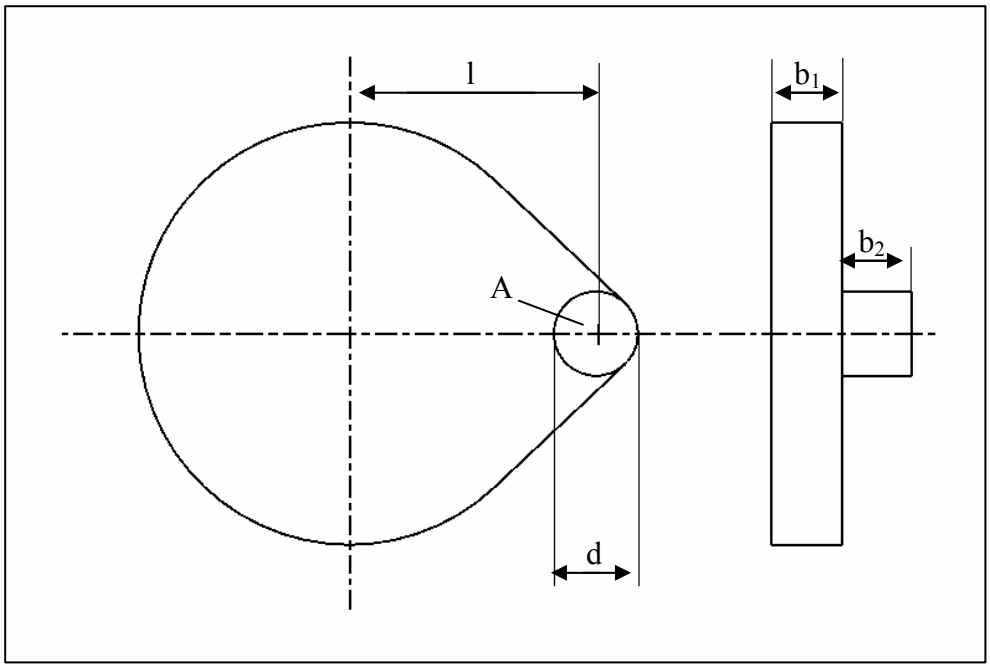

Figure 9.4: Sketch lever

Material: X20Cr13 (1.4021)

The pin of the lever is where the force is applied. Thus the occurring stresses at the pin have to be checked. If the pin is able to withstand the forces, one can assume that the whole lever is strong enough as the pin is the weakest part of the lever.

9.4.1 Bending

The maximum bending stress of the pin is **375N/mm²**; however, the present bending stress should not exceed the permissible bending stress of the bearing which has a value of **175N/mm²**.

The force which is applied at the pin can be calculated with the following equation:

$$F = \frac{M_h}{l} \qquad [N] \qquad (9.14)$$

The length l is 40mm and M_h has a value of 94,920Nmm, thus a force F of 2,373N results.

Equation of the present bending stress:

$$\sigma_b = \frac{K_A * M_b}{W_{b\,min}} \qquad [N/mm^2](9.15)$$

Where:

M_b	bending moment	[Nmm]
$W_{b\,min}$	minimal section modulus	[mm^3]

The bending moment results from the following equation:

$$M_b = b_2 * F \qquad [Nmm] \quad (9.16)$$

The length b_2 is 10mm and from this follows a bending moment of 23,730Nmm.

The minimal section modulus can be calculated as follows:

$$W_{b\,min} = \frac{\pi * d^3}{32} \qquad [N/mm^2](9.17)$$

With a value of d of 12mm, a section modulus of 170mm^3 results.

The outcome of this is a present bending stress of **174N/mm²**. /13, 15, 16/

9.4.2 Shear

The maximum shear stress which the pin can withstand can be calculated as follows:

$$\tau_{spermissible} = \frac{R_{p0.2}}{1.5} \qquad [N/mm^2](9.18)$$

Where:

$R_{p0.2}$	elastic limit	[N/mm^2]

The elastic limit of the lever material is 550N/mm^2. Hence, a permissible shear stress of **367N/mm²** results.

The present shear stress can be established using the following equation:

$$\tau_s = \frac{K_A * F}{A} \qquad [N/mm^2](9.19)$$

With an area of 113mm^2 a present shear stress of **26N/mm²** results. /13, 15/

9.4.3 Contact pressure

The maximum permissible contact pressure of the bearing (HSM-1214-10) is **90N/mm²**.

Equation of the present contact pressure:

$$p = \frac{K_A * F}{A_{proj}} \qquad [N/mm^2] \quad (9.20)$$

Where:

A_{proj} projection screen [mm²]

Equation of the projection screen:

$$A_{proj} = b_2 * d \qquad [mm^2] \quad (9.21)$$

The projection screen is equal to 120mm² and a contact pressure of **25N/mm²** results. /13, 15, 16/

9.5 Link

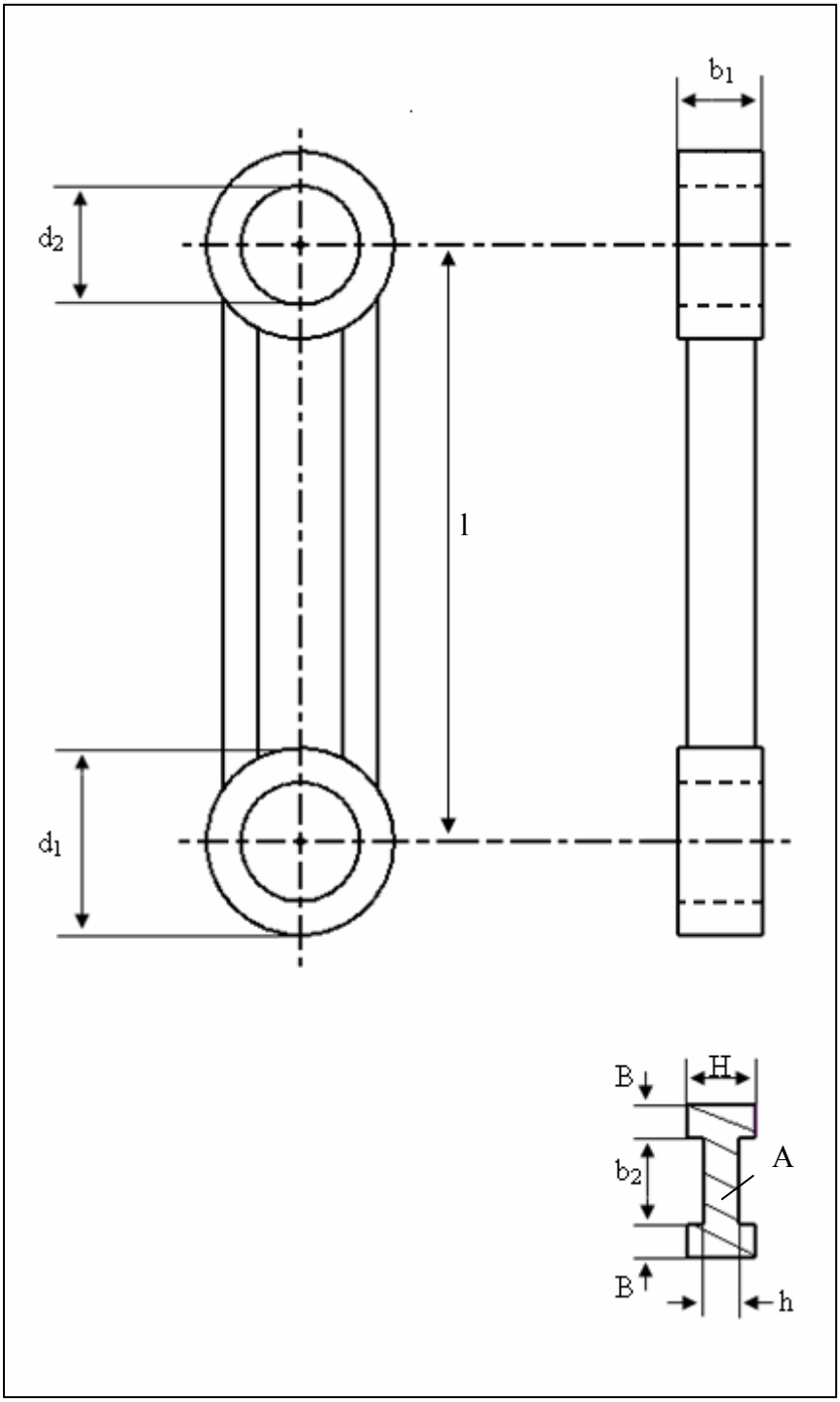

Figure 9.5: Sketch link

Material: X3CrNb17 (1.4511)

9.5.1 Buckling

The link is clamped between the lever and the crosshead as in buckling case II. Thus, buckling length l_k is equal to length l and has a value of 70mm.

The thickness ratio of the link can be established with the following equation:

$$\lambda = l_k * \sqrt{\frac{A}{I_{min}}} \qquad [-] \qquad (9.22)$$

Where:

I_{min} minimal axial moment of inertia [mm^4]

The minimal axial moment of inertia can be calculated as follows:

$$I_{min} = \frac{2 * B * H^3 + b_2 * h^3}{12} \qquad [mm^4] \qquad (9.23)$$

The outcome of this is a minimal moment of inertia of 395mm^4.

The area A is 104mm^2 and a thickness ratio of 36 results from the equation (9.22).

The marginal thickness ratio $\lambda_{g0.2}$ can be determined using the following equation:

$$\lambda_{g0,2} = \pi * \sqrt{\frac{E}{\sigma_{d0.2}}} \qquad [-] \qquad (9.24)$$

Where:

E elastic modulus [N/mm^2]

$\sigma_{d0.2}$ elastic limit ($R_{p0.2}$) [N/mm^2]

The steel 1.4511 has an elastic modulus of 220,000N/mm^2 and an elastic limit of 230N/mm^2. Hence, a marginal thickness ratio of 97 results.

Since the thickness ratio of the link is smaller than the marginal thickness ratio $\lambda_{g0.2}$, the present buckling stress has to be calculated with the following equation:

$$\sigma_k = \frac{K_A * F}{A} \qquad [N/mm^2] \qquad (9.25)$$

Force F which is applied at the link is the same force as in Section 9.4 which has a value of 2,373N. Thus a present buckling stress of **29N/mm²** results. The permissible buckling stress is equal to the permissible compression stress which is **170N/mm²**. Accordingly, the present buckling stress is within the permitted range. /13, 15/

9.5.2 Stress calculation of the links eye

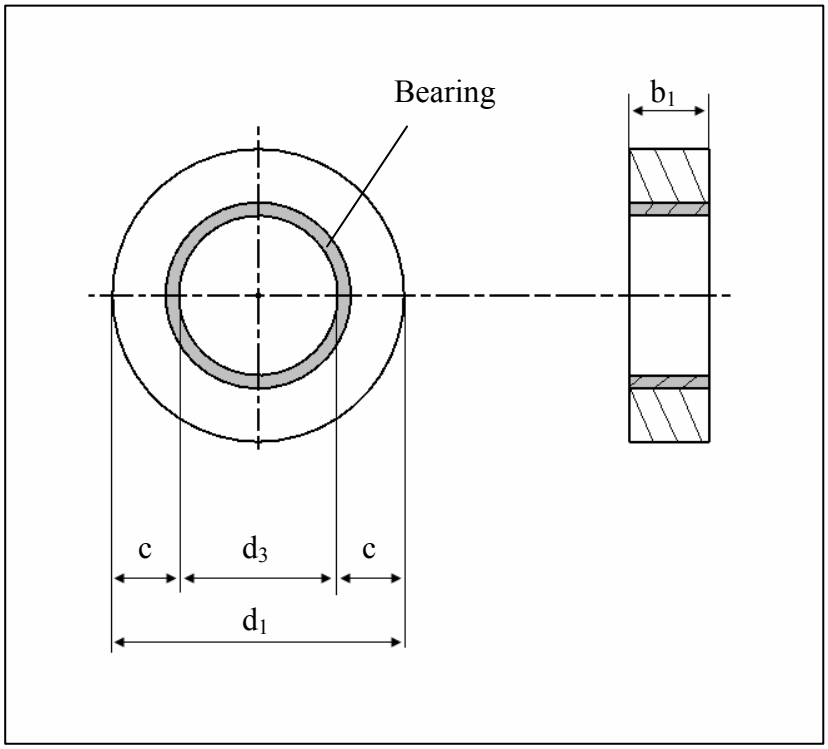

Figure 9.6: Sketch of the eye

The eye of the link is the point where the most stress occurs. To calculate the stress which appears at the eye the following equation can be used:

$$\sigma = \frac{K_A * F}{2 * c * b_1} * \left[1 + \frac{3}{2} * \left(\frac{d_3}{c} + 1\right)\right] \qquad [N/mm^2](9.26)$$

The permissible stress can be determined with the following equation:

$$\sigma_{permissible} = 0{,}5 * R_m \qquad [N/mm^2](9.27)$$

Where:

R_m tensile strength [N/mm²]

The tensile stress is 420N/mm^2, thus a permissible stress of **210N/mm^2** results.

The values which are needed to calculate the stress in the eye are as follows:

F= 2,373N

c=5mm

b_1=10mm

d_3=12mm

Accordingly, a stress of **181N/mm^2** results from equation (9.26). The present stress is smaller than the permissible stress, thus the dimension of the eye is sufficient. /15/

9.6 Crosshead

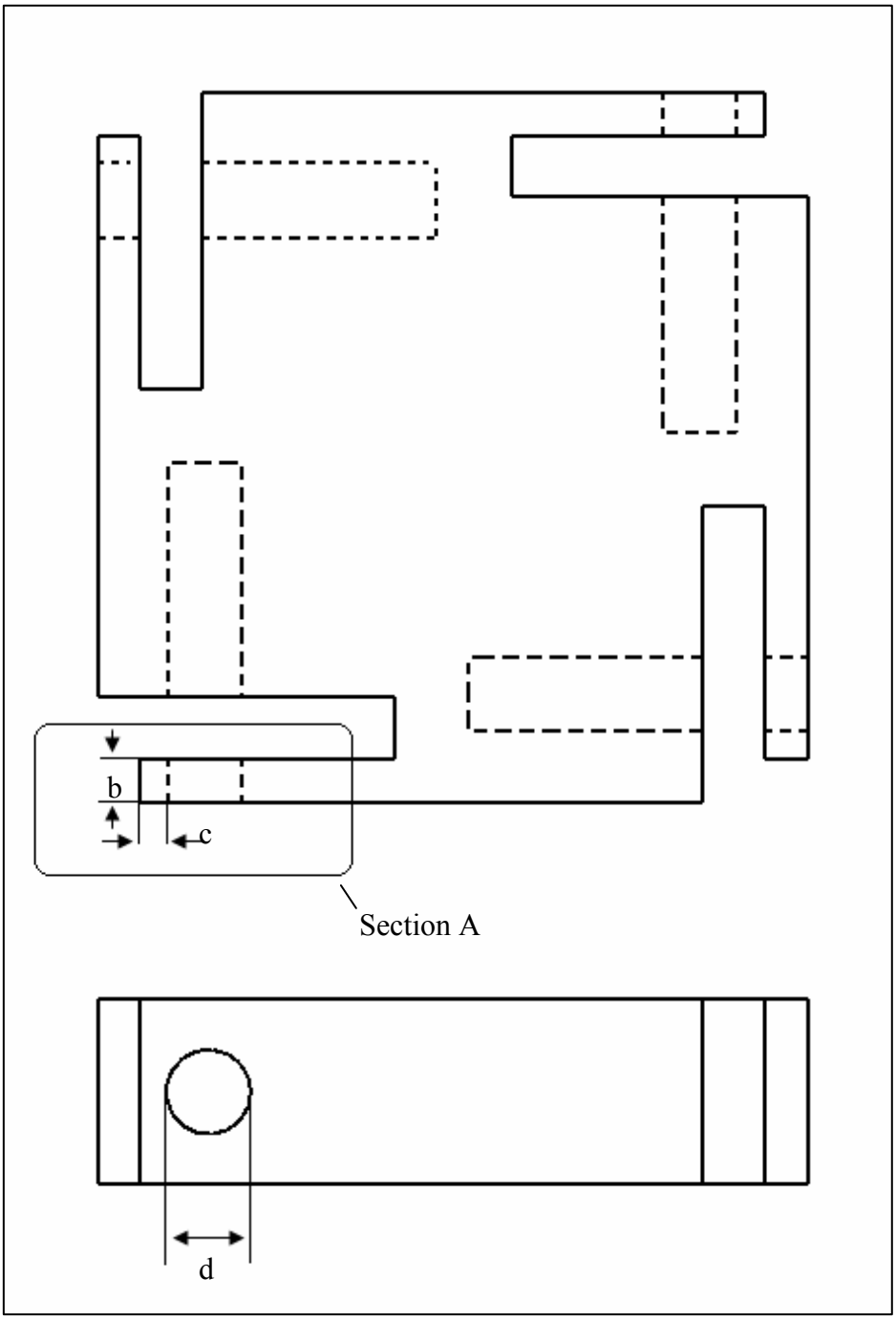

Figure 9.7: Sketch of the crosshead

Material: X20Cr13 (1.4021)

In section A, the crosshead has the weakest point. If this point can withstand the occurring stress, it can be assumed that the whole crosshead is safe against failure. The principle of this stress analysis is the same as in Section 9.5.2.

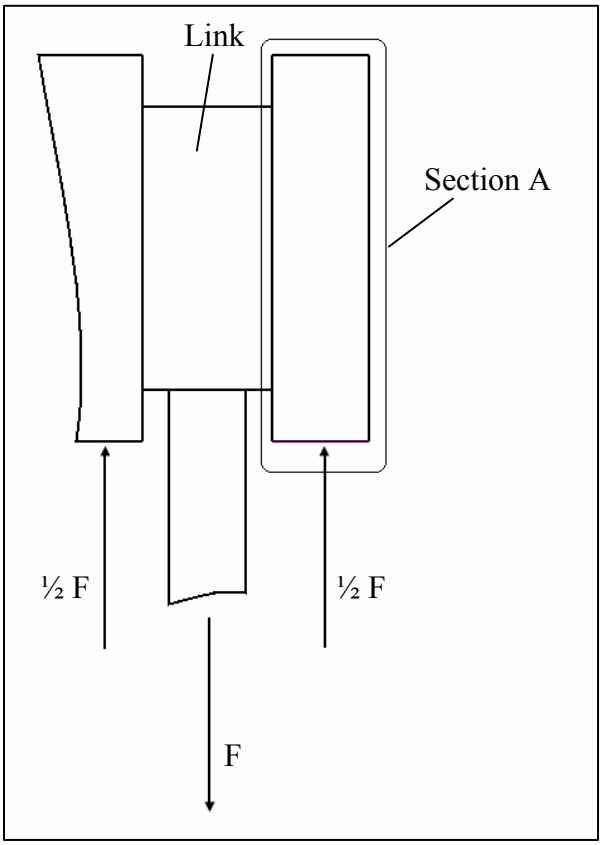

Figure 9.8: Clamping of the link in the crosshead

The force which is applied at section A is the half of the force which applies at the link. The stress which applies in section A can be calculated as follows:

$$\sigma = \frac{K_A * \frac{1}{2} F}{2 * c * b} * \left[1 + \frac{3}{2} * \left(\frac{d}{c} + 1\right)\right] \qquad [N/mm^2](9.28)$$

The permissible stress is defined as:

$$\sigma_{permissible} = 0{,}5 * R_m \qquad [N/mm^2](9.29)$$

Where:

R_m tensile strength [N/mm²]

The tensile stress is 750N/mm², thus a permissible stress of **375N/mm²** results.

The outcome of this is a present stress of **113N/mm** using the following values:

F= 2,373N

c=5mm

b=8mm

d=12mm

The section A can withstand the present stress; this means that the dimension of the whole cross head is sufficient. /15/

9.7 Bolt

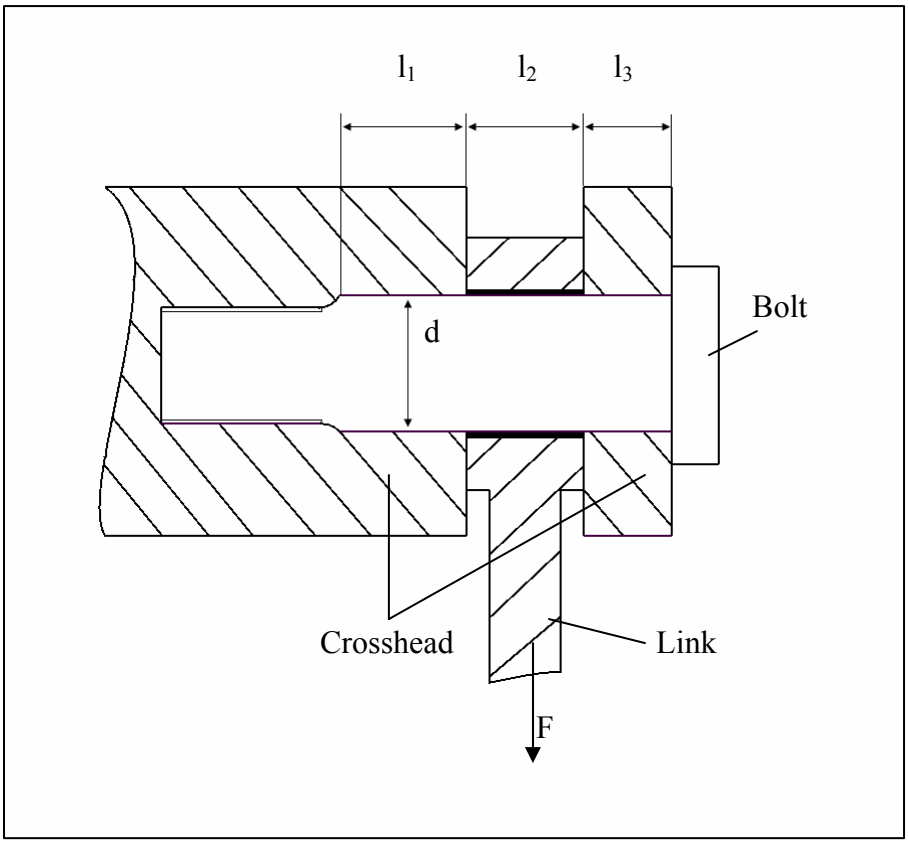

Figure 9.9: Sketch of the bolt connection

Bolt: DIN 1445-12h11x17x55

Material: X6CrMoS17 (1.4105)

9.7.1 Bending

The permissible bending stress is **215N/mm²**.

The present bending stress is defined as:

$$\sigma_b = \frac{K_A * M_b}{W_{b\,min}} \qquad [N/mm^2](9.30)$$

Where:

M_b	bending moment	[Nmm]
$W_{b\,min}$	minimal section modulus	[mm^3]

Depending on the fitting of the bolt, the bending moment has to be calculated in different ways. The bolt has a clearance fit over the lengths l_1, l_2, and l_3. Thus, to calculate the bending moment the following equation must be used:

$$M_b = \frac{F * (l_1 + l_2 + l_3)}{8} \quad \text{[Nmm]} \quad (9.31)$$

The force F has a value of 2,373N and the relevant lengths are as follows:

l_1=20mm

l_2=10mm

l_3=8mm

Thus a bending moment of 11,272Nmm results.

The section modus can be established with the following equation:

$$W_{b\,min} = \frac{\pi * d^3}{32} \quad [mm^3] \quad (9.32)$$

The bolt has a diameter d of 12mm and the outcome of this a section modus of 170mm^3. Thus a present bending stress of **<u>83N/mm^2</u>** results from equation (9.30). /15/

9.7.2 Shear

At the bolt calculation, the maximum permissible shear stress can be determined using the following equation:

$$\tau_{spermissible} = 0.2 * R_m \quad [N/mm^2] (9.33)$$

Where:

R_m	tensile strength	[N/mm^2]

The tensile strength has a value of 430N/mm^2; so a maximum shear stress of **86N/mm^2** is permitted.

The present shear stress is defined as:

$$\tau_s = \frac{4}{3} * \frac{K_A * F}{A_S * 2} \qquad [N/mm^2](9.34)$$

Where:

A_s cross section area of the bolt [mm]

With a diameter of 12mm, it follows a cross section area of 113mm^2. Force F is 2,373N; so a present shear stress of **18N/mm^2** results from equation (9.34). /15/

9.7.3 Contact pressure

At the bolt contact pressure is applied which is caused by the link and the contact pressure caused by the crosshead.

The permissible contact pressure can be established using the following equation:

$$p_{permissible} = 0.35 * R_m \qquad [N/mm^2](9.35)$$

The tensile strength is, as in the previous section 430N/mm^2 and a permissible contact pressure of **151N/mm^2** results.

The respective present contact pressure can be established using the following equation:

$$p = \frac{K_A * F}{A_{proj}} \qquad [N/mm^2](9.36)$$

Where:

A_{proj} projection screen of the link alternatively of the crosshead [mm^2]

Crosshead:

The projection screen of the crosshead can be established as follows:

$$A_{proj} = (l_1 + l_3) * d \qquad [mm^2] \quad (9.37)$$

With a projection screen of 336mm^2 a present contact pressure of **9N/mm^2** follows.

Link:

The projection screen of the link is defined as:

$$A_{proj.link} = l_2 * d \qquad [mm^2] \qquad (9.38)$$

The projection area of the link is 120mm and the present contact pressure of **<u>25N/mm²</u>** results from equation (9.36). /15/

9.8 Shaft

The shaft has to withstand four times force F of 2,373N, which was calculated in Section 9.4. Assuming that the shaft is clamped as in the buckling case II, the buckling length l_k is equal to the length of the shaft which has the value of 3300mm.

The thickness ratio of the link can be established with the following equation:

$$\lambda = l_k * \sqrt{\frac{A}{I_{min}}} \qquad [-] \qquad (9.39)$$

Where:

I_{min} minimal axial moment of inertia [mm^4]

The minimal axial moment of inertia can be calculated as follows:

$$I = \frac{\pi * d^4}{64} \qquad [mm^4] \qquad (9.40)$$

The diameter of the shaft is 60mm; so an axial moment of inertia of 636,173mm^4 results.

With an area A of 2,827mm, a thickness ratio of 220 results from equation (9.39)

The marginal thickness ratio $\lambda_{g0.2}$ can be determined using the following equation:

$$\lambda_{g0,2} = \pi * \sqrt{\frac{E}{0.8 * \sigma_{d0.2}}} \qquad [-] \qquad (9.41)$$

Where:

E elastic modulus [N/mm^2]

$\sigma_{d0.2}$ elastic limit ($R_{p0.2}$) [N/mm^2]

The elastic modulus is 220,000N/mm^2 and the elastic limit is 230N/mm^2; the outcome of this is a marginal thickness ratio of 109. Since the marginal thickness ratio is smaller than the thickness ratio, the following equation has to be used to calculate the present stress:

$$\sigma_k = \frac{K_A * \pi^2 * E}{\lambda^2} \qquad [N/mm^2](9.42)$$

A present buckling stress of **56N/mm²** follows from equation (9.42); this is less than the permissible buckling stress of **170N/mm²**. /13, 14/

9.9 Hub

The hub has to absorb the moment caused by the tangential force and the contact pressure caused by the resulting force. A stress analysis for the hub is not necessary. The wall thickness of the hub is much bigger than the wall thickness of the axle. Since the axle is able to withstand the occurring tensional stress, the hub should also withstand it. The contact pressure which occurs at the hub must be calculated in the same way as in Section 9.3.1. In reference to this section, it can be assumed that the contact pressure at the hub is within the permitted range.

10 CALCULATION OF THE SCREWS

The screw calculation is rather bulked and the procedure of it is always pretty much the same; thus just the calculation of the first screw connection will be detailed. In the following sections, only the main results will be presented.

10.1 Screw connection of the lever and the pivot

Step1: Pre-selection of the screw

The following two motive forces are acting at the screw connection:

1. Longitudinal force which is equal to the centrifugal force
2. Shear force which is caused by the hydraulic moment M_h

In Section 5.5, a maximum centrifugal force of 68,922N was established. Three screws are supposed to be used for the connection; thus a longitudinal force F_{Bs} of 22,974N results for each screw. According to Table 14.4 in the Appendix, a M12 screw of the strength class 12.9 can be chosen.

The shear force is defined as:

$$F_Q = \frac{K_A * M_h}{r} \qquad [mm] \qquad (10.1)$$

Where:

r radius of the hole circle diameter

The holes are arranged at a radius of 15mm and the hydraulic moment has a value of 94,920Nmm; a shear forces F_{Qs} of 7,910N results from this. This means that each screw has to absorb 2,637N. The screws chosen based on the longitudinal force are also adequate accordingly for the shear force.

Step2: Rough calculation of the contact pressure

The occurring contact pressure can approximately be calculated as follows:

$$p = \frac{F_{sp}}{0{,}9 * A_p} \qquad [N/mm^2] (10.2)$$

Where:

F_{sp}	tension force	[N]
A_p	contact surface of the screw head	[mm^2]

A tension force of 68.5kN can be read off Table 14.5 in the Appendix and the contact surface of the screw head can be determined as follows:

$$A_p = \frac{\pi * (d_w^2 - d_h^2)}{4} \quad [mm^2] \quad (10.3)$$

Where:

d_w	outer diameter of the annular surface of the screw head	[mm]
d_h	hole diameter	[mm]

Diameter d_w is equal to 18mm and the diameter of the hole is 13mm (see Table 14.6). The outcome of this is a contact surface of 122mm^2 and from this follows a contact pressure of **624N/mm^2**. However, the permissible contact pressure of the lever is only **300N/mm^2.** Hence, a washer must be used to decrease the contact pressure. The outer diameter of the washer must now be used in equation (10.3) instead of diameter d_w. With the new outer d_2 diameter of 24mm (see table 14.6) a contact surface of 320mm^2 results and a contact pressure of **238N/mm^2** follows, which is in the permitted range.

Step3: Calculation of the required assembly preload force

The assembly preload force is defined as:

$$F_{VM} = k_A * [F_{Kl} + F_{Bs} * (1 - \Phi) + F_Z] \quad [N] \quad (10.4)$$

Where:

k_A	snap factor	[-]
F_{Kl}	clamping force	[N]
F_B	longitudinal force per screw	[N]
Φ	force ratio	[-]
F_Z	preload force loss	[N]

The snap factor can be read off the Table 14.8 which is in the Appendix. Since the screws are supposed to be manually tightened by torque wrench, the snap factor

has a value of **1.6.** As already mentioned, the longitudinal force per screw is **22,974N**.

The clamping force can be determined with the following equation:

$$F_{Kl} = \frac{F_Q}{\mu * z} \quad [N] \quad (10.5)$$

Where:

μ	friction factor	[-]
z	number of the screws	[-]

A friction factor of 0.5 can be assumed based on the Table 14.9. Thus a clamping force of **4,218N** results from equation (10.5).

The force ratio is defined as:

$$\Phi = n * \Phi_K \quad [-] \quad (10.6)$$

Where:

n	force introduction factor	[-]
Φ_K	simplified force ratio	[-]

A force introduction factor of 0.5 is normally used. The simplified force ratio can be established using the following equation:

$$\Phi_K = \frac{\delta_T}{(\delta_T + \delta_S)} \quad [-] \quad (10.7)$$

Where:

δ_T	flexibility of the uptight parts	[mm/N]
δ_S	flexibility of the screw	[mm/N]

The flexibility of the uptight parts can be determined as follows:

$$\delta_T = \frac{l_k}{A_{ers} * E_T} \quad [mm/N] \quad (10.8)$$

Where:

l_k	clamping length	[mm]
A_{ers}	ersatz area	[mm^2]
E_T	elastic modulus of the uptight part	[N/mm^2]

The clamping length is 12.5mm and the elastic modulus of the part is 216,000N/mm^2. The ersatz area can be calculated using the following equation:

$$A_{ers} = \frac{\pi}{4} * (d_w - d_h) + \frac{\pi}{8} * d_w * (D_A - d_w) * \left[(x+1)^2 - 1\right] \quad [mm^2] \quad (10.9)$$

Where:

d_w	outer diameter of the annular surface of the screw head	[mm]
D_A	outer diameter of the uptight part	[mm]
d_h	hole diameter	[mm]
x	$\sqrt[3]{\frac{l_k * d_w}{D_A^2}}$	[mm] (10.10)

The outer diameter D_A of 30.5mm has been established using the following equation:

$$D_A = d_w + l_k \quad [mm] \quad (10.11)$$

The outcome of this is a x of 0.62. Thus an ersatz area of 147mm^2 results and a flexibility δ_T of 3.9*10^{-7}mm/N follows from equation (10.8).

The flexibility of the screws can be determined with the following equation:

$$\delta_S = \frac{1}{E_S} * \left(\frac{0{,}4 * d}{A_N} + \frac{l}{A_3} + \frac{0{,}5 * d}{A_3} + \frac{0{,}4 * d}{A_N} \right) \quad [mm/N] (10.12)$$

Where:

E_S	elastic modulus of the screws	[N/mm^2]
d	nominal diameter of the screw	[mm]
A_N	nominal cross section of the shank	[mm^2]
l	length of the non screwed part	[mm]
A_3	core cross section of the thread	[mm^2]

The elastic modulus of the screws is 220,000N/mm^2; the nominal diameter of the screw is 12mm; the length of the non screwed part is 12.5mm; the core cross section of the thread is 76.25mm^2 (see Table 14.10). A nominal cross section of

113mm^2 results out of the circular area equation. A flexibility of the screws of $1.5*10^{-6}$mm/N results from equation (10.12).

The results of equation (10.12) and (10.8) must be put in equation (10.7) and from this a simplified force ratio of 0.21 results. This result has to be used in equation (10.6) and a force ratio of **0.105** results. Only the value of the preload force loss is still missing by which to calculate the assembly preload force.

Equation of the preload force loss:

$$F_Z = \frac{f_Z}{(\delta_S + \delta_T)} \qquad [N] \qquad (10.13)$$

Where:

f_Z setting amount [mm]

The setting amount is a recommended value which can be established using Table 14.11 from the Appendix. The setting amount is 0.023mm. Hence, a preload forces loss of **12,169N** results. Finally all the values are known to establish the assembly preload force via equation (10.4) which is equal to **59,118N**. The assembly preload force is less than the tension fore; thus the screws which were chosen can be used.

Step4: Calculation of the required tightening torque

Since the screws are supposed to be tightened by a torque wrench, the tightening torque is defined as:

$$M_A = 0.9 * M_{sp} \qquad [Nm] \qquad (10.14)$$

Where:

M_{sp} tension torque [Nm]

A tension torque of 137Nm can be read off Table 14.5, the outcome of which is a tightening toque of **123Nm**.

Step5: Maximum permissible screw force

The following requirement has to be fulfilled:

$$\Phi * F_{Bs} \leq 0.1 * R_{p0.2} * A_S$$

Where:

$$\Phi * F_B = \underline{\mathbf{2{,}412N}} \quad (10.15)$$

$$0.1 * R_{p0.2} * A_S = \underline{\mathbf{9{,}104N}} \quad (10.16)$$

Thus the requirement is fulfilled. The value $R_{p0.2}$ can be determined from Table 14.12 and the value A_S can be determined from Table 14.10 from the Appendix.

Step6: Exact calculation of the contact pressure

The contact pressure is defined as:

$$p = \frac{F_{sp} + \Phi * F_{Bs}}{A_p} \quad [N/mm^2] \quad (10.17)$$

All the values are already known from the previous calculation and an exact contact pressure of **<u>222N/mm²</u>** results from equation (10.17). This exactly contact pressure is even less than the contact pressure which was roughly determined; thus the chosen material can be taken. /15/

<u>Chosen screw: ISO 4017 M12x25 class 12.9</u>

10.2 Screw connection between the blade and the pivot

Step1: Pre-selection of the screw

The longitudinal force has a value of 68,922N. The connection exists out of 8 screws. Thus a longitudinal force of 8,615N results for each screw. The shear force per screw is 424N. Hence, an M8 screw of class 12.9 is chosen.

Step2: Roughly calculation of the contact pressure

When using washers, the determined contact pressure has a value of 225N/mm². The material of the blade is able to withstand a contact pressure of up to 360N/mm².

Step3: Calculation of the required assembly preload force

The assembly preload force has to be less than the tension force of 29.5kN. The established assembly preload force is 27.19kN, which is within the permitted limit.

Step4: Calculation of the required tightening torque

The required tightening torque has a value of 35.73Nm.

Step5: Maximum permissible screw force

The maximum permissible screw force of 3,953N is not exceeded.

Step6: Exact calculation of the contact pressure

The accurate contact pressure has a value of 208N/mm^2. /15/

Chosen screw: DIN 7984 M8x12 class 12.9

10.3 Screw connection between the upper and the middle hub

Step1: Pre-selection of the screw

The longitudinal force of 14,052N follows from the sum of the axial force and the weight of the blade. Eight screws should be used for the connection; thus a longitudinal force of 1,757N results per screw. The shear force is 21,061N, which means that each screw has to absorb a shear force of 2,633N. An M8 screw of the class 12.9 is sufficient for the longitudinal force as well as for the shear force.

Step2: Roughly calculation of the contact pressure

When using washers the occurring contact pressure is 192N/mm^2 which is okay, since the chosen material of the upper hub has a maximum permissible contact pressure of 210N/mm^2.

Step3: Calculation of the required assembly preload force

The required assembly preload force for this screw connection is 25.19kN. The tension force, which has a value of 29.5kN, of the screw has to be higher than the assembly preload force; this requirement is fulfilled.

Step4: Calculation of the required tightening torque

The torque which is necessary to tighten the screw has a value of 35.7Nm.

Step5: Maximum permissible screw force

It exits no danger to exceed the permissible screw force.

Step6: Exact calculation of the contact pressure

Using the accurate equation to determine the contact pressure, a result of 203N/mm^2 results. Thus the material of the upper hub is able to withstand the occurring contact pressure. /15/

Chosen screw: DIN 7984 M8x16 class 12.9

10.4 Screw connection between the middle and the lower hub

The screw connection between the middle and the lower hub hardly has to absorb forces. The longitudinal force results just from the weight of the lower hub and has a value of 49.05N. Also the shear force is so little that it does not have an important influence on the connection. Thus, four M8 screws of class 4.6 are chosen for this connection. Due to the little forces, a check-up of the screws is not necessary; one can assume that the connection is strong enough.

Chosen screw: DIN 7984 M8x16 class 4.6

11 EXPLANATION OF THE RUNNER DESIGN

The principle of the adaptation mechanism of the runner can be seen in Figure 11.1. The blade is connected to a pivot which is connected with a lever; the lever is connected to the crosshead using a simple link. Through upwards and downwards movements of the crosshead, the blade can be adjusted. To realize the movements, the crosshead is welded to a shaft which is interfaced, for example, to an electric motor.

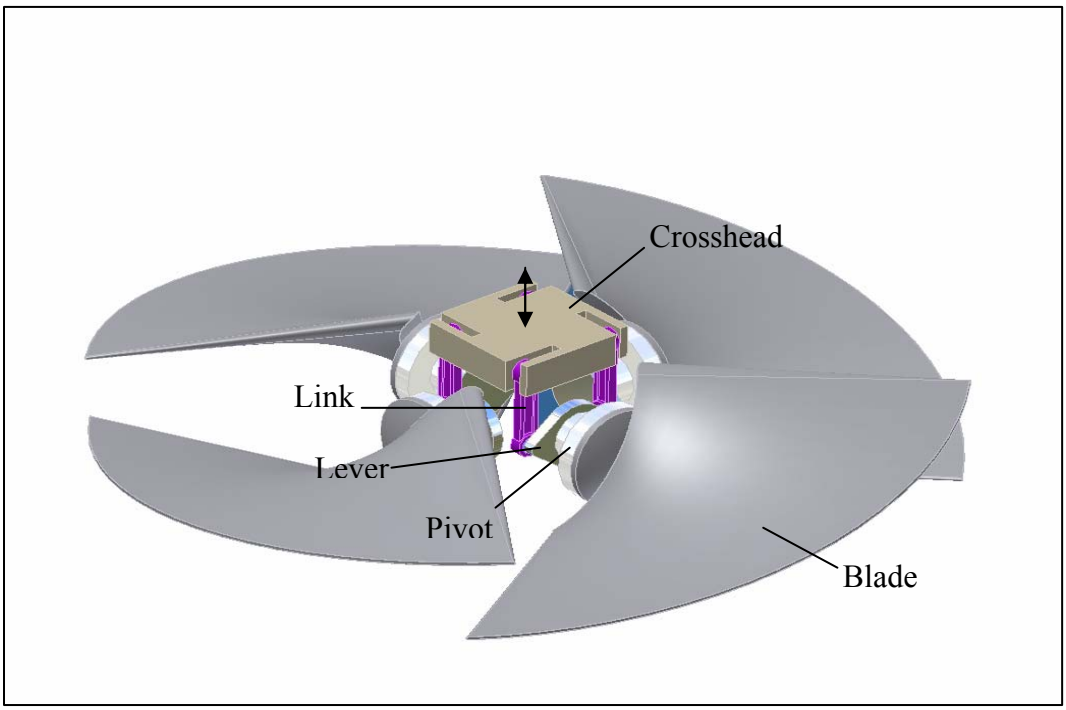

Figure 11.1: Sketch of the adaptation mechanism

The adjustment of the blade can be made in quite a wide range. As can be seen in Figure 11.2, the crosshead fits into the axle. Thus the upturn of the crosshead is, theoretical, unlimited. The middle hub is the barrier of the downturn. In the practice, the blades can be turned about 69°.

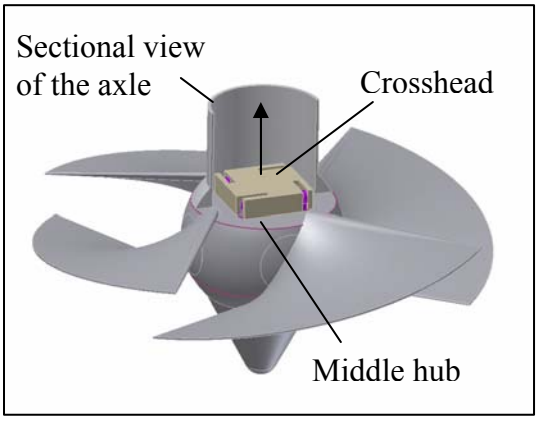

Figure 11.2: Sketch of the crosshead inside the axle

The parts of the runner can be manufactured by machining or casting; whereas the smaller parts, such as the pivot, the lever, the link and the crosshead can be produced at the Tampere Polytechnic. Other parts, such as, the bearings, the shaft and the axle are standard parts and can be purchased. The parts can be connected by screws or by welding. The parts of the adaptation mechanism are mostly connected by screws and thus they can be changed quite easy in the case of damage or wearing.

Since the adaptation mechanism is working without the input of oils or greases, the runner does not contaminate the water. Also, it is of no concern if some water does penetrate the runner as all parts are made out of stainless steel and some water in the runner will not influence its efficiency. Thus seals are not needed.

12 ASSEMBLING

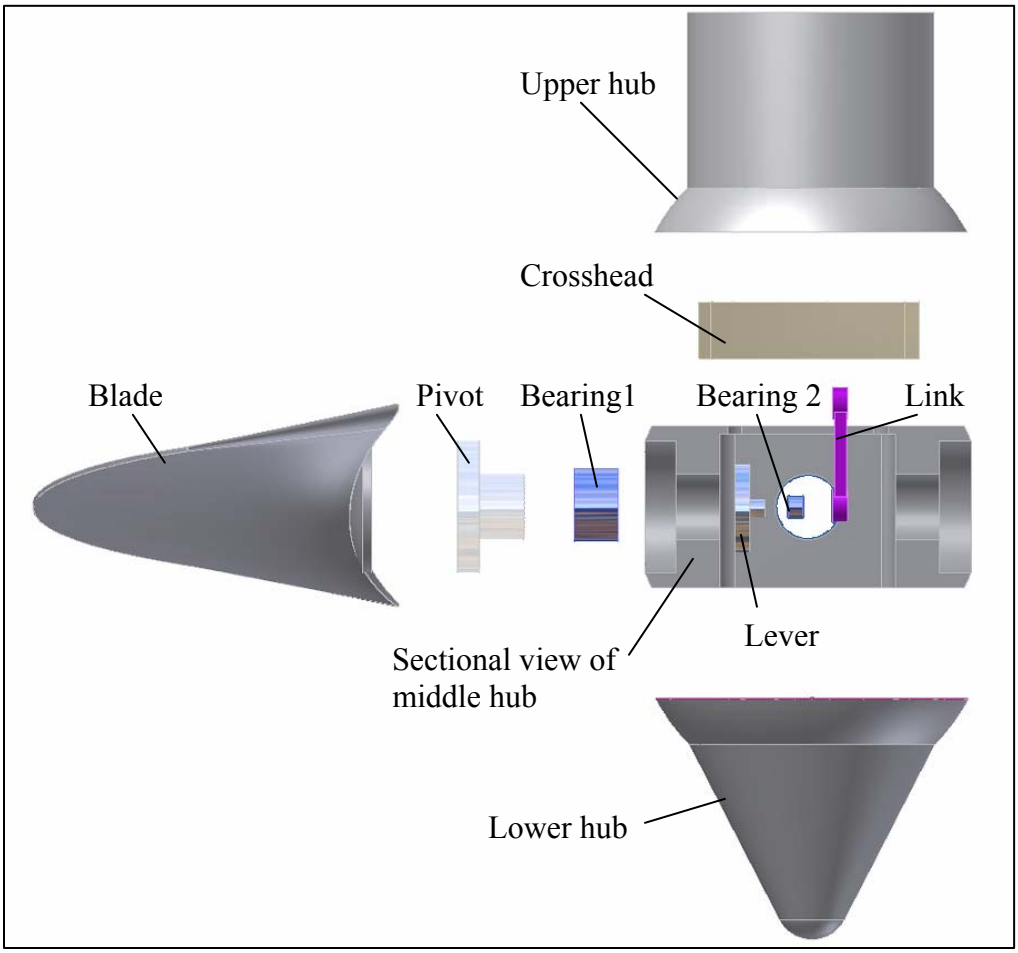

Figure 12.1: Parts of the runner

Figure 12.1 explains the assembly of the runner step by step.

Step1: Bearing 1 is attached to the middle hub with a tight fit.

Step2: Bearing 2 is attached to the link with a tight fit

Step3: The pivot is fit into bearing 1

Step4: The lever is connected to the pivot using screws

Step5: The link is fit to the pin of the lever; a spring cotter secures the link

Step6: Repeat steps 1 to 5 with the other three sides

Step7: The links are connected to the crosshead using a bolt connection

Step8: The upper and middle hub are connected by screws

Step9: The middle and lower hub are connected by screws

Step10: The blades and the pivots are connected by screws

13 CONCLUSION

The adaptation mechanism in this thesis is different to the adaptation mechanisms found in the literature. This is based on the small space the hub provides. However, even though the space of the hub is little, it is enough to fit a proper mechanism with which to adjust the blades.

The stress analysis and the screw calculation show that the adaptation mechanism should be able to withstand the occurring forces. To design the runner some simplifications and assumptions had to be made, as it is only tests can really confirm that the adaptation mechanism is sufficient. However, the safety factor used in the stress analysis should be high enough to avoid any significant malfunction.

Since the design of the runner is just based on theory, it can not be assumed to be 100% practicable – some variances to the theory always appear in practice. Hence, for example, the profile of the blade maybe needs to be change somewhat to improve the manner of the water flow.

On some points, the sources which were used to design the runner give different information and thus it was not altogether clear which of the sources should be used. Furthermore, the only book providing a step-by step design of the blade was in Finnish. Therefore, in designing the blade I was heavily dependent on my Finnish supervisor Mr Jaakko Mattila.

The drawings were compiled using the program Inventor Professional 11 similar to the Solid Edge program taught at the Fachhochschule Hannover. The most of the drawings were simple. But the blade is a quite complex part; so it caused a lot of difficulties to draw the blade in a proper way. To keep the English number system also in the drawings, they were made according to the JSI. Due to setup issues of the plotter it was not possible to plot the drawings exactly according to the standard sizes A2 and A1; the drawing areas just have approximately the correct size.

To write the final thesis in English was a very big challenge and it was not always easy. Especially technical terms were not that easy to translate into English. But the thereby gained experience is irreplaceable.

14 APPENDIX

14.1 Calculation of the mains characteristics

$Q = 3m^3/s$

$H = 3.7m$

$\eta_h = 0.9$

$\rho = 998kg/m^3$

$g = 9.81m/s^2$

14.1.1 Power

$$P = Q * H * \eta_h * \rho * g \quad => \quad P = 3 * 3.7 * 0.9 * 998 * 9.81 = \underline{\mathbf{97{,}806W = 98kW}}$$

Specific speed

$$n_{QE} = \frac{2.294}{H_n^{0.486}}$$

$$H_n = H * \eta_h \quad => \quad H_n = 3.7 * 0.9 = 3.33m$$

$$=> \quad n_{QE} = \frac{2.294}{3.33^{0.486}} = \underline{\mathbf{1.28}}$$

14.1.2 Rational speed

$$n_{QE} = \frac{n * \sqrt{Q}}{E^{3/4}} \quad => \quad n = \frac{n_{QE} * E^{3/4}}{\sqrt{Q}}$$

$$E = H_n * g \quad => \quad E = 3.33 * 9.81 = 32.7 J/kg$$

$$=> \quad n = \frac{1.28 * 32.7^{3/4}}{\sqrt{3}} = \underline{\mathbf{10s^{-1}}}$$

14.1.3 Runaway speed

$$n_{max} = 3.2 * n \quad => \quad n_{max} = 3.2 * 10 = \underline{\mathbf{32s^{-1}}}$$

14.1.4 Runner diameter

$$D_e = 84.5 * (0.79 + 1.602 * n_{QE}) * \frac{\sqrt{H_n}}{60 * n}$$

$$=> D_e = 84.5 * (0.79 + 1.602 * 1.28) * \frac{\sqrt{3.33}}{60 * 10} = \underline{\mathbf{0.73m}}$$

14.1.5 Hub diameter

$$D_i = \left(0.25 + \frac{0.0951}{n_{QE}}\right) * D_e \quad => D_i = \left(0.25 + \frac{0.0951}{1.28}\right) * 0.73 = \underline{\mathbf{0.24m}}$$

14.2 Cavitation

p_{atm} = 101,300Pa

p_v = 2,985.7Pa (see table 14.1)

ρ = 998kg/m^3

g = 9.81m/s^2

c_4 = 2m/s

H_n = 3.33m

Suction head

$$H_s = \frac{p_{atm} - p_v}{\rho * g} + \frac{c_4^2}{2 * g} - \sigma * H_n$$

$$\sigma = 1.5241 * n_{QE}^{1.46} + \frac{c_4^2}{2 * g * H_n} \quad => \sigma = 1.5241 * 1.28^{1.46} + \frac{2^2}{2 * 9.81 * 3.33} = 2.2$$

$$=> H_s = \frac{101{,}300 - 2{,}985.7}{998 * 9.81} + \frac{2^2}{2 * 9.81} - 2.2 * 3.33 = \underline{\mathbf{2.9m}}$$

14.3 Design of the blade

The calculation of the blade characteristics is rather bulky; thus all the established values were calculated via Excel. But for a better understanding the calculation of the diameter D_e is listed below.

14.3.1 Velocities and the angles angle of distortion (180°-β_∞)

$d = D_e = 0.73m$

$n = 10s^{-1}$

$H_n = 3.33m$

$H_1 = 3.26m$

$H_2 = 3.4m$

$Q = 3m^3/s$

$D_i = 0.24m$

$$u = \pi * n * d \quad => u = \pi * 10 * 0.73 = \underline{\mathbf{22.93m/s}}$$

$$c_{u1} = \frac{H_1 * g}{u} \quad => c_{u1} = \frac{3.26 * 9.81}{22.93} = \underline{\mathbf{1.39m/s}}$$

$$c_{u2} = \frac{H_2 * g}{u} \quad => c_{u2} = \frac{3.4 * 9.81}{22.93} = \underline{\mathbf{1.45m/s}}$$

$$w_{u1} = c_{u1} - u \quad => w_{u1} = 1.39 - 22.93 = \underline{\mathbf{-21.54m/s}}$$

$$w_{u2} = c_{u2} - u \quad => w_{u2} = 1.45 - 22.93 = \underline{\mathbf{-21.48m/s}}$$

$$w_{u\infty} = \frac{w_{u1} + w_{u2}}{2} \quad => w_{u\infty} = \frac{-21.54 + (-21.48)}{2} = \underline{\mathbf{-21.51m/s}}$$

$$w_m = \frac{Q}{A_\infty}$$

$$A_\infty = \frac{\pi * \left(D_e^2 - D_i^2\right)}{4} \quad => A_\infty = \frac{\pi * \left(0.73^2 - 0.24^2\right)}{4} = 0.37$$

$$=> w_m = \frac{3}{0.37} = \underline{\mathbf{8m/s}}$$

$$w_1 = \sqrt{w_{u1}^2 + w_m^2} \quad => w_1 = \sqrt{-21.54^2 + 8^2} = \underline{\mathbf{22.98m/s}}$$

$$w_2 = \sqrt{w_{u2}^2 + w_m^2} \quad => w_2 = \sqrt{-21.48^2 + 8^2} = \underline{\mathbf{22.92m/s}}$$

$$w_\infty = \sqrt{w_{u\infty}^2 + w_m^2} \quad => w_\infty = \sqrt{-21.51^2 + 8^2} = \underline{\mathbf{22.95m/s}}$$

$$\beta_\infty = \arccos\frac{w_{u\infty}}{w\infty} \quad => \beta_\infty = \arccos\frac{-21.51}{22.95} = \underline{\mathbf{160°}}$$

$$\left(180^\circ - \beta_\infty\right) = 180^\circ - 160^\circ = \underline{\mathbf{20°}}$$

14.3.2 Calculation of the blade characteristics

Lifting coefficient 1

$w_2 = 22.92m/s$

$w_\infty = 22.95m/s$

$p/\gamma = 10m$

$H_s = 0.45$

$p_{min}/\gamma = 2$

$\eta_s = 0.9$

$c_4 = 2m/s$

$K = 2.6$

$Q = 3m^3/s$

$$\zeta_a = \frac{w_2^2 - w_\infty^2 + 2*g*\left(\frac{p}{\gamma} - H_s - \frac{p_{min}}{\gamma} - \eta_s * \frac{c_3^2 - c_4^2}{2*g}\right)}{K*w_\infty^2}$$

$$c_3 = \frac{Q}{A_3}$$

$$A_3 = \frac{\pi * D_e^2}{4} \quad => A_3 = \frac{\pi * 0.73^2}{4} = 0.42m^2$$

$$=> c_3 = \frac{3}{0.42} = 7.2m/s$$

$$=> \zeta_a = \frac{22.92^2 - 22.95^2 + 2*9.81*\left(10 - 0.45 - 2 - 0.9*\frac{7.2^2 - 2^2}{2*9.81}\right)}{2.6*22.95^2} = \underline{\mathbf{0.08}}$$

Ratio l/t

$\eta_h = 0.9$

$H = 3.7m$

$c_m = w_m = 8m/s$

$w_\infty = 22.95m/s$

$u = 22.93m/s$

$\beta_\infty = 160°$

$\zeta_a = 0.08$

$\lambda = 3°$ (assumption)

$$\frac{l}{t} = \frac{g*\eta_h*H}{w_\infty^2} * \frac{c_m}{u} * \frac{\cos\lambda}{\sin(180 - \beta_\infty - \lambda)} * \frac{1}{\zeta_a}$$

$$=> \frac{l}{t} = \frac{9.81*0.9*3.7}{22.95^2} * \frac{8}{22.93} * \frac{\cos 3}{\sin(180 - 160 - 3)} * \frac{1}{0.08} = \underline{\mathbf{0.92}}$$

This value of l/t does not match exactly with the value in Section 6.2.1 which has a value of 0.95. The values in Section 6.2.1 were established using precise numerical data; however, in the calculation above the numerical data were rounded. This impreciseness will also arise in some of the following calculation. However, these calculations are supposed to show the exact procedure to establish the main characteristics of the blade and thus the impreciseness can be neglected.

Reciprocal value of l/t

$$t/l = \frac{1}{l/t} \quad => t/l = \frac{1}{0.92} = \underline{\mathbf{1.1}}$$

Lifting coefficient ζ_A

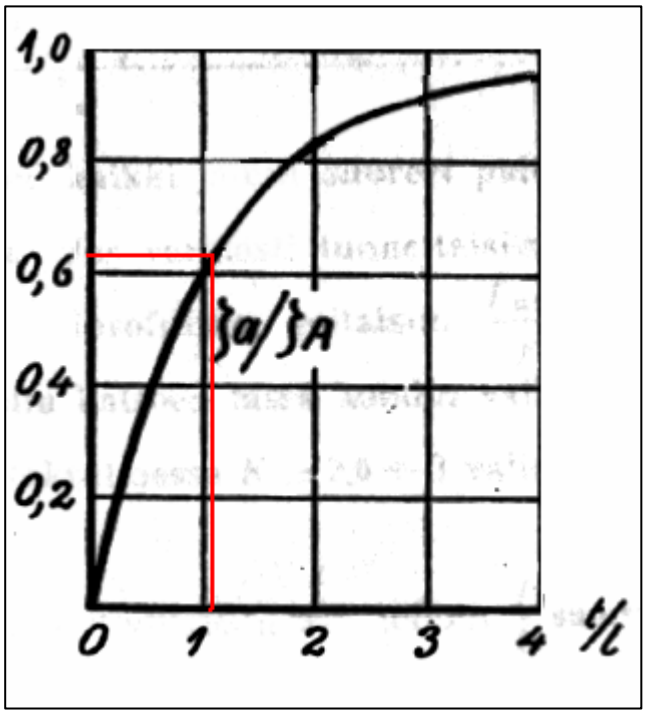

$$=> \zeta_a/\zeta_A = 0.62 \quad => \zeta_A = 0.08/0.62 = \underline{\mathbf{0.13}}$$

Drag coefficient ζ_W

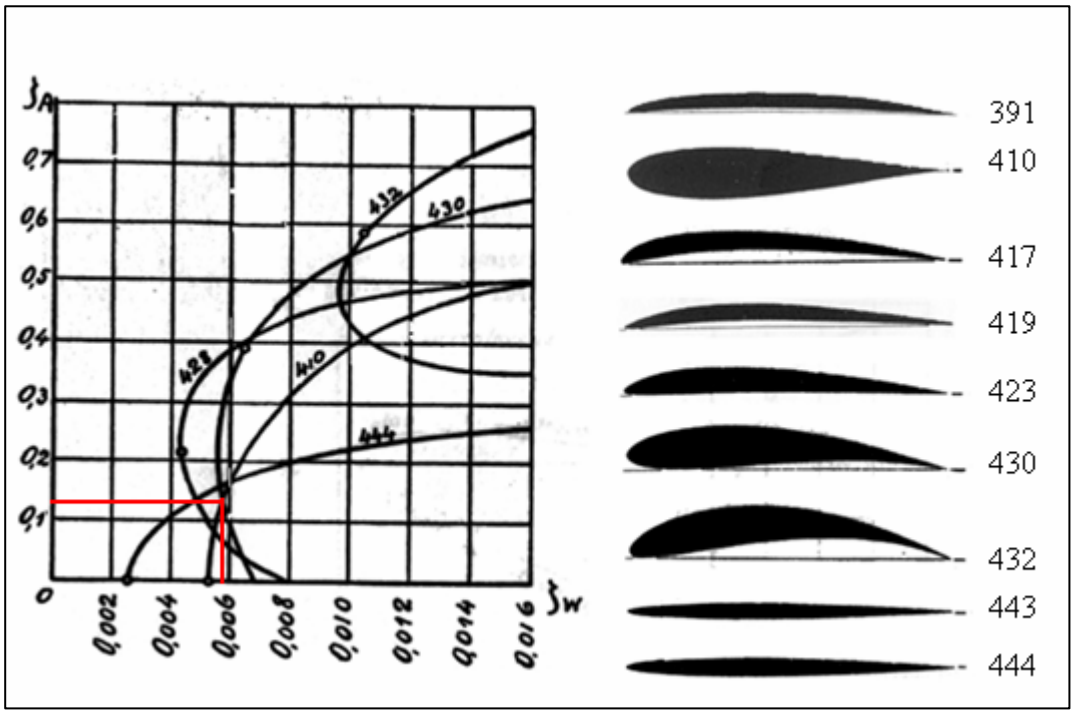

=> ζ_W = **0.0062**

Angle of slip λ

$$\lambda = \arctan\frac{\zeta_W}{\zeta_A} \quad \Rightarrow \lambda = \arctan\frac{0.0062}{0.13} = \underline{\mathbf{2.7°}}$$

It can be assumed that the assumed angle of 3° and the calculated angle are close enough. (In the calculations with the precise values in Section 6.2.1 the calculated angle of slip is even 2.9)

Angle of attack

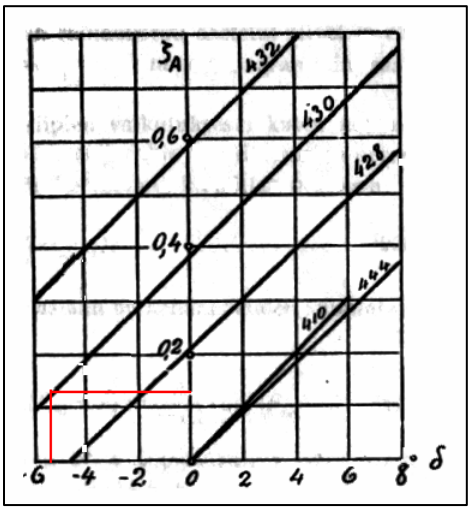

=> δ = **-5.4°**

Exact angle of distortion

$(180° - \beta_\infty - \delta) = 180° - 160° - (-5.4°) = 25.4°$

Now all the significant values of the diameter D_e are known.

14.4 Calculation of the forces

14.4.1 Tangential force

$P = 98kW$

$n = 10s^{-1}$

$z = 4$

$R_e = 0.365m$

$R_i = 0.12m$

$$F_t = \frac{P}{2 * \pi * n * z * r}$$

$$r = \sqrt{\frac{R_e^2 + R_i^2}{2}} \quad => r = \sqrt{\frac{0.365^2 + 0.12^2}{2}} = 0.272m$$

$$=> F_t = \frac{98{,}000}{2 * \pi * 10 * 4 * 0.272} = \underline{\mathbf{1434N}}$$

14.4.2 Axial force

$H_n = 3.33m$

$\alpha = 80°$

$\beta_\infty = 152°$

$\delta = -3.1°$

Via water pressure

$$F_a = g * \rho * H_n * A_b$$

$$A_b = \frac{\pi * \alpha * \left(R_e^2 - R_i^2\right)}{360^\circ} \quad => A_b = \frac{\pi * 80 * \left(0.365^2 - 0.12^2\right)}{360} = 0.083m^2$$

$$=> F_a = 9.81 * 998 * 3.33 * 0.083 = \underline{\mathbf{2{,}706N}}$$

Via the tangential force and blade distortion:

$$F_a = \frac{F_t}{\tan(180^\circ - \beta_\infty - \delta)} \quad => F_a = \frac{1434}{\tan 31} = \underline{\mathbf{2{,}387N}}$$

14.4.3 Resulting force

$$F_r = \sqrt{F_t^2 + F_a^2} \quad => F_r = \sqrt{1434^2 + 2706^2} = \underline{\mathbf{3{,}062N}}$$

14.4.4 Hydraulic moment

$F_r = 3{,}062N$

$A_b = 0.083m^2$

$R_e = 0.365m = 365mm$

$R_i = 0.12m = 120mm$

$\alpha = 80° => \hat{\alpha} = 1.396$

$\varepsilon = 20°$

$$M_h = F_r * e_y$$

$$e_y = \frac{I_s}{y_s * A_b}$$

$$I_s = \frac{R_e^4 - R_i^4}{4} * \left(\frac{\hat{\alpha}}{2} - \sin\frac{\alpha}{2} * \cos\frac{\alpha}{2}\right)$$

$$=> I_s = \frac{365^4 - 120^4}{4} * \left(\frac{1.396}{2} - \sin\frac{80}{2} * \cos\frac{80}{2} \right) = 901{,}718{,}555\text{mm}^4$$

$$y_s = \frac{F_a}{g * \rho * A_b * \cos\varepsilon} \quad => y_s = \frac{2{,}706}{9.81 * 998 * 0.083 * \cos 20} = 3.5\text{m}$$

$$=> e_y = \frac{901{,}718{,}555}{3.5 * 10^3 * 0.083 * 10^6} = 3.1\text{mm}$$

$$=> M_h = 3{,}062 * 3.1 = 9{,}492\text{Nmm}$$

14.4.5 Centrifugal force

$n_{max} = 32s^{-1}$

$\Sigma G_i = 7.65\text{kg}$

$\Sigma G_i * R_i = 1{,}706\text{kgmm}$

$$F_c = M_G * R_{cg} * \omega^2$$

$$M_G = \sum G_i = 7.65\text{kg}$$

$$R_{cg} = \frac{\sum G_i * R_i}{\sum G_i} \quad => R_{cg} = \frac{1{,}706}{7.65} = 223\text{mm} = 0.223\text{m}$$

$$\omega = 2 * \pi * n_{max} \quad => \omega = 2 * \pi * 32 = 201s^{-1}$$

$$=> F_c = 7.65 * 0.223 * 201^2 = \underline{\mathbf{68{,}922N}}$$

14.5 Critical speed

G = 54.2kg

E = 220,000N/mm^2

D = 168.3mm

d = 159.3mm

l = 2m

$$n_c = \frac{1}{2*\pi} * \sqrt{\frac{c_q}{G}}$$

$$c_q = \frac{3*E*I}{l^3}$$

$$I = \frac{\pi}{64} * \left(D^4 - d^4\right) => I = \frac{\pi}{64} * \left(168.3^4 - 159.3^4\right) = 7{,}772{,}160\text{mm}^4$$

$$=> c_q = \frac{3*220{,}000*7{,}772{,}160}{200^3} = 641{,}203\text{N/mm}$$

$$=> n_c = \frac{1}{2*\pi} * \sqrt{\frac{641{,}203}{54.2}} = \underline{\mathbf{17.3s^{-1}}}$$

14.6 Stress analysis

14.6.1 Axle

$\tau_{t\ permissible}$ = 125N/mm^2

r = 272mm

F_t = 1434N

D = 168.3mm

d = 159.3mm

K_A = 1.25

Present tensional stress

$$\tau_t = \frac{K_A * M_t}{W_t}$$

$$M_t = 4 * r * F_t \quad => M_t = 4 * 272 * 1{,}434 = 1{,}560{,}192\text{Nmm}$$

$$W_t = \frac{\pi}{16} * \frac{D^4 - d^4}{D} \quad => W_t = \frac{\pi}{16} * \frac{168.3^4 - 159.3^4}{168.3} = 184{,}722\text{mm}^3$$

$$=> \tau_t = \frac{1.25 * 156{,}0192}{184{,}722} = \underline{\mathbf{10.6N/mm^2}} < 125\text{N/mm}^2$$

14.6.2 Blade

Bending:

The calculation to establish the thickness of the blade should be shown on the basis of the radius R_e.

$F_r = 3062\text{N}$

$\sigma_{bpermissible} = 450\text{N/mm}^2$

$h = 60\text{mm}$

$R_e = 365\text{mm}$

$r = R_i = 120\text{mm}$ (variable)

$$y = \sqrt{\frac{6 * F_r * z}{h * \sigma_{bpermissible}}}$$

$$z = R_e - r \quad => z = 365 - 120 = 245\text{mm}$$

$$=> y = \sqrt{\frac{6 * 3{,}062 * 245}{60 * 450}} = \underline{\mathbf{13mm}}$$

Torsion:

$\tau_{t\ permissible} = 270N/mm^2$

$M_h = 94{,}920Nmm$

$y = 8mm$

$K_A = 1.25$

Present tensional sterss

$$\tau_t = \frac{K_A * M_h}{W_t}$$

$$W_t = \frac{c_1}{c_2} * h * y^2$$

$$\frac{h}{y} = \frac{60}{8} = 7.5 \quad \Rightarrow c_1 = 0.307 \text{ and } c_2 = 0.999 \text{ (see table 14.3)}$$

$$\Rightarrow W_t = \frac{0.307}{0.999} * 60 * 8^2 = 1{,}180$$

$$\Rightarrow \tau_t = \frac{1.25 * 94{,}920}{1{,}180} = \underline{\mathbf{101N/mm^2}} < 270N/mm^2$$

14.6.3 Pivot

Contact pressure:

$p_{permissible} = 90N/mm^2$

$F_r = 3{,}062$

$d = 45mm$

$b = 30mm$

$K_A = 1.25$

Present contact pressure

$$p = \frac{K_A * F_r}{A_{proj}}$$

$$A_{proj} = b * d \quad => A_{proj} = 30 * 45 = 1350mm^2$$

$$=> \quad p = \frac{1.25 * 3062}{1,350} = \underline{\mathbf{2.8N/mm^2}} < 90N/mm^2$$

Torsion:

$\tau_{t\ permissible} = 225N/mm^2$

$M_h = 94,920Nmm$

Present tensional stress

$$\tau_t = \frac{K_A * M_h}{W_t}$$

$$W_t = \frac{\pi * d^3}{16} \quad => W_t = \frac{\pi * 45^3}{16} = 17,892mm^3$$

$$=> \tau_t = \frac{1.25 * 94,920}{17,892} = \underline{\mathbf{6.6N/mm^2}} < 225N/mm^2$$

Bending:

$\sigma_{bpermissible} = 175N/mm^2$

$l = 212mm$

Present bending stress

$$\sigma_b = \frac{K_A * M_b}{W_{b\,min}}$$

$$M_b = l * F_r \quad => M_b = 212 * 3,062 = 649,144Nmm$$

$$W_{b\,min} = \frac{\pi * d^3}{32} \quad => W_{b\,min} = \frac{\pi * 45^3}{32} = 8,946mm^3$$

$$=> \sigma_b = \frac{1.25 * 649,144}{8,946} = \underline{\mathbf{90N/mm^2}} < 175N/mm^2$$

14.6.4 Lever

Bending:

$\sigma_{bpermissible} = 175N/mm^2$

$M_h = 94{,}920Nmm$

$l = 40$

$b_2 = 10mm$

$d = 12mm$

$K_A = 1.25$

Present bending stress

$$\sigma_b = \frac{K_A * M_b}{W_{b\,min}}$$

$$M_b = b_2 * F$$

$$F = \frac{M_h}{l} \quad => F = \frac{94{,}920}{40} = 2{,}373N$$

$$=> M_b = 10 * 2{,}373 = 23{,}730Nmm$$

$$W_{b\,min} = \frac{\pi * d^3}{32} \quad => W_{b\,min} = \frac{\pi * 12^3}{32} = 170mm^3$$

$$=> \sigma_b = \frac{1.25 * 23{,}730}{170} = \underline{\mathbf{174N/mm^2}} < 175N/mm^2$$

Shear:

$R_{p0,2} = 550N/mm^2$

$F = 2{,}373N$

Permissible shear stress

$$\tau_{spermissible} = \frac{R_{p0.2}}{1.5} \quad => \tau_{spermissible} = \frac{550}{1.5} = 367N/mm^2$$

Present shear stress

$$\tau_s = \frac{K_A * F}{A}$$

$$A = \frac{\pi * d^2}{4} \quad => A = \frac{\pi * 12^2}{4} = 113mm^2$$

$$=> \tau_s = \frac{1.25 * 2{,}373}{113} = \underline{\mathbf{26N/mm^2}} < 140N/mm^2$$

Contact pressure:

$p_{permissible} = 90N/mm^2$

Present contact pressure

$$p = \frac{K_A * F}{A_{proj}}$$

$$A_{proj} = b_2 * d \quad => A_{proj} = 10 * 12 = 120mm^2$$

$$=> p = \frac{1.25 * 2{,}373}{120} = \underline{\mathbf{25\ N/mm^2}} < 90N/mm^2$$

14.6.5 Link

Buckling:

$\sigma_{kpermissible} = 170N/mm^2$

$l = 70mm$

$B = 4mm$

$H = 8mm$

$b_2 = 10mm$

$h = 4mm$

$\sigma_{d0.2} = R_{p0.2} = 230N/mm^2$

$E = 220{,}000N/mm^2$

$F = 2373N$

$K_A = 1.25$

Buckling case II

$\Rightarrow l_k = l = 70mm$

Thickness ratio:

$$\lambda = l_k * \sqrt{\frac{A}{I_{min}}}$$

$$A = 2*B*H + b_2*h \quad \Rightarrow A = 2*4*8 + 10*4 = 104mm^2$$

$$I_{min} = \frac{2*B*H^3 + b_2*h^3}{12} \quad \Rightarrow I_{min} = \frac{2*4*8^3 + 10*4^3}{12} = 395mm^4$$

$$\Rightarrow \lambda = 70*\sqrt{\frac{104}{395}} = 36$$

Marginal thickness ratio

$$\lambda_{g0.2} = \pi*\sqrt{\frac{E}{\sigma_{d0.2}}} \quad \Rightarrow \lambda_{g0.2} = \pi*\sqrt{\frac{220{,}000}{230}} = 97 > 36$$

$$=> \sigma_k = \frac{K_A * F}{A} \quad => \sigma_k = \frac{1.25 * 2{,}373}{104} = \underline{\mathbf{29N/mm^2}} < 170N/mm^2$$

Stress calculation of the links eye:

$R_m = 420N/mm^2$

$c = 5mm$

$b_1 = 10mm$

$d_3 = 12mm$

Permissible stress

$$\sigma_{permissible} = 0.5 * R_m \quad => \sigma_{permissible} = 0.5 * 420 = 210N/mm^2$$

Present stress

$$\sigma = \frac{K_A * F}{2 * c * b_1} * \left[1 + \frac{3}{2} * \left(\frac{d_3}{c} + 1\right)\right]$$

$$=> \sigma = \frac{1.25 * 2{,}373}{2 * 5 * 10} * \left[1 + \frac{3}{2} * \left(\frac{12}{5} + 1\right)\right] = \underline{\mathbf{181N/mm^2}} < 210N/mm^2$$

14.6.6 Crosshead

$R_m = 420N/mm^2$

F = 2,373

c = 5mm

b = 8mm

d = 12mm

$K_A = 1.25$

Permissible stress

$$\sigma_{permissible} = 0.5 * R_m \quad => \sigma_{permissible} = 0.5 * 420 = 210N/mm^2$$

Present stress

$$\sigma = \frac{K_A * \frac{1}{2}F}{2 * c * b} * \left[1 + \frac{3}{2} * \left(\frac{d}{c} + 1\right)\right]$$

$$=> \sigma = \frac{1.25 * 1186.5}{2 * 5 * 8} * \left[1 + \frac{3}{2} * \left(\frac{12}{5} + 1\right)\right] = \underline{\mathbf{113N/mm^2}} < 210N/mm^2$$

14.6.7 Bolt

Bending:

$\sigma_{bpermissible} = 215N/mm^2$

F = 2,373N

$l_1 = 20mm$

$l_2 = 10mm$

$l_3 = 8mm$

d = 12mm

$K_A = 1.25$

Present bending stress

$$\sigma_b = \frac{K_A * M_b}{W_{b\,min}}$$

$$M_b = \frac{F*(l_1+l_2+l_3)}{8} \quad => M_b = \frac{2373*(20+10+8)}{8} = 11{,}272\text{Nmm}$$

$$W_{b\,min} = \frac{\pi*d^3}{32} \quad => W_{b\,min} = \frac{\pi*12^3}{32} = 170\text{mm}^3$$

$$=> \sigma_b = \frac{1.25*11{,}272}{170} = \underline{\mathbf{83N/mm^2}} < 215\text{N/mm}^2$$

Shear:

$R_m = 430\text{N/mm}^2$

Permissible shear stress

$$\tau_{spremissible} = 0.2*R_m \quad => \tau_{spremissible} = 0.2*430 = 86\text{N/mm}^2$$

Present shear stress

$$\tau_s = \frac{4}{3}*\frac{K_A*F}{A_s*2}$$

$$A_s = \frac{\pi*d^2}{4} \quad => A_s = \frac{\pi*12^2}{4} = 113\text{mm}^2$$

$$=> \tau_s = \frac{4}{3}*\frac{1.25*2{,}373}{113*2} = \underline{\mathbf{18N/mm^2}} < 86\text{N/mm}^2$$

Contact pressure:

Permissible shear stress

$$p_{premissible} = 0.35*R_m \quad => p_{premissible} = 0.35*430 = 151\text{N/mm}^2$$

Crosshead:

$$p = \frac{K_A*F}{A_{proj}}$$

$$A_{proj} = (l_1 + l_3) * d \quad => A_{proj} = (20 + 8) * 12 = 336mm^2$$

$$=> p = \frac{1.25 * 2,373}{336} = \underline{\mathbf{9N/mm^2}} < 151N/mm^2$$

Link:

$$p = \frac{K_A * F}{A_{proj}}$$

$$A_{proj} = l_2 * d \quad => A_{proj} = 10 * 12 = 120mm^2$$

$$=> p = \frac{1.25 * 2,373}{120} = \underline{\mathbf{25N/mm^2}} < 151N/mm^2$$

14.6.8 Shaft

Buckling:

$\sigma_{kpermissible} = 170N/mm^2$

$l = 3300mm$

$d = 60mm$

$\sigma_{d0.2} = R_{p0.2} = 230N/mm^2$

$E = 220,000N/mm^2$

$F = 2,373N$

$K_A = 1.25$

Buckling case II

$=> l_k = l = 3300mm$

Thickness ratio:

$$\lambda = l_k * \sqrt{\frac{A}{I_{min}}}$$

$$A = \frac{\pi * d^2}{4} \quad => A = \frac{\pi * 60^2}{4} = 2,827mm^2$$

$$I_{min} = \frac{\pi * d^4}{64} \quad => I_{min} = \frac{\pi * 60^4}{64} = 63{,}6173 mm^4$$

$$=> \lambda = 3300 * \sqrt{\frac{2{,}827}{636{,}173}} = 220$$

Marginal thickness ratio

$$\lambda_{g0.01} = \pi * \sqrt{\frac{E}{0.8 * \sigma_{d0.2}}} \quad => \lambda_{g0.01} = \pi * \sqrt{\frac{220{,}000}{0.8 * 230}} = 109 < 220$$

$$=> \sigma_k = \frac{K_A * \pi^2 * E}{\lambda^2} \quad => \sigma_k = \frac{1.25 * \pi^2 * 220{,}000}{220^2} = \underline{\mathbf{56N/mm^2}} < 170 N/mm^2$$

14.7 Calculation of the screws

14.7.1 Screw connection of the lever and the pivot

Step1: Pre-selection

$z = 3$

$F_B = 68{,}922N$

$M_h = 94{,}920$

$r = 15mm$

$K_A = 1.25$

$F_B = 68{,}922N$ => $F_{Bs} = 22{,}974kN$ per screw => M12 class 12.9 (see table 14.4)

$$F_Q = \frac{K_A * M_h}{r} \quad => F_Q = \frac{1.25 * 94{,}920}{15} = 7910N \quad => F_{Qs} = 26{,}37N \text{ per screw}$$

=> M12 class 12.9 (see table 14.4)

Step2: Roughly calculation of the contact pressure

$p_{permissible} = 300N/mm^2$

$F_{sp} = 68.5kN = 68{,}500N$ (see table 14.5)

$d_w = 18mm$ (see table 14.6)

$d_h = 13mm$ (see table 14.6)

Contact pressure

$$p = \frac{F_{sp}}{0.9 * A_p}$$

$$A_p = \frac{\pi * \left(d_w^2 - d_h^2\right)}{4} \quad => A_p = \frac{\pi * \left(18^2 - 13^2\right)}{4} = 122mm^2$$

$$=> p = \frac{68{,}500}{0.9 * 122} = 624N/mm^2 > 300N/mm^2$$

=> A washer is necessary

d_2 = 24mm (see table 14.6)

$$=> A_p = \frac{\pi * (d_2^2 - d_h^2)}{4} \quad => A_p = \frac{\pi * (24^2 - 13^2)}{4} = 320mm^2$$

$$=> p = \frac{68,500}{0.9 * 320} = \underline{\mathbf{238N/mm^2}} < 300N/mm^2$$

Step3: Calculation of the required assembly preload force

k_A = 1.6 (see table 14.8)

μ = 0.5 (see table 14.9)

n = 0.5

l_k = 12.5mm

E_T = 216,000N/mm^2

E_S = 220,000N/mm^2

d = 12mm

l = 12.5mm

A_3 = 76.25mm^2 (see table 14.10)

f_Z = 0.023 (see table 14.11)

$$F_{VM} = k_A * [F_{Kl} + F_{Bs} * (1 - \Phi) + F_Z]$$

$$F_{Kl} = \frac{F_Q}{\mu * z} \quad => F_{Kl} = \frac{6,328}{0,5 * 3} = 4,218N$$

$$\Phi = n * \Phi_K$$

$$\Phi_K = \frac{\delta_T}{(\delta_T + \delta_S)}$$

$$\delta_T = \frac{l_k}{A_{ers} * E_T}$$

$$A_{ers} = \frac{\pi}{4} * (d_w - d_h) + \frac{\pi}{8} * d_w * (D_A - d_w) * \left[(x+1)^2 - 1\right]$$

$$D_A = d_w + l_k \quad => D_A = 18 + 12.5 = 30.5\text{mm}$$

$$x = \sqrt[3]{\frac{l_k * d_w}{D_A^2}} \quad => x = \sqrt[3]{\frac{12.5 * 18}{30.5^2}} = 0.62$$

$$=> A_{ers} = \frac{\pi}{4} * (18 - 13) + \frac{\pi}{8} * 18 * (30.5 - 18) * \left[(0.62+1)^2 - 1\right] = 147\text{mm}^2$$

$$=> \delta_T = \frac{12.5}{147 * 216{,}000} = 3.9*10^{-7}\text{mm/N}$$

$$\delta_S = \frac{1}{E_S} * \left(\frac{0.4 * d}{A_N} + \frac{1}{A_3} + \frac{0.5 * d}{A_3} + \frac{0.4 * d}{A_N} \right)$$

$$A_N = \frac{\pi * d^2}{4} \quad => A_N = \frac{\pi * 12^2}{4} = 113\text{mm}^2$$

$$=> \delta_S = \frac{1}{220{,}000} * \left(\frac{0.4 * 12}{113} + \frac{12.5}{76.25} + \frac{0.5 * 12}{76.25} + \frac{0.4 * 12}{113} \right) = 1.5*10^{-6}\text{mm/N}$$

$$=> \Phi_K = \frac{3.9 * 10^{-7}}{\left(3.9 * 10^{-7} + 1.5 * 10^{-6}\right)} = 0.21$$

$$=> \Phi = 0.5 * 0.21 = 0.105$$

$$F_Z = \frac{f_Z}{(\delta_S + \delta_T)} \quad => F_Z = \frac{0.023}{\left(1.5 * 10^{-6} + 3.9 * 10^{-7}\right)} = 12{,}169\text{N}$$

$$=> F_{VM} = 1.6 * \left[4{,}218 + 22{,}974 * (1 - 0.105) + 12{,}169\right] = \underline{\mathbf{59{,}118N}} < 68{,}500\text{N}$$

Step4: Caculation of the required tightening torque

M_{sp} = 137Nm (see table 14.5)

$$M_A = 0.9 * M_{sp} \quad => M_A = 0.9 * 137 = \underline{\mathbf{123Nm}}$$

Step5: Maximum permissible screw force

$R_{p0.2}$ = 1,080N/mm^2 (see table 14.12)

A_s = 84.3mm^2 (see table 14.10)

$$\Phi * F_{Bs} \leq 0.1 * R_{p0.2} * A_s \quad => 0.105 * 22{,}974 \leq 0.1 * 1{,}080 * 84.3$$

=>**<u>2,412N ≤9,104N</u>**

Step6: Exact calculation of the contact pressure

$$p = \frac{F_{sp} + \Phi * F_{Bs}}{A_p} \quad => p = \frac{68{,}500 + 0.105 * 22{,}974}{320} = \underline{\mathbf{222N/mm^2}}$$

<u>Chosen screw: ISO 4017 M12x25 class 12.9</u>

14.7.2 Screw connection of pivot and flange

Step1: Pre-selection

$z = 8$

$F_B = 68{,}922N$

$M_h = 94{,}920$

$r = 35mm$

$K_A = 1.25$

$F_B = 68{,}922N$ => $F_{Bs} = 8{,}615N$ per screw => M8 class 12.9 (see table 14.4)

$$F_Q = \frac{K_A * M_h}{r} \quad => F_Q = \frac{1.25 * 94{,}920}{35} = 3{,}390N \quad => F_{Qs} = 424N \text{ per screw}$$

=> M8 class 12.9 (see table 14.4)

Step2: Roughly calculation of the contact pressure

$p_{permissible} = 360N/mm^2$

$F_{sp} = 29.5kN = 29{,}500N$ (see table 14.5)

$d_1 = 13mm$ (see table 14.7)

$d_h = 8.4mm$ (see table 14.6)

Contact pressure

$$p = \frac{F_{sp}}{0.9 * A_p}$$

$$A_p = \frac{\pi * (d_1^2 - d_h^2)}{4} \quad => A_p = \frac{\pi * (13^2 - 8.4^2)}{4} = 77mm^2$$

$$=> p = \frac{29{,}500}{0.9 * 77} = 426N/mm^2 > 360N/mm^2$$

=> A washer is necessary

$d_2 = 16mm$ (see table 14.6)

$$=> A_p = \frac{\pi * (d_2^2 - d_h^2)}{4} \quad => A_p = \frac{\pi * (16^2 - 8.4^2)}{4} = 146mm^2$$

$$=> p = \frac{29{,}500}{0.9 * 146} = \underline{\mathbf{225N/mm^2}} < 360N/mm^2$$

Step3: Calculation of the required assembly preload force

$k_A = 1.6$ (see table 14.8)

$\mu = 0.5$ (see table 14.9)

$n = 0.5$

$l_k = 6.6mm$

$E_T = 216{,}000N/mm^2$

$E_S = 220{,}000N/mm^2$

$d = 8mm$

$l = 6.6mm$

$A_3 = 32.84mm^2$ (see table 14.10)

$f_Z = 0.023$ (see table 14.11)

$$F_{VM} = k_A * [F_{Kl} + F_{Bs} * (1 - \Phi) + F_Z]$$

$$F_{Kl} = \frac{F_Q}{\mu * z} \quad => F_{Kl} = \frac{3{,}390}{0.5 * 8} = 848N$$

$$\Phi = n * \Phi_K$$

$$\Phi_K = \frac{\delta_T}{(\delta_T + \delta_S)}$$

$$\delta_T = \frac{l_k}{A_{ers} * E_T}$$

$$A_{ers} = \frac{\pi}{4} * (d_1 - d_h) + \frac{\pi}{8} * d_1 * (D_A - d_1) * [(x+1)^2 - 1]$$

$$D_A = d_1 + l_k \quad => D_A = 13 + 6.6 = 19.6\text{mm}$$

$$x = \sqrt[3]{\frac{l_k * d_1}{D_A^2}} \quad => x = \sqrt[3]{\frac{6.6*13}{19.6^2}} = 0.61$$

$$=> A_{ers} = \frac{\pi}{4}*(13-8.4) + \frac{\pi}{8}*13*(19.6-13)*\left[(0.61+1)^2 - 1\right] = 57\text{mm}^2$$

$$=> \delta_T = \frac{6.6}{57*216{,}000} = 5.4*10^{-7}\text{mm/N}$$

$$\delta_S = \frac{1}{E_S}*\left(\frac{0.4*d}{A_N} + \frac{1}{A_3} + \frac{0.5*d}{A_3} + \frac{0.4*d}{A_N}\right)$$

$$A_N = \frac{\pi*d^2}{4} \quad => A_N = \frac{\pi*8^2}{4} = 50.3\text{mm}^2$$

$$=> \delta_S = \frac{1}{220{,}000}*\left(\frac{0.4*12}{50.3} + \frac{6.6}{32.84} + \frac{0.5*8}{32.84} + \frac{0.4*8}{50.3}\right) = 2.2*10^{-6}\text{mm/N}$$

$$=> \Phi_K = \frac{5.4*10^{-7}}{\left(5.4*10^{-7} + 2.2*10^{-6}\right)} = 0.2$$

$$=> \Phi = 0.5*0.2 = 0.1$$

$$F_Z = \frac{f_Z}{(\delta_S + \delta_T)} \quad => F_Z = \frac{0.023}{\left(2.2*10^{-6} + 5.4*10^{-7}\right)} = 8{,}394\text{N}$$

$$=> F_{VM} = 1.6*\left[848 + 8{,}615*(1-0.1) + 8{,}394\right] = \underline{\mathbf{27{,}193N}} < 29{,}500\text{N}$$

Step4: Caculation of the required tightening torque

M_{sp} = 39.7Nm (see table 14.5)

$$M_A = 0.9 * M_{sp} \quad => M_A = 0.9 * 39.7 = \underline{\mathbf{35.73Nm}}$$

Step5: Maximum permissible screw force

$R_{p0,2}$ = 1,080N/mm^2 (see table 14.12)

A_s = 36.6mm^2 (see table 14.10)

$$\Phi * F_{Bs} \leq 0.1 * R_{p0.2} * A_s \quad => 0.1 * 8{,}521 \leq 0.1 * 1{,}080 * 36.6$$

=>**<u>852N ≤ 3,953N</u>**

Step6: Exact calculation of the contact pressure

$$p = \frac{F_{sp} + \Phi * F_{Bs}}{A_p} \quad => p = \frac{29{,}500 + 0.1 * 8{,}615}{146} = \underline{\mathbf{208N/mm^2}}$$

<u>Chosen screw: DIN 7984 M8x12 class 12.9</u>

14.7.3 Screw connection between the upper and the middle hub

Step1: Pre-selection

$z = 8$

$F_a = 2{,}706N$

$G = 53.2kg$

$g = 9.81kg/s^2$

$M_t = 1{,}560{,}192Nmm$

$r = 92.6mm$

$K_A = 1.25$

$$F_B = 4 * K_A * F_a + G * g \quad => F_B = 4 * 1.25 * 2{,}706 + 53.2 * 9.81 = 11{,}346$$

=> $F_{Bs} = 1{,}757N$ => M8 class 12.9 (see Table 14.4)

$$F_Q = \frac{K_A * M_t}{r} \quad => F_Q = \frac{1.25 * 1{,}560{,}192}{92.6} = 21{,}061N \quad => F_{Qs} = 2{,}633N \text{ per screw}$$

=> M8 class 12.9 (see table 14.4)

Step2: Roughly calculation of the contact pressure

$p_{permissible} = 230N/mm^2$

$F_{sp} = 29.5kN = 29{,}500N$ (see table 14.4)

$d_l = 13mm$ (see table 14.7)

$d_h = 8.4mm$ (see table 14.6)

Contact pressure

$$p = \frac{F_{sp}}{0.9 * A_p}$$

$$A_p = \frac{\pi * (d_l^2 - d_h^2)}{4} \quad => A_p = \frac{\pi * (13^2 - 8.4^2)}{4} = 77mm^2$$

$$\Rightarrow\ p = \frac{29{,}500}{0.9 * 77} = 426\text{N/mm}^2 > 230\text{N/mm}^2$$

=> A washer is necessary

d_2 = 16mm (see table 14.3)

$$\Rightarrow A_p = \frac{\pi * \left(d_2^2 - d_h^2\right)}{4} \quad \Rightarrow\ A_p = \frac{\pi * \left(16^2 - 8.4^2\right)}{4} = 146\text{mm}^2$$

$$\Rightarrow\ p = \frac{29{,}500}{0.9 * 146} = \underline{\mathbf{225\text{N/mm}^2}} < 230\text{N/mm}^2$$

Step3: Calculation of the required assembly preload force

k_A = 1.6 (see table 14.8)

μ = 0.5 (see table 14.9)

n = 0.5

l_k = 6.6mm

E_T = 200,000N/mm^2

E_S = 220,000N/mm^2

d = 8

l = 6.6

A_3 = 32.84mm^2 (see table 14.10)

f_Z = 0.023 (see table 14.11)

$$F_{VM} = k_A * \left[F_{Kl} + F_{Bs} * (1 - \Phi) + F_Z\right]$$

$$F_{Kl} = \frac{F_Q}{\mu * z} \quad \Rightarrow\ F_{Kl} = \frac{21{,}061}{0.5 * 8} = 5{,}265\text{N}$$

$$\Phi = n * \Phi_K$$

$$\Phi_K = \frac{\delta_T}{(\delta_T + \delta_S)}$$

$$\delta_T = \frac{l_k}{A_{ers} * E_T}$$

$$A_{ers} = \frac{\pi}{4} * (d_1 - d_h) + \frac{\pi}{8} * d_1 * (D_A - d_1) * \left[(x+1)^2 - 1\right]$$

$$D_A = d_1 + l_k \quad => D_A = 13 + 6.6 = 19.6\text{mm}$$

$$x = \sqrt[3]{\frac{l_k * d_1}{D_A^2}} \quad => x = \sqrt[3]{\frac{6.6*13}{19.6^2}} = 0.61$$

$$=> A_{ers} = \frac{\pi}{4} * (13 - 8.4) + \frac{\pi}{8} * 13 * (19.6 - 13) * \left[(0.61+1)^2 - 1\right] = 57\text{mm}^2$$

$$=> \delta_T = \frac{6{,}6}{57 * 200{,}000} = 5.8*10^{-7}\text{mm/N}$$

$$\delta_S = \frac{1}{E_S} * \left(\frac{0{,}4*d}{A_N} + \frac{1}{A_3} + \frac{0{,}5*d}{A_3} + \frac{0{,}4*d}{A_N} \right)$$

$$A_N = \frac{\pi * d^2}{4} \quad => A_N = \frac{\pi * 8^2}{4} = 50.3\text{mm}^2$$

$$=> \delta_S = \frac{1}{220{,}000} * \left(\frac{0.4*8}{50.3} + \frac{6.6}{32.84} + \frac{0.5*8}{32.84} + \frac{0.4*8}{50.3} \right) = 2*10^{-6}\text{mm/N}$$

$$=> \Phi_K = \frac{5.8*10^{-7}}{\left(5.8*10^{-7} + 2*10^{-6}\right)} = 0.22$$

$$=> \Phi = 0.5 * 0.21 = 0.11$$

$$F_Z = \frac{f_Z}{(\delta_S + \delta_T)} \quad => F_Z = \frac{0.023}{\left(2*10^{-6} + 5.8*10^{-7}\right)} = 8{,}915\text{N}$$

=> $F_{VM} = 1.6 * [5{,}265 + 1757 * (1 - 0.11) + 8{,}915] =$ **25,190N** < 29,500N

Step4: Calculation of the required tightening torque

M_{sp} = 39.7Nm (see table 14.5)

$M_A = 0.9 * M_{sp}$ => $M_A = 0.9 * 39.7 =$ **35.7Nm**

Step5: Maximum permissible screw force

$R_{p0,2}$ = 1,080N/mm^2 (see table 14.12)

A_s = 36.6mm^2 (see table 14.10)

$\Phi * F_{Bs} \leq 0.1 * R_{p0.2} * A_s$ => $0.11 * 1418 \leq 0.1 * 1{,}080 * 36.6$

=>**193N ≤3,953N**

Step6: Exact calculation of the contact pressure

$p = \frac{F_{sp} + \Phi * F_{Bs}}{A_p}$ => $p = \frac{29{,}500 + 0.11 * 1{,}757}{146} =$ **203N/mm^2**

Chosen screw: DIN 7984 M8x16 class 12.9

14.8 Drawings

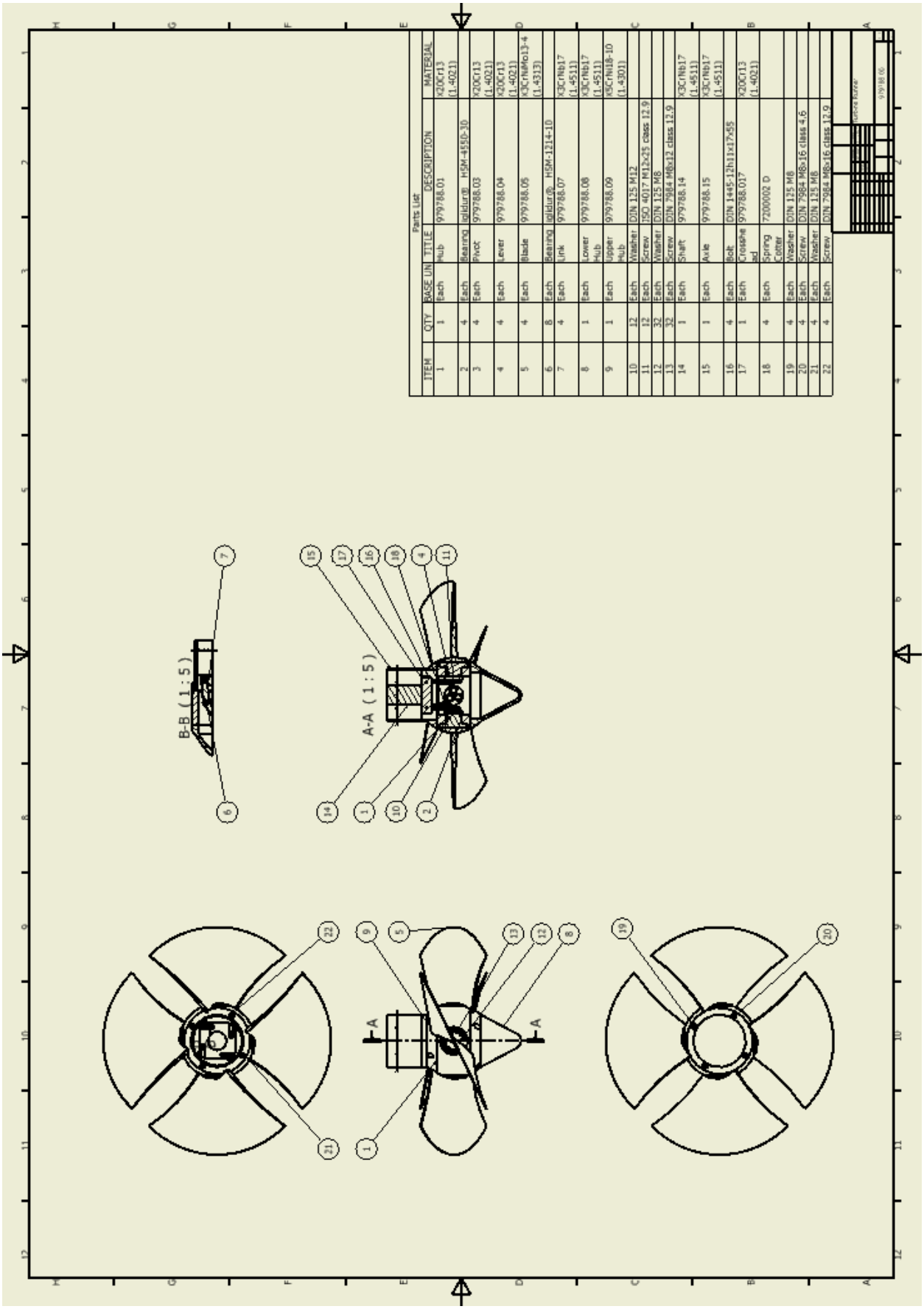

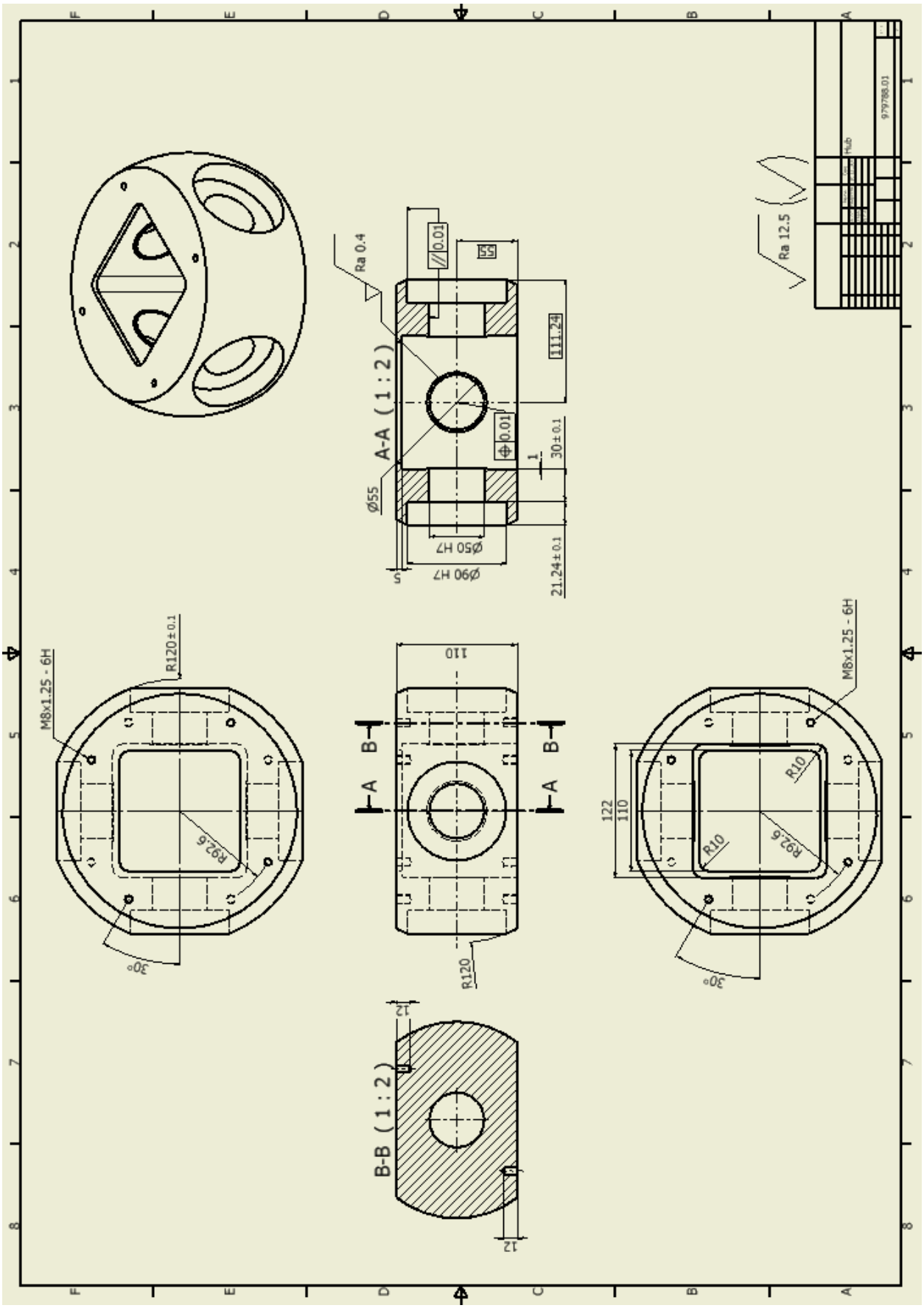
A-A (1 : 2)
B-B (1 : 2)
Ra 0.4
Ra 12.5
0.01
55
111.24
30±0.1
21.24±0.1
Ø55
Ø50 H7
Ø90 H7
5
1
110
R120
R120±0.1
M8x1.25 - 6H
R92.6
30°
122
R10
12
A
B
979788.01
Hub

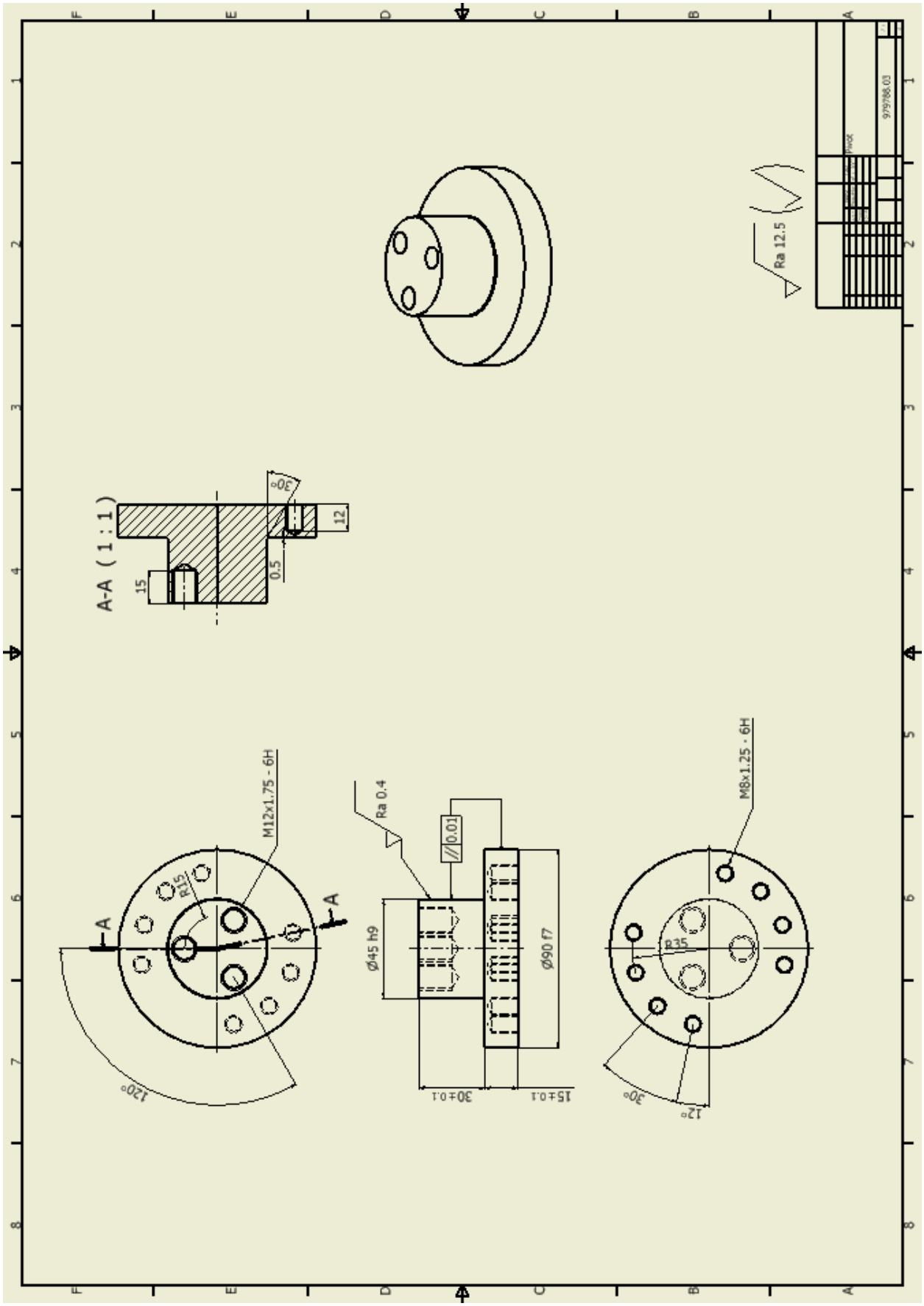
A-A (1 : 1)
15
0.5
12
30°
M12x1.75 - 6H
R15
A
A
120°
Ø45 h9
Ra 0.4
//0.01
30±0.1
15±0.1
Ø90 f7
M8x1.25 - 6H
R35
30°
12°
Ra 12.5
979786.03

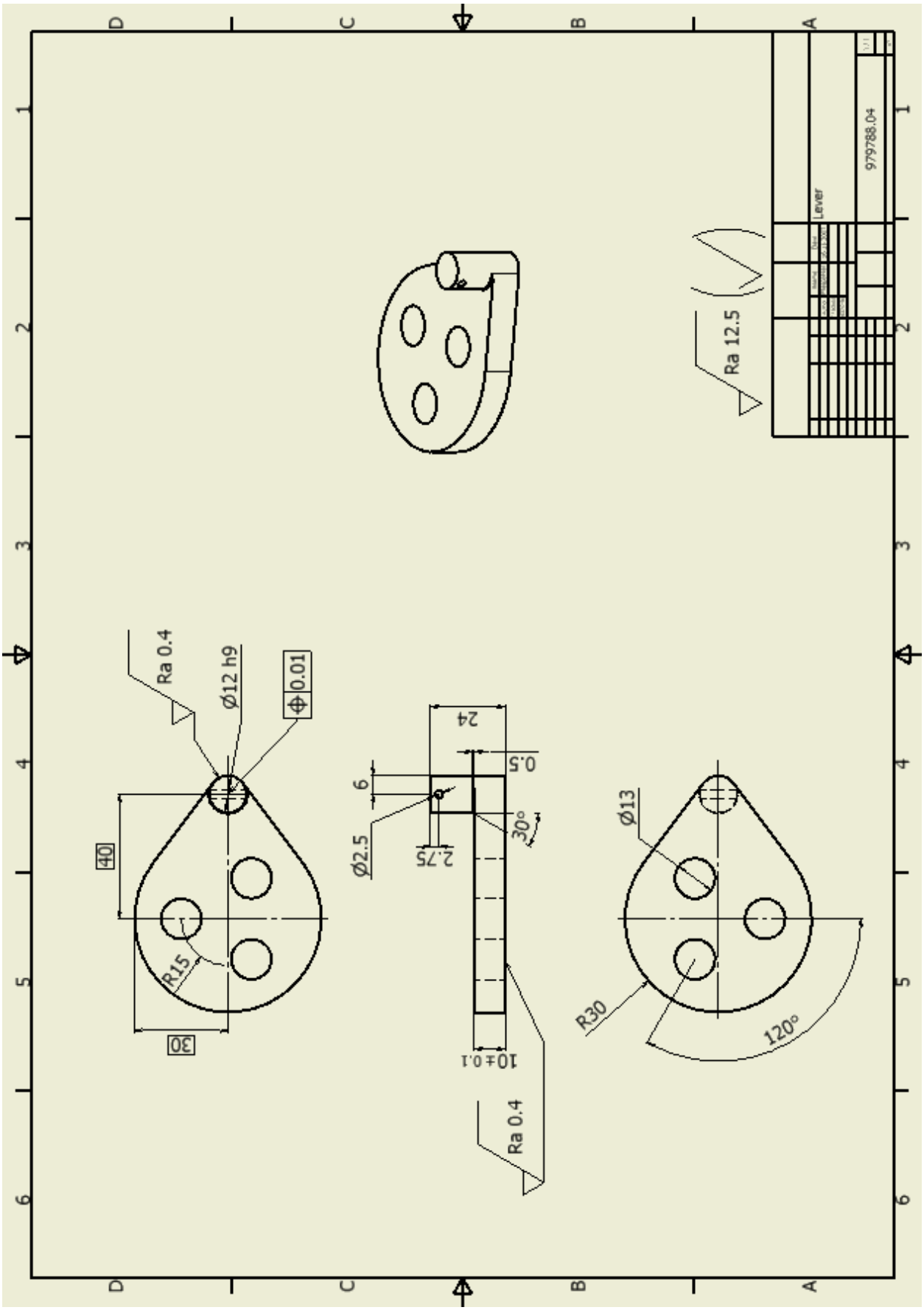
Ra 0.4
Ø12 h9
0.01
40
30
R15
Ø2.5
6
2.75
24
0.5
30°
10±0.1
Ra 0.4
Ø13
R30
120°
Ra 12.5
Lever
979788.04

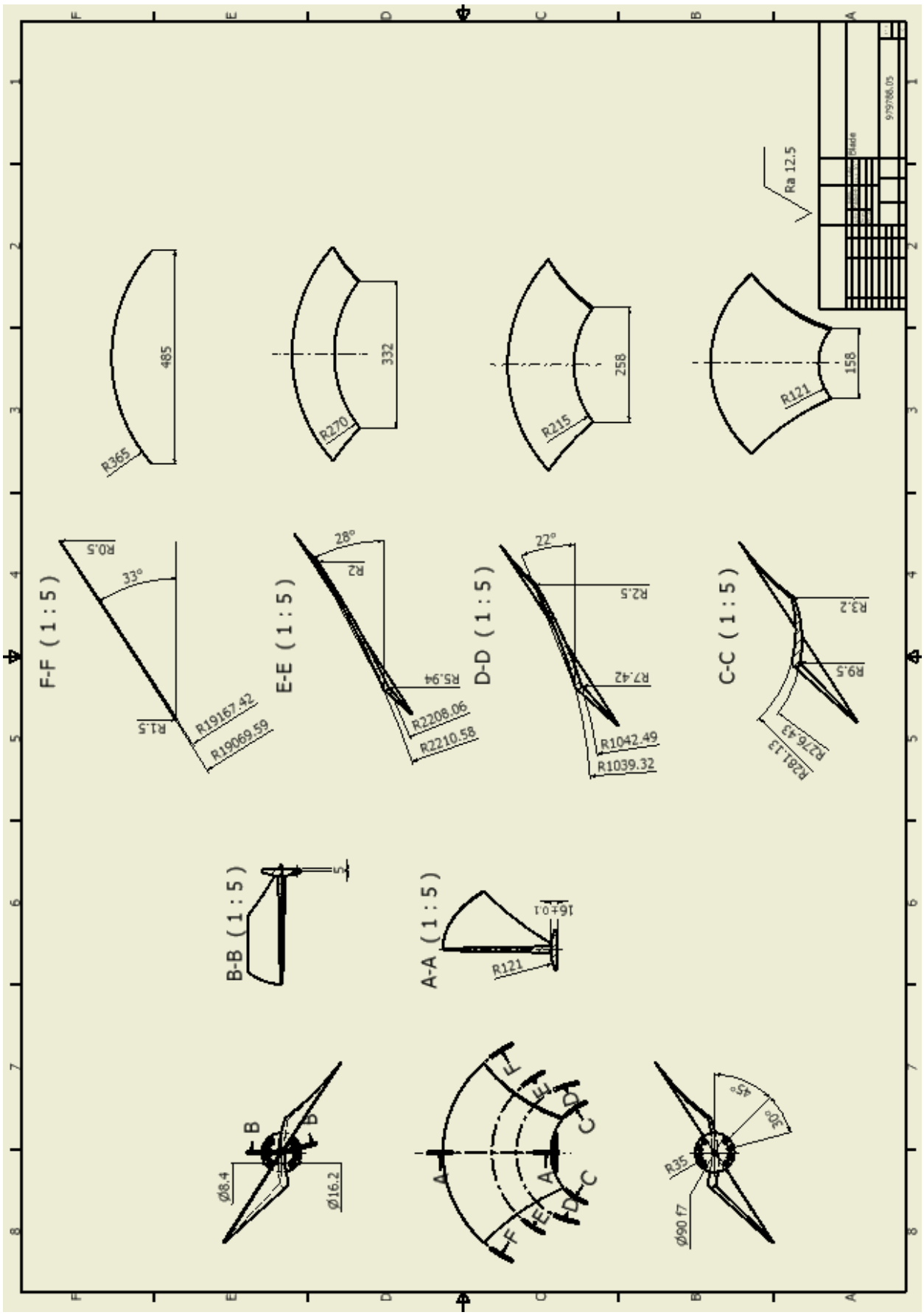
F-F (1 : 5)
E-E (1 : 5)
D-D (1 : 5)
C-C (1 : 5)
B-B (1 : 5)
A-A (1 : 5)
Ra 12.5
R365
485
R270
332
R215
258
R121
158
R0.5
33°
R1.5
R19167.42
R19069.59
28°
R2
R5.94
R2208.06
R2210.58
22°
R2.5
R7.42
R1042.49
R1039.32
R3.2
R9.5
R276.43
R281.13
Ø8.4
Ø16.2
16±0.1
R35
Ø90 f7
30°
45°

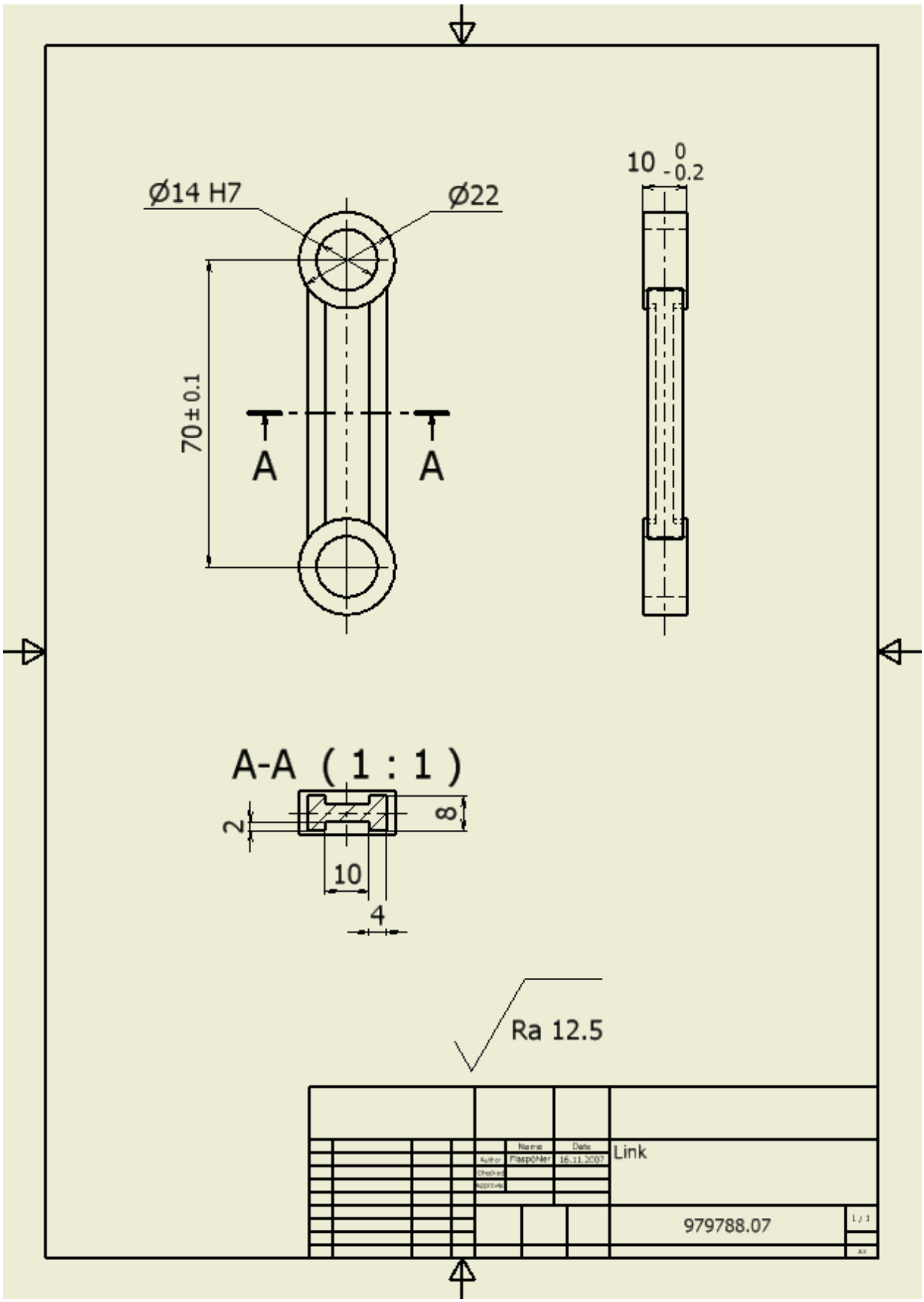
Ø14 H7
Ø22
10 0 -0.2
70 ± 0.1
A
A
A-A (1 : 1)
2
8
10
4
Ra 12.5
Author
Name
Date
Flaspöhler
16.11.2007
Link
979788.07

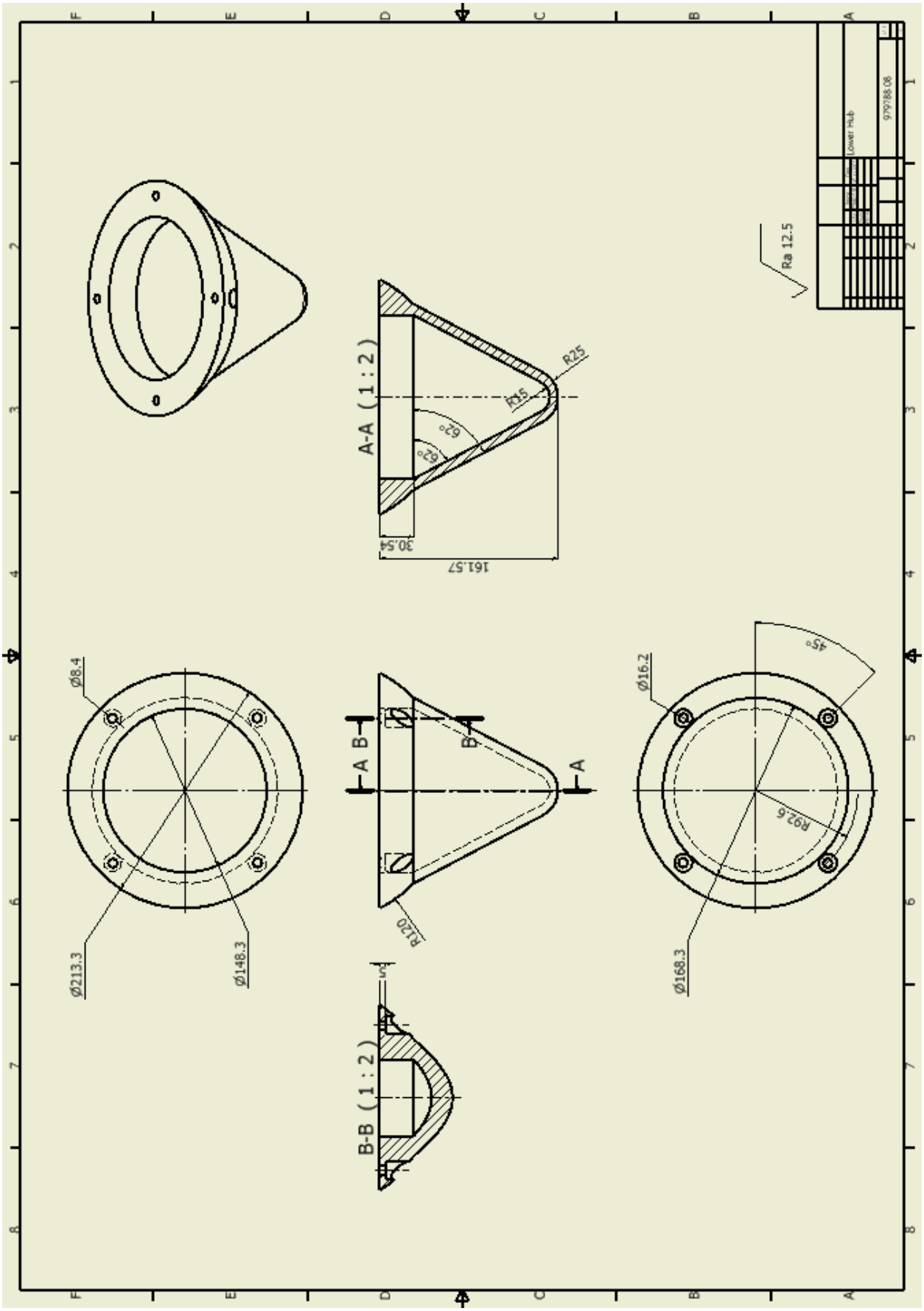
A-A (1 : 2)
R25
R25
62°
62°
30.54
161.57
Ø8.4
Ø213.3
Ø148.3
A B
B
A
R120
B-B (1 : 2)
Ø16.2
45°
R92.6
Ø168.3
Ra 12.5
Lower Hub
979188.08

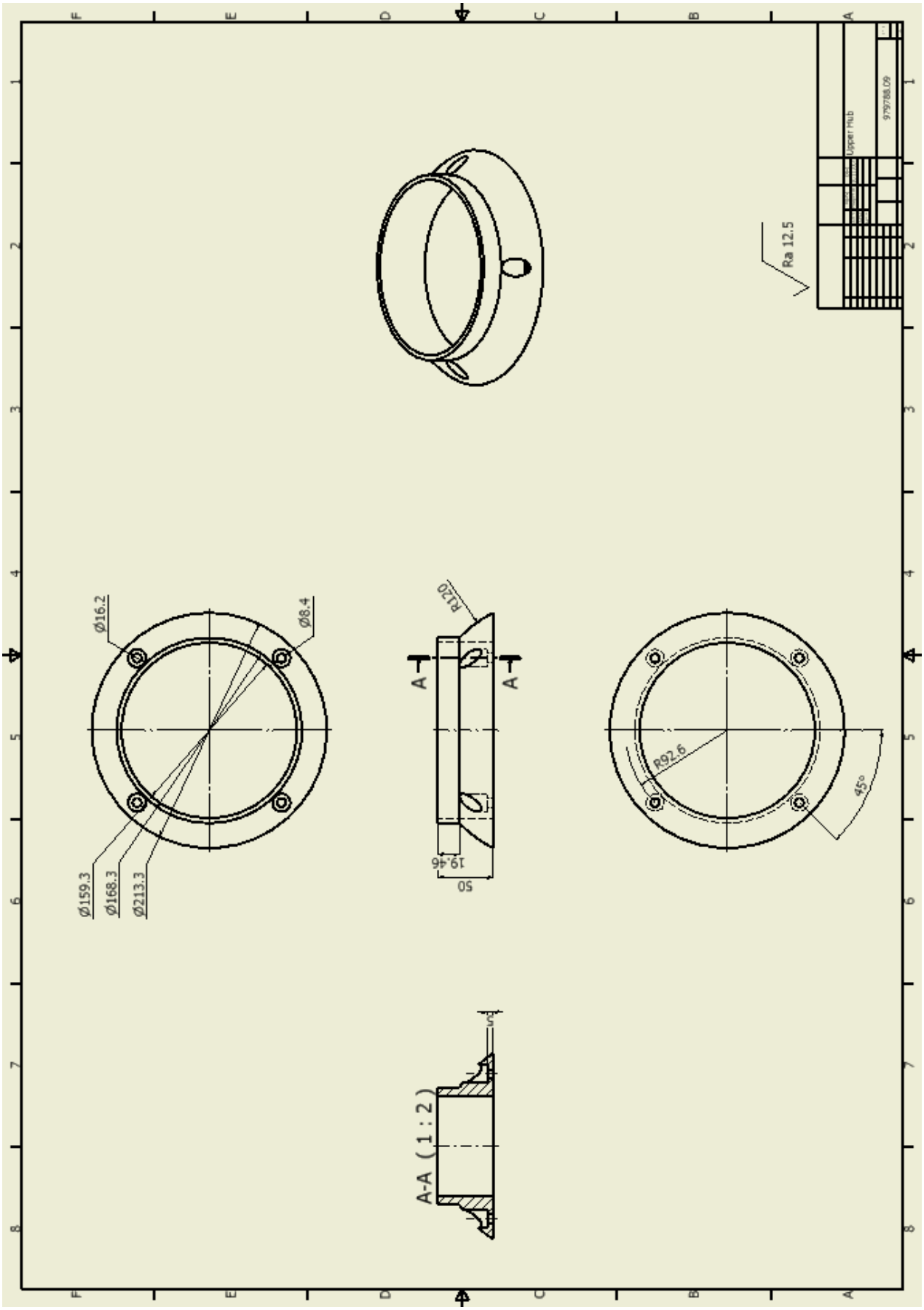
Ø16.2
Ø8.4
Ø159.3
Ø168.3
Ø213.3
R1.20
A
A
50
19.46
R92.6
45°
A-A (1 : 2)
Ra 12.5
Upper Hub
979788.09

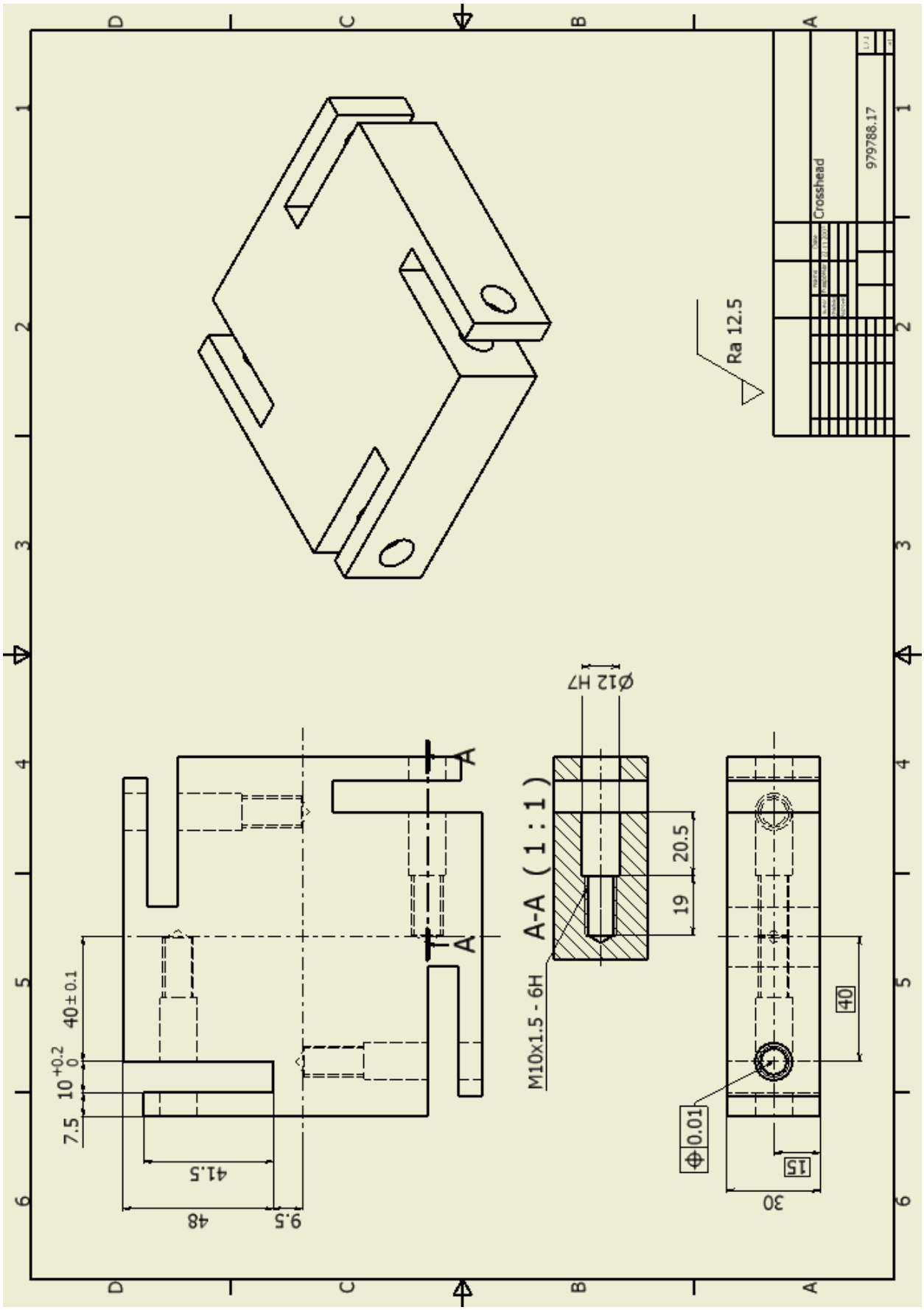
Crosshead
979788.17
Ra 12.5
A-A (1 : 1)
M10x1.5 - 6H
Ø12 H7
20.5
19
40
15
30
0.01
40±0.1
10 +0.2 0
7.5
41.5
48
9.5

14.9 Tables

Table 14.1: Vapor pressure of water /10/

t/°C	0	2	4	6	8	10	12	14	16	18
0	0.6112	0.706	0.8135	0.9353	1.0729	1.2281	1.4027	1.5989	1.8187	2.0646
20	2.3392	2.6452	2.9857	3.3638	3.7809	4.2452	4.7582	5.324	5.9472	6.6324
40	7.3848	8.2096	9.1126	10.1	11.117	12.352	13.632	16.023	16.534	18.173
60	1.,948	21.869	23.946	26.188	28.605	31.21	34.013	37.01	40.24	43.704
80	47.416	51.388	55.636	60.174	65.018	70.183	75.685	81.542	87.771	94.39
100	101.42	108.87	116.78	125.15	134.01	143.38	153.25	163.74	174.77	186.41

Table 14.2: Strength factors /15/

Stahlsorte Kurzname	Werkstoffnummer	A % min.	R_{mN} min.	R_{eN} $R_{p0,2N}$ min.	σ_{zdWN} (σ_{zdSchN})	σ_{bWN} (σ_{bSchN})	τ_{tWN} (τ_{tSchN})	relative Werkstoffkosten[3)]	Eigenschaften und Verwendungsbeispiele	
i) Nichtrostende Stähle nach DIN EN 10088 und SEW 400 Behandlungszustand: Ferritische und austenitische Stähle: geglüht (+A) Martensitische Stähle: vergütet (+QT) Praktisch kein technologischer Größeneinfluss									zeichnen sich durch besondere Beständigkeit gegen chemisch angreifende Stoffe aus; enthalten mindestens 12 % Cr und höchstens 1,2 % C; Beständigkeit beruht auf der Bildung von Deckschichten durch den chemischen Angriff	
X3CrNb17	1.4511	23	420	230	170 (230)	210 (275)	125 (160)		Bauwesen; Beschläge, Regale, Bekleidungen	**Ferritische Stähle** gute Schweißeignung, warmfest, besondere magnetische Eigenschaften, schlecht zerspanbar, kaltumformbar $E=220000\,N/mm^2$
X6CrMoS17	1.4105	20	430	250	170 (250)	215 (300)	130 (175)		Automatenstahl; Bolzen, Befestigungselemente	
X6Cr13	1.4000	19	400	240	160 (240)	200 (290)	120 (165)		Chips-Träger, Bestecke, Innenausbau	
X6Cr17	1.4016	20	450	240	180 (240)	225 (290)	135 (165)		Verbindungselemente, tiefgezogene Formteile	
X20Cr13	1.4021	10	750	550	300 (480)	375 (560)	225 (380)	3,2	Armaturen, Flansche, Federn, Turbinenteile	**Martensitische Stähle** härtbar, gut zerspanbar, hohe Festigkeit, magnetisch, bedingt schweißbar $E=216000\,N/mm^2$
X39CrMo17-1	1.4122	12	750	500	300 (480)	375 (560)	225 (345)		Rohre, Wellen, Spindeln, Verschleißteile	
X14CrMoS17	1.4102	11	640	450	255 (410)	320 (480)	190 (310)		Automatenstahl; Drehteile, Apparatebau	
X50CrMoV15	1.4116	12	850	–	340 (545)	425 (635)	255 (410)		Fleischverarbeitung: Wellen, Muffen, Schneidwerkzeuge	
X12Cr13	1.4006	12	650	450	260 (415)	325 (485)	195 (310)		Verbindungselemente, Schneidwerkzeug, verschleißbeanspruchte Bauteile	
X3CrNiMo13-4	1.4313	11	900	800	360 (575)	450 (675)	270 (460)			
X17CrNi16-2	1.4057	14	750	550	300 (480)	375 (560)	225 (380)	4,0		
X5CrNi18-10	1.4301	40	520	210	210 (210)	250 (250)	145 (145)		universeller Einsatz; Bauwesen, Fahrzeugbau, Lebensmittelindustrie	**Austenitische Stähle** gute Schweißeignung, gut kaltumformbar, schwer zerspanbar, unmagnetisch $E=200000\,N/mm^2$
X8CrNiS18-9	1.4305	35	500	190	190 (190)	230 (230)	130 (130)		Automatenstahl; Maschinen- und Verbindungselemente	
X6CrNiTi18-10	1.4541	40	500	200	200 (200)	240 (240)	140 (140)	5,8	Schienenfahrzeugbau, Baugruppen Sanitärbereich	
X2CrNiMo17-12-2 X2CrNiMoN17-13-3	1.4404 1.4429	40 35	520 580	220 295	220 (220) 230 (295)	260 (260) 290 (355)	150 (150) 175 (205)		Offshore-Technik, geschweißte Konstruktionsteile, Achsen, Wellen, Wärmetauscher	
X5CrNiMo17-12-2	1.4401	40	520	220	220 (220)	260 (260)	150 (150)		Bleichereien, Lebensmittelindustrie, Außenfassaden	
X6CrNiMoTi17-12-2	1.4571	40	520	220	220 (220)	260 (260)	150 (150)		Behälter (Tankwagen), Heizkessel, Dacheindeckungen	
X2CrNiN24-4 **X3CrNiMoN27-5-2** **X2CrNiMoN22-5-3**	1.4362 1.4460 1.4462	25 20 30	600 600 640	400 450 450	240 (385) 240 (385) 255 (410)	300 (450) 300 (450) 320 (480)	180 (275) 180 (305) 190 (310)		Textilindustrie, Apparatebau; geschweißte Bauteile mit hoher Beanspruchung	**Austenitisch-ferritische Stähle** (Duplex-Stähle) beständig gegen Spannungsrisskorrosion $E=200000\,N/mm^2$

Table 14.3: Values of c_1 and c_2 /13/

h/b =	1	1,5	2	3	4	6	8	10	∞
c_1	0,141	0,196	0,229	0,263	0,281	0,298	0,307	0,312	0,333
c_2	0,675	0,852	0,928	0,977	0,990	0,997	0,999	1,000	1,000
c_3	1,000	0,858	0,796	0,753	0,745	0,743	0,743	0,743	0,743

Table 14.4: Nominal diameter of the screws depending on the force /15/

Festigkeitsklasse	Nenndurchmesser in mm für Schaftschrauben bei Kraft je Schraube[1)] F_B bzw. F_Q in kN bis												
	stat. axial	1,6	2,5	4	6,3	10	16	25	40	63	100	160	250
	dyn. axial	1	1,6	2,5	4,0	6,3	10	16	25	40	63	100	160
	quer	0,32	0,5	0,8	1,25	2	3,15	5	8	12,5	20	31,5	50
4.6		6	8	10	12	16	20	24	27	33	–	–	–
4.8, 5.6		5	6	8	10	12	16	20	24	30	–	–	–
5.8, 6.8		4	5	6	8	10	12	14	18	22	27	–	–
8.8		4	5	6	8	8	10	14	16	20	24	30	–
10.9		–	4	5	6	8	10	12	14	16	20	27	30
12.9		–	4	5	5	8	8	10	12	16	20	24	30

Table14.5: Tension force and tension torque /15/

Regel- bzw. Feingewinde	μ_{ges} $= \mu_G$ $= \mu_K$	Schaftschrauben Spannkraft F_{sp} in kN bei Festigkeitsklasse[1)]			Schaftschrauben Spannmoment M_{sp} in Nm bei Festigkeitsklasse[1)]			Dehnschrauben ($d_T \approx 0{,}9\,d_3$) Spannkraft F_{sp} in kN bei Festigkeitsklasse[1)]			Dehnschrauben ($d_T \approx 0{,}9\,d_3$) Spannmoment M_{sp} in Nm bei Festigkeitsklasse[1)]		
		8.8	10.9	12.9	8.8	10.9	12.9	8.8	10.9	12.9	8.8	10.9	12.9
M5	0,08	7,16	10,5	12,3	4,3	6,3	7,3	4,98	7,31	8,55	3,0	4,4	5,1
	0,10	6,90	10,1	11,9	4,9	7,2	8,5	4,75	6,97	8,16	3,4	5,0	5,8
	0,12	6,63	9,74	11,4	5,5	8,1	9,5	4,52	6,64	7,77	3,8	5,5	6,5
	0,14	6,36	9,34	10,9	6,0	8,9	10,4	4,30	6,31	7,39	4,1	6,0	7,0
M6	0,08	10,1	14,9	17,4	7,4	10,9	12,7	6,97	10,2	12,0	5,1	7,5	8,8
	0,10	9,74	14,3	16,7	8,5	12,5	14,7	6,65	9,76	11,4	5,8	8,6	10
	0,12	9,35	13,7	16,1	9,5	14	16,4	6,32	9,29	10,9	6,4	9,5	11,1
	0,14	8,97	13,2	15,4	10,4	15,3	17,9	6,01	8,83	10,3	7,0	10,3	12
M8	0,08	18,5	27,2	31,9	17,9	26,2	30,7	12,9	19	22,2	12,5	18,3	21,4
	0,10	17,9	26,2	30,7	20,6	30,3	35,5	12,3	18,1	21,2	14,2	20,9	24,5
	0,12	17,2	25,2	29,5	23,1	34	39,7	11,8	17,3	20,2	15,8	23,2	27,2
	0,14	16,5	24,2	28,3	25,3	37,2	43,6	11,2	16,4	19,2	17,2	25,3	29,6
M8 × 1	0,08	20,3	29,7	34,8	18,8	27,7	32,4	14,6	21,5	25,1	13,6	20	23,4
	0,10	19,6	28,7	33,6	22	32,3	37,7	14	20,5	24	15,7	23,1	27
	0,12	18,8	27,7	32,4	24,8	36,4	42,6	13,4	19,6	23	17,6	25,8	30,2
	0,14	18,1	26,6	31,1	27,3	40,1	47	12,7	18,7	21,9	19,2	28,2	33
M10	0,08	29,5	43,3	50,7	36	53	61	20,7	30,4	35,6	25	37	43
	0,10	28,4	41,8	48,9	41	61	71	19,8	29,1	34	29	42	50
	0,12	27,3	40,2	47	46	68	80	18,9	27,7	32,4	32	47	55
	0,14	26,2	38,5	45,1	51	75	88	17,9	26,4	30,8	35	51	60
M10 × 1,25	0,08	31,6	46,5	54,4	37	55	64	22,8	33,5	39,2	27	40	46
	0,10	30,6	44,9	52,5	44	64	75	21,9	32,1	37,6	31	46	53
	0,12	29,4	43,2	50,6	49	72	84	20,9	30,6	35,9	35	51	60
	0,14	28,3	41,5	48,6	54	80	93	19,9	29,2	34,2	38	56	65
M12	0,08	43	63,1	73,9	61	90	105	30,3	44,6	52,1	43	63	74
	0,10	41,4	60,9	71,2	71	104	122	29	42,6	49,8	50	73	85
	0,12	39,9	58,5	68,5	80	117	137	27,6	40,6	47,5	55	81	95
	0,14	38,3	56,2	65,8	87	128	150	26,3	38,6	45,2	60	88	103
M12 × 1,25	0,08	48,2	70,8	82,8	65	96	112	35,5	52,1	61	48	71	83
	0,10	46,6	68.4	80,1	77	113	132	34,1	50	58,5	56	82	96
	0,12	44,9	66	77,2	87	128	150	32,6	47,8	56	63	93	108
	0,14	43,2	63,5	74,3	96	141	165	31,1	45,7	53,4	69	102	119
M14	0,08	59	86,7	101	97	143	167	41,8	61,4	71,8	69	101	118
	0,10	56,9	83,6	97,8	113	165	194	39,9	58,6	68,6	79	116	136
	0,12	54,7	80,4	94,1	127	186	218	38,1	55,9	65,4	88	129	151
	0,14	52,6	77,2	90,3	139	205	239	36,2	53,2	62,3	96	141	165
M16	0,08	81	119	139	147	216	253	58,4	85,8	100	106	156	183
	0,10	78,2	115	134	172	252	295	55,9	82,2	96,2	123	180	211
	0,12	75,3	111	130	194	285	333	53,4	78,5	91,8	137	202	236
	0,14	72,4	106	124	214	314	367	50,9	74,8	87,5	150	221	258
M16 × 1,5	0,08	88	129	151	154	227	265	65,5	96,2	113	115	169	197
	0,10	85,2	125	147	182	267	313	62,9	92,4	108	134	197	231
	0,12	82,2	121	141	207	304	355	60,2	88,4	104	151	222	260
	0,14	79,2	116	136	229	336	394	57,5	84,5	98,9	166	244	286
M20	0,08	131	186	218	298	424	496	94,2	134	157	215	306	358
	0,10	126	180	210	347	494	578	90,2	128	150	248	354	414
	0,12	121	173	202	392	558	653	86,1	123	144	278	396	463
	0,14	117	166	194	431	615	719	82,1	117	137	304	432	506
M20 × 1,5	0,08	149	212	248	320	456	533	113	160	188	242	345	403
	0,10	144	206	240	379	540	632	108	154	181	285	406	475
	0,12	139	199	232	433	617	722	104	148	173	323	460	538
	0,14	134	191	224	482	686	803	99,4	142	166	356	508	594
M24	0,08	188	268	313	512	730	854	136	193	226	370	566	616
	0,10	182	259	303	597	850	995	130	185	216	427	608	712
	0,12	175	249	291	673	959	1122	124	177	207	478	680	796
	0,14	168	239	280	742	1057	1237	118	168	197	522	743	870
M24 × 2	0,08	210	299	350	544	775	907	158	224	263	409	582	681
	0,10	203	290	339	643	916	1072	152	216	253	479	683	799
	0,12	196	280	327	733	1044	1222	145	207	242	542	772	904
	0,14	189	269	315	814	1159	1357	139	198	231	598	851	966

Table 14.6: Main characteristic of headless screws /15/

1	2	3	4	5	6	7	8	9	10	11	12	13	14
ISO DIN EN DIN	272, 4014, 4032 u.a. 24014, 24032 u.a. 475		4014 24014	4014 24017	4017 24017	4014 24014	4014 24014	4032 24032	4035 24035	935	ISO 1234	125	
Gewinde	Schlüsselweite SW	Eckenmaß	Kopfhöhe	Nennlängenbereich	Nennlängenbereich	Gewindelänge für $l \leq 125$ mm	Gewindelänge für $l \leq 125$ bis 200 mm	Mutterhöhe Typ 1	Mutterhöhe niedrige Form	Kronenmutter	Splint	Scheiben	
d	s	e	k	$l^{1)}$	$l^{1)}$	b	b	$m^{2)}$	m	h	$d_1 \times l_1$	d_2	s_1
M 3	5,5	6,01	2	20 ... 30	6 ... 30	12	–	2,4	1,8	–	–	7	0,5
M 4	7	7,66	2,8	25 ... 40	8 ... 40	14	–	3,2	2,2	5	1 × 10	9	0,8
M 5	8	8,79	3,5	25 ... 50	10 ... 50	16	–	4,7	2,7	6	1,2 × 12	10	1
M 6	10	11,05	4	30 ... 60	12 ... 60	18	–	5,2	3,2	7,5	1,6 × 14	12	1,6
M 8	13	14,38	5,3	40 ... 80	16 ... 80	22	–	6,8	4	9,5	2 × 16	16	1,6
M10	16	17,77	6,4	45 ... 100	20 ... 100	26	–	8,4	5	12	2,5 × 20	20	2
M12	18	20,03	7,5	50 ... 120	25 ... 120	30	–	10,8	6	15	3,2 × 22	24	2,5
M14	21	23,38	8,8	60 ... 140	30 ... 140	34	40	12,8	7	16	3,2 × 25	28	2,5
M16	24	26,75	10	65 ... 160	30 ... 200	38	44	14,8	8	19	4 × 28	30	3
M20	30	33,53	12,5	80 ... 200	40 ... 200	46	52	18	10	22	4 × 36	37	3
M24	36	39,98	15	90 ... 240	50 ... 200	54	60	21,5	12	27	5 × 40	44	4
M30	46	51,28	18,7	110 ... 300	60 ... 200	66	72	25,6	15	33	6,3 × 50	56	4
M36	55	61,31	22,5	140 ... 360	70 ... 200	–	84	31	18	38	6,3 × 63	66	5

15	16	17	18	19	20	21	22	23	24	25	26	
273 20273				76	3129	3110	74T3 (974T2)					ISO DIN EN DIN
Durchgangsloch[4)] Reihe			Kopf- bzw. Mutterauflagefläche in mm²	Grundlochüberhang (Regel)	Steckschlüsseleinsatz Außendurchmesser	Maulschlüsselbreite	Form R	Form SA TA	Form SB TB	Form SA SB	Form TA TB	
fein	mittel	grob					Ansenkung für rohe Flächen	für Steckschlüssel, Steckschlüsselein-sätze nach DIN 3124	für gekröpfte Ringschlüssel Steckschlüsselein-sätze nach DIN 3129	für Schraubenköpfe ohne Unterlegteile	für Muttern ohne Unterlegteile	Gewinde
d_h	d_h	d_h	A_p[5)]	e_1	d_5	b_1	d_3	d_4	d_4	t_1	t_1	d
3,2	3,4	3,6	7,5	2,8	9,7	19	9	11	11	2,4	2,8	M 3
4,3	4,5	4,8	11,4	3,8	12,8	20	10	13	15	3,4	3,8	M 4
5,3	5,5	5,8	13,6	4,2	15,3	22	11	15	18	4,2	4,7	M 5
6,4	6,6	7	28	5,1	17,8	27	13	18	20	4,8	5,8	M 6
8,4	9	10	42	6,2	21,5	34	18	24	26	6,5	7,5	M 8
10,5	11	12	72,3	7,3	27,5	38	22	28	33	8	9	M10
13	13,5	14,5	73,2	8,3	32,4	44	26	33	36	9	11	M12
15	15,5	16,5	113	9,3	36,1	49	30	36	43	10	12	M14
17	17,5	18,5	157	9,3	42,9	56	33	40	46	11,5	14,5	M16
21	22	24	244	11,2	50,4	66	40	46	53	14,5	17,5	M20
25	26	28	356	13,1	64,2	80	48	57	71	16,5	20,5	M24
31	33	35	576	15,2	76,7	96	61	71	82	21	26	M30
37	39	42	856	16,8	87,9	–	71	82	92	25	31	M36

Table 14.7: Main characteristic of countersink screws /15/

1	2	3	4	5	6	7	8	9	10	11	12	13	14	15	16	17	18	19	20	21	22	23	24	25	26	27	28	29	30	
DIN EN ISO DIN		4762	6912	7984	1207	4762 6912	7984	4762	6912	7984	1207	4762	6912 7984	4762 6912	7991	963	7991	2009	7991	7991	2009	74T2				74T1				DIN EN ISO DIN
Gewinde	Kopfdurchmesser	Kopfhöhe				Schlüssel-weite		Nennlängenbereich[1]				Gewindelänge	Gewindelänge für $l \leq 125$	Kopfauflage-fläche in mm²	Kopf-durch-messer		Kopf-Höhe		Schlüsselweite	Nennlängenbereich[1) 4)]		Form HJK	Form H für DIN EN ISO 1207 und DIN 7984	Form J für DIN 6912	Form K für DIN EN ISO 4762	Form A für DIN 963	Form B für DIN 7991	Form A für DIN 963	Form B für DIN 7991	Gewinde
d	d_1	k_1	k_2	k_3	k_4	s_1	s_2	l_1	l_2	l_3	l_4	b_1	b_2[2]	A_p[3]	d_2	d_3	k_5	k_6	s_3	l_5	l_6	d_4	t	t	t	d_5	d_5	$\approx t_1$	$\approx t_1$	d
M 3	5,5	3		2	2	2,5	2	5 … 30		5 … 20	4 … 30	18	12	11,1	6	5,6	1,7	1,65	2	8 … 30 (20)	4 … 30 (22)	6	2,4	–	3,4	6,5	6,6	1,6	1,6	M 3
M 4	7	4	2,8	2,8	2,6	3	2,5	6 … 40	10 … 50	6 … 25	5 … 40	20	14	17,6	8	7,5	2,3	2,2	2,5	8 … 40 (25)	5 … 40 (25)	8	3,2	3,4	4,6	8,6	9	2,1	2,3	M 4
M 5	8,5	5	3,5	3,5	3,3	4	3	8 … 50	10 … 60	8 … 30	6 … 50	22	16	26,9	10	9,2	2,8	2,5	3	8 … 50 (30)	6 … 50 (30)	10	4	4,2	5,7	10,4	11	2,5	2,8	M 5
M 6	10	6	4	4	3,9	5	4	10 … 60	10 … 70	10 … 40	8 … 60	24	18	34,9	12	11	3,3	3	4	8 … 50 (35)	8 … 50 (35)	11	4,7	4,8	6,8	12,4	13	2,9	3,2	M 6
M 8	13	8	5	5	5	6	5	12 … 80	12 … 80	12 … 60	10 … 80	28	22	55,8	16	14,5	4,4	4	5	10 … 60 (40)	10 … 55 (40)	15	6	6	9	16,4	17,2	3,7	4,1	M 8
M10	16	10	6,5	6	6	8	7	16 … 100	16 … 90	16 … 70	12 … 80	32	26	89,5	20	18	5,5	5	6	12 … 70 (40)	12 … 60 (50)	18	7	7,5	11	20,4	21,5	4,7	5,3	M10
M12	18	12	7,5	7	–	10	8	20 … 120	16 … 100	20 … 80	–	36	30	90	24	22	6,5	6	8	20 … 70 (50)	20 … 80 (60)	20	8	8,5	13	23,9	25,5	5,2	6	M12
M14	21	14	8,5	8	–	12	10	25 … 140	20 … 120	30 … 80	–	40	34	131	27	25	7	7	10	25 … 80 (50)	22 … 80 (60)	24	9	9,5	15	26,9	28,5	5,7	6,5	M14
M16	24	16	10	9	–	14	12	25 … 160	20 … 140	30 … 80	–	44	38	181	30	29	7,5	8	10	30 … 90 (60)	25 … 100 (70)	26	10,5	11,5	17,5	31,9	31,5	7,2	7	M16
M20	30	20	12	11	–	17	14	30 … 200	30 … 180	40 … 100	–	52	46	274	36	36	8,5	10	12	35 … 100 (70)	30 … 100 (80)	33	12,5	13,5	21,5	40,4	38	9,2	8	M20
M24	36	24	14	13	–	19	17	40 … 200	60 … 200	50 … 100	–	60	54	421	39	–	14	–	14	50 … 100 (90)	–	40	14,5	15,5	25,5	–	41	–	13,5	M24
M30	45	30	17,5	–	–	22	–	45 … 200	70 … 200		–	72	66	638	–	–	–	–	–	–	–	48	–	19,5	32	–	–	–	–	M30

Table 14.8: Snap factor /15/

Anziehverfahren	Streuung der Vorspannkräfte	vorzuschreibendes Anziehdrehmoment	Anziehfaktor k_A
Streckgrenzgesteuertes oder *drehwinkelgesteuertes Anziehen* von Hand oder motorisch	entspricht der Streckgrenze der Schraube	entfällt	1,0
Drehmomentgesteuertes Anziehen mit *Drehmomentschlüssel* ohne oder mit Vormontage durch Schlagschrauber, oder *Drehschrauber* mit Einstellen über Verlängerungsmessungen der montierten Schrauben oder über das Nachziehmoment sowie stetiger Nachkontrolle	±20 %	0,9 M_{sp}	1,6
Impulsgesteuertes Anziehen mit *Schlagschrauber*. Einstellung über Verlängerungsmessungen der montierten Schrauben oder über jeweils 10 Versuche (pro Los bzw. Tag), d. h. *Kontrolle* durch Drehmomentschlüssel	±40 %	0,85 M_{sp}	2,5
Impulsgesteuertes Anziehen mit *Schlagschrauber ohne Einstellkontrollen* oder *Anziehen von Hand* ohne Messung des Anziehmomentes	±60 %	entfällt	4,0

Table 14.9: Friction factor /15/

Reibungsart	Reibungszustand	Zwischenstoff	Reibungszahl μ
Gleitreibung	Festkörperreibung – Metall/Metall – Keramik/Keramik – Kunststoff/Metall	ohne (trocken)	 0,3 ... 1,5 0,2 ... 1,5 0,1 ... 1,5
	Grenzreibung	molekularer Schmierstofffilm	0,01 ... 0,2
	Mischreibung	partieller Schmierstofffilm	0,01 ... 0,1
	Flüssigkeitsreibung	Schmierstoff	ca. 10^{-3}
	Gasreibung	Gas	ca. 10^{-4}
Rollreibung		Wälzkörper	0,001 ... 0,005
Haftreibung (Ruhereibung)		ohne	ca. 0,5

Table 14.10: Nominal cross section of the shank and core cross section of the thread /15/

Gewinde-Nenndurchmesser $d = D$		Steigung	Flankendurchmesser	Kerndurchmesser		Gewindetiefe		Spannungsquerschnitt[1] A_s	Kernquerschnitt[1] A_3	Steigungswinkel[1] φ
Reihe 1	Reihe 2	P	$d_2 = D_2$	d_3	D_1	h_3	H_1	mm²	mm²	Grad
1		0,25	0,838	0,693	0,729	0,153	0,135	0,460	0,377	5,43
1,2		0,25	1,038	0,893	0,929	0,153	0,135	0,732	0,626	4,38
1,6		0,35	1,373	1,170	1,221	0,215	0,189	1,27	1,075	4,64
2		0,4	1,740	1,509	1,567	0,245	0,217	2,07	1,788	4,19
2,5		0,45	2,208	1,948	2,013	0,276	0,244	3,39	2,980	3,71
3		0,5	2,675	2,387	2,459	0,307	0,271	5,03	4,475	3,41
	3,5	0,6	3,110	2,765	2,850	0,368	0,325	6,78	6,000	3,51
4		0,7	3,545	3,141	3,242	0,429	0,379	8,78	7,749	3,60
	4,5	0,75	4,013	3,580	3,688	0,460	0,406	11,3	10,07	3,41
5		0,8	4,480	4,019	4,134	0,491	0,433	14,2	12,69	3,25
6		1	5,350	4,773	4,917	0,613	0,541	20,1	17,89	3,41
8		1,25	7,188	6,466	6,647	0,767	0,677	36,6	32,84	3,17
	(9)	1,25	8,188	7,466	7,647	0,767	0,677	48,1	43,78	2,78
10		1,5	9,026	8,160	8,376	0,920	0,812	58,0	52,30	3,03
	(11)	1,5	10,026	9,160	9,376	0,920	0,812	72,3	65,90	2,73
12		1,75	10,863	9,853	10,106	1,074	0,947	84,3	76,25	2,94
	14	2	12,701	11,546	11,835	1,227	1,083	115	104,7	2,87
16		2	14,701	13,546	13,835	1,227	1,083	157	144,1	2,48
	18	2,5	16,376	14,933	15,294	1,534	1,353	193	175,1	2,78
20		2,5	18,376	16,933	17,294	1,534	1,353	245	225,2	2,48
	22	2,5	20,376	18,933	19,294	1,534	1,353	303	281,5	2,24
24		3	22,051	20,319	20,752	1,840	1,624	353	324,3	2,48
	27	3	25,051	23,319	23,752	1,840	1,624	459	427,1	2,18
30		3,5	27,727	25,706	26,211	2,147	1,894	561	519,0	2,30
	33	3,5	30,727	28,706	29,211	2,147	1,894	694	647,2	2,08
36		4	33,402	31,093	31,670	2,454	2,165	817	759,3	2,19
	39	4	36,402	34,093	34,670	2,454	2,165	976	913,0	2,00
42		4,5	39,077	36,477	37,129	2,760	2,436	1121	1045	2,10
	45	4,5	42,077	39,479	40,129	2,760	2,436	1306	1224	1,95
48		5	44,752	41,866	42,587	3,067	2,706	1473	1377	2,04
	52	5	48,752	45,866	46,587	3,067	2,706	1758	1652	1,87
56		5,5	52,428	49,252	50,046	3,374	2,977	2030	1905	1,91
	60	5,5	56,428	53,252	54,046	3,374	2,977	2362	2227	1,78
64		6	60,103	56,639	57,505	3,681	3,248	2676	2520	1,82
	68	6	64,103	60,639	61,505	3,681	3,248	3055	2888	1,71

Table 14.11: Setting amount /15/

		Längskraft			Querkraft		
Rautiefe der Oberfläche R_z in µm		<10	10 … <40	40 … <160	<10	10 … <40	40 … <160
f_z in µm	im Gewinde	3	3	3	3	3	3
	je Kopf- oder Mutterauflage	2,5	3	4	3	4,5	6,5
	je innere Trennfuge	1,5	2	3	2	2,5	3,5
	Summe[1]	9,5	11	14	11	14,5	19,5

Table 14.12: Strength factors of the screws /15/

Festigkeits-klasse (Kennzeichen)	Werkstoff und Wärmebehandlung	Zug-festigkeit[2] R_m N/mm²	Streckgrenze[2] bzw. 0,2 %-Dehngrenze R_{eL} bzw. $R_{p0,2}$ N/mm²	Bruch-dehnung A_5 % min
3.6[3]	Stahl mit niedrigem C-Gehalt (z. B. QSt 36-2)	300 (330)	180 (190)	25
4.6[3]	Stahl mit niedrigem oder mittlerem C-Gehalt (z. B. UQSt 38-2)	400	240	22
4.8[3]		400 (420)	320 (340)	14
5.6	Stahl mit niedrigem oder mittlerem C-Gehalt (z. B. Cq22, Cq35)	500	300	20
5.8[3]		500 (520)	400 (420)	10
6.8[3]		600	480	8
8.8 ≤M16	Stahl mit niedrigem C-Gehalt und Zusätzen (z. B. Bor, Mn, Cr) oder mit mittlerem C-Gehalt, jeweils abgeschreckt und angelassen (z. B. 22B2, Cq45)	800	640	12
8.8 >M16		800 (830)	640 (660)	
9.8[4]		900	720	10
10.9	Stahl mit niedrigem C-Gehalt und Zusätzen[1] (z. B. Bor, Mn, Cr) bzw. mittlerem C-Gehalt, abgeschreckt und angelassen; oder mit mittlerem C-Gehalt mit Zusätzen oder legierter Stahl (z. B. 35B2, 34Cr4)	1000 (1040)	900 (940)	9
12.9	legierter Stahl, abgeschreckt und angelassen (z. B. 34CrMo4)	1200 (1220)	1080 (1100)	8

15 REFERENCES

1. *http://www.esha.be/index.php?id=39*
   Guide on how to develop a Small Hydropower Plant, Accessed 11 May 2007
2. Gordon, J.L. *Hydraulic turbine efficiency*. Article. Canada. 2001
3. Dixon, S.L. *Fluid mechanics and thermodynamics of turbomachinery*. Burlington, United States of America: Butterworth-Heinemann, 1998
4. *http://www.worldofenergy.com.au/factsheet_water/07_fact_water_hydro.html*
   THE FACTS ABOUT WATER ENERGY, modified 27 February 2007. Accessed 31 July 2007
5. *http://www.ept.ntnu.no/vk/publikasjoner/pdf/ArneKjolle/chapter8.pdf*
   Kaplna Turbines, Accessed 22 May 2007
6. *http://www.pienvesivoimayhdistys.fi/*
   Pienvesivoima on puhtainta uusiutuvaa energiaa, Accessed 31 July 2007
7. *http://www.maakaasu.fi/pdf/Energy_consumption.pdf*
   Primary energy consumption in Finland, Accessed 24 July 2007
8. *http://www.nordpool.com/*
   Spot market data, monthly prices. Accessed 19 November 2007
9. Menny, Klaus. Strömungsmaschinen: *Hydraulische und thermische Kraft- und Arbeitsmaschinen*. Wiesbaden, Germany: Teubner, 2006. ISBN-10 3-519-6317-2
10. *http:www.kayelaby.npl.co.uk/chemistry/3_4/3_4_2.html*
    Vapour pressure of water at temperatures between 0 and 360°C, Accessed 24 September 2007
11. Kovale, N. N. *Hydroturbines*. Moscow, Russia: Mashinostroitel'noi Literatury, 1961.
12. Ahlfors, K. Axel. *Vesiturbiinit*. Helsinki, Finland: Porvoo, 1932
13. Gieck, K., R. Gieck. *Technische Formelsammlung*. Germering, Germany: Gieck, 1995. ISBN 3 920379 21 7
14. Fischer, U., Heinzler M., Kilgus, R.,Näher, F., Paetold, H., Röhrer, W., Schilling K., A. Stephan. *Tabellenbuch Metall*. Haan-Gruiten, Germany: Lehrmittel, 1999. ISBN 3-8085-1712-2

15. Becker, Manfred., Jannasch, Dieter., Matek, Wilhelm., Muhs, Dieter., Herbert. Wittel. Roloff/Matek: *Maschinenelemente*. Braunschweig/ Wiesbaden, Germany: Vieweg, 2001. ISBN 3-528-94028-X
16. *http://www.igus.de/iPro/iPro_02_0008_00_DEde.htm?ArtNr=&C=DE&L=de* Iglidur® H, Accessed 14 September 2007
17. *http://www.kleinsorge.de/html/katalog/produktdetail.asp?id={46C6CDEF-8E73-4BD2-9962-BA9F3D75163C}&catID={7DAD2090-B7AC-46E3-98CF-3D16A0E0FEF1}&lang=0* kleinsorge-Verbindungstechnik, Accessed 7 November 2007
18. Hoischen, Hans. *Technisches Zeichnen*. Berlin, Germany: Cornelsen, 2003. ISBN 3-464-48009-7

Tampere, 04.12.2007

Timo Flaspöhler